

USE OF VORONOI GRIDDING IN WELL TEST DESIGN

A THESIS SUBMITTED TO  
THE GRADUATE SCHOOL OF NATURAL AND APPLIED SCIENCES  
OF  
MIDDLE EAST TECHNICAL UNIVERSITY

BY  
FUAD RAHIMOV

IN PARTIAL FULFILLMENT OF THE REQUIREMENTS  
FOR  
THE DEGREE OF MASTER OF SCIENCE  
IN  
PETROLEUM AND NATURAL GAS ENGINEERING

SEPTEMBER 2015



Approval of the thesis:

**USE OF VORONOI GRIDDING IN WELL TEST DESIGN**

submitted by **FUAD RAHIMOV** in partial fulfillment of the requirements for the degree of **Master of Science in Petroleum and Natural Gas Engineering Department, Middle East Technical University** by,

Prof. Dr. M. Gülbin Dural Ünver  
Dean, Graduate School of **Natural and Applied Sciences**

\_\_\_\_\_

Prof. Dr. Mustafa Verşan Kök  
Head of Department, **Petroleum and Natural Gas Eng.**

\_\_\_\_\_

Assist. Prof. Dr. Çağlar Sınayuç  
Supervisor, **Petroleum and Natural Gas Eng. Dept., METU**

\_\_\_\_\_

**Examining Committee Members:**

Prof. Dr. Mahmut Parlaktuna  
Petroleum and Natural Gas Engineering Dept., METU

\_\_\_\_\_

Asst. Prof. Dr. Çağlar Sınayuç  
Petroleum and Natural Gas Engineering Dept., METU

\_\_\_\_\_

Prof. Dr. Mustafa Verşan Kök  
Petroleum and Natural Gas Engineering Dept., METU

\_\_\_\_\_

Asst. Prof. Dr. İsmail Durgut  
Petroleum and Natural Gas Engineering Dept., METU

\_\_\_\_\_

Asst. Prof. Dr. Emre Artun  
Petroleum and Natural Gas Engineering Dept., METU NCC

\_\_\_\_\_

**Date:** 01.09.2015

**I hereby declare that all information in this document has been obtained and presented in accordance with academic rules and ethical conduct. I also declare that, as required by these rules and conduct, I have fully cited and referenced all material and results that are not original to this work.**

**Name, Last Name:** Fuad, Rahimov

**Signature:**

## **ABSTRACT**

### **USE OF VORONOI GRIDDING IN WELL TEST DESIGN**

Rahimov, Fuad

M.S., Department of Petroleum and Natural Gas Engineering

Supervisor: Asst. Prof. Dr. Çağlar Sınayuç

September 2015, 152 pages

One of the most efficient tools to accurately characterize the reservoir and its nature is well testing. In the literature, well testing sometimes is referred as Pressure Transient Analysis (PTA). For the development strategy of the field both technical and economic considerations are involved. In order to perform well testing, firstly it needs to be correctly designed, otherwise well testing will not yield reliable information about the reservoir. There are both analytical and numerical techniques for the well testing.

One of the main aim of this study is to compare analytical methods commonly used in well test design against the numerical simulators by taking into account different reservoir models. These models were built using a commercial black oil simulator called as CMG IMEX by considering various scenarios, such as simple oil reservoir models with and without gas phase, reservoir models in different shapes, models with different fault channel orientations with respect to grid orientations (vertical and inclined), one well model versus two wells model in which they are producing close to each other to see the superposition effect on well test design. For this part it can be concluded that under ideal circumstances, analytical calculations can be somewhat reliable, but with more complex reservoirs where inclined faults, availability of a gas phase and several wells, numerical simulators yield more accurate and reliable information for the well test design procedure. In the second part, the aim is to assess unstructured gridding simulation – Voronoi gridding applicability in well test design

procedure by comparing against structured gridding simulation results. Comparisons showed that under simple and ideal reservoir parameters, they can yield somewhat similar pressure results. But with inclined fault model that is built by using Ecrin Rubis module, it is concluded that Voronoi gridding gives more realistic and accurate results due to its flexibility on representing deviated fault channels.

Six different cases of different values of production time, production rate, and shut-in time are studied to check how these variations affect the well test design. Based on the comparisons done using Horner plots generated for each case it is concluded that using a numerical simulator is the best way to appropriately design a test in order to select optimum value for each parameter.

**Keywords:** Reservoir, well testing design, Voronoi gridding, Horner Plots, CMG IMEX, Ecrin Rubis, fault

## ÖZ

### VORONOİ IZGARALARIN KUYU TESTLERİNDE KULLANIMI

Rahimov, Fuad

Yüksek Lisans. Petrol ve Doğal Gaz Mühendisliği

Tez Yöneticisi: Yrd. Doç. Dr. Çağlar Sınayuç

Eylül 2015, 152 sayfa

Rezervuar karakterizasyonu için en etkili yöntemlerden biri de kuyu testleridir. Literatürde kuyu testleri Süreksiz Basınç Analizi olarak da adlandırılır. Saha geliştirme sürecinde teknik ve ekonomik veriler değerlendirilmelidir. Kuyu testlerini etkin şekilde uygulayabilmek için öncelikli olarak doğru bir tasarım gereklidir. Aksi takdirde testler rezervuar hakkında güvenilir sonuçlar üretmeyebilir. Kuyu testlerini analiz ederken analitik ve sayısal yöntemler kullanılır.

Bu çalışmanın temel amaçlarından bir tanesi, kuyu testleri tasarımında sıklıkla kullanılan analitik yöntemler ile sayısal yöntemlerin farklı rezervuar modelleri için karşılaştırılmasıdır. Bu sayısal modeller düzenli simülasyon ızgaraları için ticari bir petrol simülatörü olan CMG IMEX kullanılarak, Voronoi ızgaraları için ise Ecrin Rubis yazılımı kullanılarak oluşturulmuştur. Rezervuarda petrol dışında gazın olup olmaması, farklı şekildeki rezervuarlar, ızgara yönüne göre dik ya da eğik olan fay hatlarının olup olmaması, bir kuyulu ya da birbirleri ile olan etkileşimlerini incelemek için iki kuyulu sistemler gibi durumlar için çalışmalar yapılmıştır. Analitik denklemlerin ideal şartlar altında güvenilebilir olabileceğini göstermesine rağmen, fay hatlarının ya da gaz fazının varlığı, çok sayıda kuyunun bulunması gibi karışık rezervuarlarda sayısal simülatörlerin test tasarımında daha yakın ve güvenilir

sonuç verdiđini göstermiřtir. İkinci olarak, Voronoi gibi düzensiz ızgaraların simülatörde kullanılmasının sonuçların nasıl etkilendiđi deđerlendirilmiřtir. Karřılařtırılmalar göstermiřtir ki, basit ve ideal řartlar altında, her iki ızgara yöntemi de benzer sonuçlar verirken, Ecrin Rubis yazılımı ile oluřturulan eđik fay modelinde de görüldüđu üzere Voronoi ızgaraları, esnek oluřları ve fay hatlarını temsil etmedeki üstünlükleri nedeniyle daha gerçeđçi ve yakın sonuçların alınmasını sađlamıřtır.

Altı farklı model kullanılarak yapılan alıřmalar ile farklı üretim süresi, üretim debisi, ve kuyu kapatma süresinin kuyu test tasarımının nasıl etkilediđi deđerlendirilmiřtir. Horner grafikleri kullanılarak yapılan karřılařtırmalarda sayısal yöntemlerin analitik yöntemlere göre tasarım aşamasında en uygun parametrelerin seçiminde özellikle heterojen ve doymuř rezervuarlarda gerekli olduđu, voronoi ızgara kullanımının da fay gibi yapısal özelliklerin önemli olduđu yerlerde kullanılmasının faydalı olduđu sonucuna varılmıřtır.

**Anahtar Kelimeler:** Rezervuar, kuyu testleri, Voronoi ızgaraları, Horner grafikleri, CMG IMEX, fay

## **ACKNOWLEDGEMENTS**

All prays for Allah that has never left me alone any single moment of my life.

I'd like to personally thank my supervisor Asst. Prof. Dr. Çağlar Sınayuç for his relentless contribution, enthusiastic involvement and continuous efforts on my thesis work. I wish also to thank him for his time that was spent on my study.

I also want to acknowledge the contribution of all my professors for their precious courses and efforts at Middle East Technical University.

Ultimately, I want to express my gratitude to my family for their understanding, contribution, and everlasting support irrespective of any hurdles that I've faced.

## TABLE OF CONTENTS

ABSTRACT.....	v
ÖZ.....	vii
ACKNOWLEDGEMENTS.....	ix
TABLE OF CONTENTS.....	x
LIST OF FIGURES .....	xiii
LIST OF TABLES.....	xix
CHAPTERS	
1 INTRODUCTION .....	1
2 WELL TESTING.....	5
2.1 Well Testing Objectives .....	10
2.2 Typical Flow Regimes .....	13
2.3 Well Tests .....	16
2.3.1 Drawdown Testing.....	16
2.3.2 Build-up Testing.....	20
2.3.3 Interference Testing .....	26
2.3.4 Pulse Testing .....	27
3 WELL TEST DESIGN .....	29
3.1 Variable Dependency.....	30
3.2 Test Duration .....	31
3.3 Flow Rate Consideration.....	33
3.4 Computer Aided Well Test Interpretation .....	34
3.5 Optimization of Well Test Design and Steps for Workflow.....	36

4 RESERVOIR SIMULATION.....	41
4.1 Introduction to Reservoir Simulation.....	41
4.2 Structured Grid Simulation .....	44
4.2.1 Corner-Point Geometry Grids .....	45
4.3 Unstructured Grid Simulation .....	46
4.4 Use of Voronoi Gridding on Simulation.....	47
4.4.1 Grid Generation.....	50
4.4.2 Assignment of Physical Properties .....	52
4.4.3 Use of Voronoi Gridding Simulation for Heterogeneous Reservoirs .....	54
4.5 Numerical Well Testing Using Unstructured Voronoi Gridding.....	57
5 PRESSURE ANALYSIS METHODS IN HETEREGENEOUS OIL RESERVOIRS .....	59
5.1 Introduction.....	59
5.2 Effect of Pressure on Rock Properties .....	59
5.3 Pressure Responses Near to No-Flow Boundary.....	60
6 STATEMENT OF THE PROBLEM .....	63
7 METHODOLOGY.....	65
7.1 Introduction.....	65
7.2 Part-1. Use of CMG IMEX and ECRIN Saphir.....	66
7.2.1 OILWATER Model .....	66
7.2.2 BLACKOIL Model.....	71
7.2.3 Reservoir Models with Different Shapes .....	73
7.2.4 Reservoir Models with Two Wells .....	75
7.2.5 Reservoir Model with Vertical Fault .....	78
7.2.6 Reservoir Model with Inclined Fault .....	81

7.3 Part-2. Use of ECRIN Rubis and CMG IMEX.....	82
7.3.1 Undersaturated.....	83
7.3.2 Saturated.....	100
8 RESULTS AND DISCUSSIONS.....	111
8.1 Results and Discussions for Part-1.....	111
8.1.1 OILWATER Model.....	111
8.1.2 BLACKOIL Model.....	111
8.1.3 Reservoir Models with Different Shapes.....	112
8.1.4 Reservoir Model with Two Wells.....	113
8.1.5 Reservoir Model with Vertical Fault.....	113
8.1.6 Reservoir Model with Inclined Fault.....	114
8.2 Results and Discussions for Part-2.....	114
8.2.1 Undersaturated.....	114
8.2.2 Saturated.....	131
9 CONCLUSIONS.....	145
10 FUTURE WORK.....	147
REFERENCES.....	149

## LIST OF FIGURES

### FIGURES

<b>Figure 2-1.</b> Characteristic Pressure Transient graphs yielding different reservoir characteristics (Schlumberger, 1994).....	6
<b>Figure 2-2.</b> Drawdown and build-up well testing (Steward, 2011).....	8
<b>Figure 2-3.</b> Common test sequence in oil wells (Schlumberger, 1994).....	9
<b>Figure 2-4.</b> 3 flow regimes in a reservoir (Schlumberger, 1994).....	15
<b>Figure 2-5.</b> Drawdown Test (Tarek, 2001). ....	16
<b>Figure 2-6.</b> Drawdown semilog plot (Schlumberger, 1994). ....	18
<b>Figure 2-7.</b> Flow-rate and pressure behaviour for an ideal buildup (Schlumberger, 1994). ....	21
<b>Figure 2-8.</b> Horner Plot for a buildup (Schlumberger, 1994).....	21
<b>Figure 2-9.</b> Impact of wellbore storage on a build-up (Schlumberger, 1994).....	23
<b>Figure 2-10.</b> Procedure for determination the Middle Time Region pressure at 1 hour (Schlumberger, 1994). ....	26
<b>Figure 2-11.</b> Influence region for interference or pulse testing, (Chaudhry, 2004)..	27
<b>Figure 2-12.</b> Pulse Test methodology (SPE, 1983).....	28
<b>Figure 3-1.</b> Well Test Design Optimization Workflow (Kumar et al., 2010).....	39
<b>Figure 4-1.</b> Reservoir Simulation Workflow (Cheng, 2011). ....	42
<b>Figure 4-2.</b> Reservoir Simulation Grids (Souche, 2003).....	45
<b>Figure 4-3.</b> Voronoi Grid and Delaunay mesh (Palagi, 1994). ....	48
<b>Figure 4-4.</b> Special cases of Voronoi Gridding (Palagi, 1994). ....	49
<b>Figure 4-5.</b> Different modules for grid generation (Palagi, 1994). ....	50
<b>Figure 4-6.</b> Hypothetical use of different modules (Palagi, 1994).....	51
<b>Figure 4-7.</b> Assignment of physical properties to each block (Palagi, 1994). ....	53
<b>Figure 4-8.</b> Specifying of physical properties to each Voronoi grid blocks and its connections (Ballin et al, 1993). ....	56
<b>Figure 5-1.</b> Effect of pressure-dependent permeability on drawdown and build-up tests (Chaundry, 2004). ....	60

<b>Figure 7-1.</b> Well bottom-hole pressure change over the production and build-up period. ....	68
<b>Figure 7-2.</b> Diagnostic log-log plot of the OILWATER Reservoir Model.....	69
<b>Figure 7-3.</b> Bottom-hole Pressure of the well located on the centre of reservoir taken from CMG IMEX .irf file. ....	71
<b>Figure 7-4.</b> Diagnostic log-log plot of the BLACKOIL Reservoir Model. ....	72
<b>Figure 7-5.</b> Rectangular shaped reservoir model log-log plot result.....	73
<b>Figure 7-6.</b> ECRIN build-up testing results for the squared reservoir model. ....	74
<b>Figure 7-7.</b> 2 wells producing close to each other in a reservoir model. ....	75
<b>Figure 7-8.</b> Bottom-hole pressure value for the Observation Well with another well operating adjacent to it.....	76
<b>Figure 7-9.</b> Bottom hole pressure value for the Observation well without another well producing close to it.....	76
<b>Figure 7-10.</b> Build-up log-log testing plot in a reservoir model with 2 wells.....	77
<b>Figure 7-11.</b> Pressure drop value differences between analytical and numerical results. ....	78
<b>Figure 7-12.</b> Reservoir Model with a well producing close to vertical fault. ....	79
<b>Figure 7-13.</b> ECRIN build-up log-log plot for the reservoir with the vertical fault. ....	79
<b>Figure 7-14.</b> ECRIN build-up testing results for the reservoir model without any fault. ....	80
<b>Figure 7-15.</b> Reservoir model with inclined fault built in CMG IMEX simulator. ..	81
<b>Figure 7-16.</b> Build-up result on a reservoir model with inclined fault model by use of ECRIN software. ....	82
<b>Figure 7-17.</b> Voronoi Gridded reservoir model built in Ecrin Rubis.....	84
<b>Figure 7-18.</b> Pressure-Rate plot for Undersaturated case taken from Ecrin Rubis. ..	84
<b>Figure 7-19.</b> Reservoir gridding built and taken from CMG IMEX. ....	85
<b>Figure 7-20.</b> Well bottom-hole pressure for Well-1 taken from CMG IMEX.....	85
<b>Figure 7-21.</b> Ecrin Saphir log-log build-up plot for case 1.....	86
<b>Figure 7-22.</b> Pressure-Rate plot for the case 2 taken from Ecrin Rubis.....	87
<b>Figure 7-23.</b> Ecrin Saphir build-up results for case 2. ....	87
<b>Figure 7-24.</b> Pressure-Rate plot for case 3.....	88
<b>Figure 7-25.</b> Build-up log-log plot testing on Ecrin Saphir. ....	89
<b>Figure 7-26.</b> Rubis pressure-rate plot for the case 4. ....	89
<b>Figure 7-27.</b> Ecrin Saphir build-up log-log plot for the case 4. ....	90

<b>Figure 7-28.</b> Ecrin Rubis pressure-rate plot for the case 5.....	90
<b>Figure 7-29.</b> Ecrin Saphire log-log build-up testing for the case 5. ....	91
<b>Figure 7-30.</b> Ecrin Rubis pressure-rate plot for the case 6.....	91
<b>Figure 7-31.</b> Ecrin Saphir build-up log-log plot for the case 6. ....	92
<b>Figure 7-32.</b> Ecrin Rubis module for the under-saturated horizontal fault. ....	93
<b>Figure 7-33.</b> Ecrin Rubis under-saturated reservoir model with horizontal fault. ....	93
<b>Figure 7-34.</b> Rubis Pressure-rate plot for the undersaturated reservoir model with horizontal fault. ....	94
<b>Figure 7-35.</b> CMG IMEX Model with horizontal fault for the under-saturated reservoir case.....	94
<b>Figure 7-36.</b> Bottom-hole pressure change for well-1 taken from CMG IMEX.....	95
<b>Figure 7-37.</b> Ecrin Saphir build-up log-log plot based on Rubis pressure values for under-saturated reservoir model.....	95
<b>Figure 7-38.</b> Ecrin Saphir build-up log-log plot for the undersaturated reservoir model with fault by using CMG IMEX pressure values.....	96
<b>Figure 7-39.</b> Undersaturated reservoir model with inclined fault built on Ecrin Rubis. ....	97
<b>Figure 7-40.</b> Ecrin Rubis Module representing inclined fault model for undersaturated reservoir case. ....	97
<b>Figure 7-41.</b> Ecrin Rubis pressure-rate plot for the undersaturated reservoir model with inclined fault. ....	98
<b>Figure 7-42.</b> CMG IMEX undersaturated reservoir model with inclined fault channel. ....	98
<b>Figure 7-43.</b> CMG IMEX under-saturated reservoir model with inclined fault depicting bottom-hole pressure value change. ....	99
<b>Figure 7-44.</b> Ecrin Saphir build-up log-log plot for under-saturated reservoir model with inclined fault by using Rubis data.....	99
<b>Figure 7-45.</b> Ecrin Saphir build-up log-log plot for under-saturated reservoir model with inclined fault by using CMG data. ....	100
<b>Figure 7-46.</b> Ecrin Rubis pressure-rate plot for the saturated reservoir model. ....	101
<b>Figure 7-47.</b> CMG IMEX Bottom-hole pressure change for the well. ....	102
<b>Figure 7-48.</b> Ecrin Saphir log-log build-up plot by using Rubis pressure data.....	102
<b>Figure 7-49.</b> Ecrin Saphir build-up results by using CMG IMEX pressure data. ...	103
<b>Figure 7-50.</b> Relative Permeability data for both models. ....	103

<b>Figure 7-51.</b> Ecrin Rubis pressure-rate plot for the saturated reservoir model with horizontal fault. ....	104
<b>Figure 7-52.</b> CMG IMEX plot describing bottom-hole pressure change for the well located in saturated reservoir model with horizontal fault. ....	105
<b>Figure 7-53.</b> Ecrin Saphir build-up testing on saturated reservoir model with horizontal fault by using Rubis pressure data. ....	105
<b>Figure 7-54.</b> Ecrin Saphir pressure build-up testing log-log plot for the saturated reservoir model with horizontal fault by using CMG IMEX data. ....	106
<b>Figure 7-55.</b> Ecrin Rubis pressure-rate plot for the saturated reservoir model with inclined fault. ....	107
<b>Figure 7-56.</b> CMG IMEX plot illustrating bottom-hole pressure change in a well for the saturated reservoir model with deviated fault. ....	108
<b>Figure 7-57.</b> Ecrin Saphir pressure data for saturated reservoir model with deviated fault channel based on Ecrin Rubis pressure data. ....	108
<b>Figure 7-58.</b> Ecrin Saphir pressure data for saturated reservoir model with deviated fault channel based on CMG IMEX pressure data. ....	109
<b>Figure 8-1.</b> CMG IMEX-Ecrin Rubis pressure match. ....	115
<b>Figure 8-2.</b> Horner Plot for the Case-1. ....	115
<b>Figure 8-3.</b> CMG IMEX pressure values match with Ecrin Rubis ....	116
<b>Figure 8-4.</b> Horner Plot for Case 2. ....	117
<b>Figure 8-5.</b> Horner Plot for the Case 3. ....	118
<b>Figure 8-6.</b> Pressure change history plot for the case 3. ....	118
<b>Figure 8-7.</b> Pressure change history plot for the case 4. ....	119
<b>Figure 8-8.</b> Horner Plot for the Case 4. ....	119
<b>Figure 8-9.</b> Horner Plot for the case 5. ....	120
<b>Figure 8-10.</b> Horner Plot for Case-6. ....	121
<b>Figure 8-11.</b> CMG-IMEX pressure values comparison with Ecrin Rubis module. ....	122
<b>Figure 8-12.</b> Horner plot by using CMG IMEX pressure values. ....	123
<b>Figure 8-13.</b> CMG IMEX Plots describing fault effect. ....	123
<b>Figure 8-14.</b> Horner plot based on CMG IMEX pressure values. ....	124
<b>Figure 8-15.</b> Horner Plot generated based on Ecrin Rubis pressure values. ....	125
<b>Figure 8-16.</b> Horner Plot for Rubis Pressure Values. ....	125
<b>Figure 8-17.</b> CMG IMEX pressure values match with Ecrin Rubis module. ....	126
<b>Figure 8-18.</b> Horner Plot based on Ecrin Rubis values. ....	127

<b>Figure 8-19.</b> Horner Plot based on Rubis pressure values with straight lines.....	128
<b>Figure 8-20.</b> Horner Plot based on CMG IMEX pressure values. ....	128
<b>Figure 8-21.</b> Horner Plot based on CMG IMEX pressure values with 2 straight lines. .....	129
<b>Figure 8-22.</b> Horner Plot based on CMG IMEX and ECRIN Rubis pressure values. .....	130
<b>Figure 8-23.</b> Ecrin Rubis Pressure Values comparison for horizontal and inclined faults.....	130
<b>Figure 8-24.</b> CMG IMEX Pressure values difference for horizontal and inclined fault models.....	131
<b>Figure 8-25.</b> CMG IMEX Pressure values match with Ecrin Rubis for saturated reservoir model.....	132
<b>Figure 8-26.</b> Horner Plot by using Ecrin Rubis Pressure Values.....	132
<b>Figure 8-27.</b> Horner plot based on Ecrin Rubis pressure values with straight line.	133
<b>Figure 8-28.</b> Horner Plot based on CMG IMEX pressure values. ....	133
<b>Figure 8-29.</b> Horner Plot by using CMG IMEX values with straight line. ....	134
<b>Figure 8-30.</b> CMG IMEX-Ecrin Rubis pressure values match for saturated reservoir with horizontal fault. ....	135
<b>Figure 8-31.</b> Horner Plot by using Ecrin Rubis pressure values for saturated reservoir model with a horizontal fault. ....	136
<b>Figure 8-32.</b> Horner Plot for Saturated reservoir model with horizontal fault by using Rubis pressure values. ....	136
<b>Figure 8-33.</b> Horner Plot based on CMG IMEX pressure values for the saturated reservoir model with horizontal fault. ....	137
<b>Figure 8-34.</b> Horner Plot by using CMG IMEX pressure values.....	138
<b>Figure 8-35.</b> CMG IMEX pressure values comparison with Ecrin Rubis for the saturated reservoir model with inclined fault.....	139
<b>Figure 8-36.</b> Horner Plot based on Ecrin Rubis values for saturated reservoir with inclined fault.....	140
<b>Figure 8-37.</b> Horner Plot based on CMG IMEX pressure value for saturated reservoir with inclined fault. ....	140
<b>Figure 8-38.</b> Horner Plot based on Ecrin Rubis pressure values for the saturated reservoir with inclined fault. ....	141

**Figure 8-39.** Horner Plot based on CMG IMEX pressure values for saturated reservoir model with inclined fault. .... 142

## LIST OF TABLES

### TABLE

<b>Table 7-1.</b> Reservoir Model specifications from CMG IMEX Builder. ....	67
<b>Table 7-2.</b> Reservoir Model specifications from CMG IMEX Builder. ....	67
<b>Table 7-3.</b> Results of Build-up testing with reservoir parameters taken from Ecrin Saphir. ....	70
<b>Table 7-4.</b> Results of Build-up testing of BLACKOIL reservoir model. ....	72
<b>Table 8-1.</b> End of Transient flow regime comparison. ....	143
<b>Table 8-2.</b> End of transient regime comparison for 6 different cases .....	143
<b>Table 8-3.</b> Well to Fault distance estimation for different reservoir models. ....	144



## CHAPTER 1

### INTRODUCTION

One of the most efficient tool to accurately determine the reservoir characterization and its nature is well testing (Lee, 1997). In literature, well testing sometimes is referred as Pressure Transient Analysis (PTA). For the development strategy of the field both the technical and economic considerations are involved (Dominic, 2002). In order to adequately implement the optimization of the field, some sort of accurate reservoir model is required through which realistic forecasts of dynamic reservoir behaviour can be made. For instance, an engineer would be more interested in predictions about production rate and fluid recovery as the reservoir is produced. Such kind of model can be built based on geological, geophysical and well test data (Robert, 1997). Some required data can be gained from direct measurements such as from cores, cuttings, fluid samples and etc. On the other hand, some indirect measurements can be performed such as surface seismic, well logs, well tests, PVT analysis and so on. Seismic data combined with well logs can inform about static description of the field, whereas it's only well testing through which dynamic reservoir response can be acquired and interpreted. This is too crucial for the correct reservoir model establishment.

For building the reservoir model representing actual reservoir features, it needs to be discretized into small blocks (Aziz et al., 1979). Most of the reservoir simulators use structured grids by Cartesian or corner block geometries. The heterogeneity of the rock properties has to be represented in these models. Sometimes it poses some challenge to focus on certain regions of the structured models. However this technique increases the number of blocks and hence the simulation time. Voronoi diagrams can be used to discretise the reservoir so that the smaller blocks can be

placed wherever needed. Such as around a well or along a fault line, etc. Therefore this study will develop the understanding the usage of Voronoi diagrams in reservoirs through well testing procedure. In this study a well test design will be performed by using a hypothetical Voronoi gridded reservoir. The Voronoi diagrams are capable of simulating the fluid flow in the reservoir.

Well testing design starts with the simulation study where the amount of rate, the duration of the test, the choice of the observation well, etc. need to be understood before actually doing the test on the real field (Steward. 2001).

Different stages of drilling, production, and completion may undergo well testing operations (Lee, 1997). The test purposes can range from a mere identification of produced fluids up to complex reservoir descriptions. Whatever the reason is, well testing is an unimpeachable important tool for precise description of reservoir performance as well as for realistic forecasts.

Productivity well testing enables to get information about produced fluid identification, collection of representative samples, and determination of reservoir productivity, whereas descriptive well testing are carried out to estimate reservoir parameters, to identify vertical and horizontal heterogeneities of the reservoirs as well as to evaluate reservoir extent (Schlumberger, 1994).

Transient tests are carried out by changing abruptly the production rate in surface and recording the corresponding bottom-hole pressure change (Tarek, 2001). These production changes generate pressure disturbances and can extend much farther through the reservoir and making these tests useful for reservoir characterization. In literature, these tests are referred as descriptive or reservoir tests. These pressure disturbances can be affected by reservoir rock features, and obviously can behave differently. For instance, these pressure transients will have difficulty entering low-permeable zones, conversely they can penetrate in more-permeable zones unimpeded. That's why a record of well-bore pressure change will yield a curve whose shape appears to be representative for the reservoir characteristics. Interpreting this pressure transient curves and corresponding reservoir characteristics are the essential purposes of well testing (Clark, 1951).

The previous production history can also alter the shape of the pressure transient curve, especially if the field has been producing for quite some time (Kamal et. al.,

1997). More precisely, each production change will generate some pressure disturbances in the reservoir, and it will be combined with the previous pressure pulses. As a result, the superposition of these pressure pulses will have an impact of the wellbore pressure change (Kamal et. al., 1997). So, analysing these pressure transient curves will yield some significant reservoir parameters from which further reservoir management and development decisions are made.

These curves are even irreplaceable in well test design procedure which is the core focus of our study. In this, the thesis is divided into two parts. The first part is dedicated the advantages of using numerical simulators such as CMG IMEX, and Ecrin Rubis module over the analytical methods. CMG IMEX is a powerful commercial simulator which is commonly used in petroleum industry. Ecrin Rubis module is also well known tool that is used in especially well testing studies. Ecrin Rubis module is not used in management studies though since it is not designed to give pressure distributions in the reservoir. In order to highlight the advantages of using the numerical simulators over the analytical calculations, different reservoir models were run using the mentioned simulators. Different scenarios, such as oil with and without gas phase, different reservoir shapes, reservoir model with and without fault (including inclined fault model also), and one well producing close to another well to see the superposition principle effect on well test design parameters are applied throughout the study. For each case analytical calculations will be compared against CMG IMEX and Ecrin Rubis output results. Based on these comparisons, the reliability of using analytical calculations in well test design by taking into consideration of the aforementioned scenarios and results were discussed in this study.

In the second part, the applicability of Voronoi gridding in well test design is assessed by using Ecrin Rubis module. For this purpose a reservoir model in CMG IMEX and the same model with the same fluid properties in Ecrin Rubis software has been built and run. Then the results from both softwares are compared. Based on this comparison it can be judged the applicability of unstructured reservoir gridding as opposed to structured reservoir gridding. Two cases are studied: under-saturated and saturated reservoirs. Under-saturated model case accounts for the simple model without any fault and as the name implies there is only oil phase without gas phase. In order to have one phase throughout the whole production, bubble point pressure is

set as low as possible for the reservoir pressure to remain above the bubble point pressure. Different scenarios are introduced, such as reducing and increasing production rate, setting different build-up and production times in the model so that the effects of these variations can be seen on well test design parameters, because the design is strictly depended upon these parameters as well. Then selection of optimum production and build-up times for the reasonable well test design based on Horner plots for these different scenarios could be accomplished.

Second case accounts for the gas phase as well where a fault is also introduced to the model with both straight and inclined with respect to the orientations of the structured grids, and build-up testing in Ecrin Saphir based on Ecrin Rubis pressure values is performed to assess voronoi gridding applicability on the well test design. Then, the same reservoir model with the same fluid and fault properties is built on CMG IMEX and build-up testing on Ecrin Saphir based on CMG IMEX pressure values is performed. Then, these two results are compared to judge the applicability of unstructured gridding on reservoir models with faults based on these comparisons.

## CHAPTER 2

### WELL TESTING

Petroleum Engineering phases require detailed and accurate information about the reservoir and its conditions in order to properly implement reservoir management work. Reservoir Engineer needs to get informed about reservoir *in-situ* conditions in order to be able to foresee the production accurately with minimum loss, and in order to assess reservoir deliverability in an accurate manner (Sattar, 2008). When it comes the information for the production and injection wells location and condition in a reservoir to get the most authentic reservoir performance, it's the responsibility of production engineer who in turn can get this information through well testing.

Well testing is a quite important topic in both Reservoir and Production Engineering. It can be sub-divided further into various tests such as build-up, drawdown, falloff, injectivity, and interference tests which are the heart of Petroleum Engineering discipline (Ronald, 1990). As the name implies, pressure transient analysis involves creating and interpreting pressure variation in the well, and as a result identifying rock, fluid, and well properties. To put in different words, PTA is a quantitative estimation of flow rate, pressure, and time (Ronald, 1990). Usually, the data that is obtained from the flowing well can be “distorted”, therefore the data being acquired from shut-in period is interpreted. Obviously, pressure differentials can be created when a well is closed or opened. Therefore, by virtue of generation of pressure disturbance, this pressure differential gradually reaches the boundary of the reservoir, and the radius of interest zone increases in a square-root of time fashion (Dake, 1975). Naturally, the longer the duration of PTA, the more engineer will be well-versed in reservoir *in-situ* conditions.

The nature of PTA in both oil and gas wells is somewhat similar – identification of flowing bottom hole pressure (FBHP). Nevertheless, when the well is flowing, it

opposes a significant challenge to adequately estimate FBHP from bottom-hole, that's the reason why it is measured from surface nowadays (Steward, 2010).

Various pressure responses can be achieved depending on the reservoir parameters. For instance, some of these responses are shown in Figure 1.1.

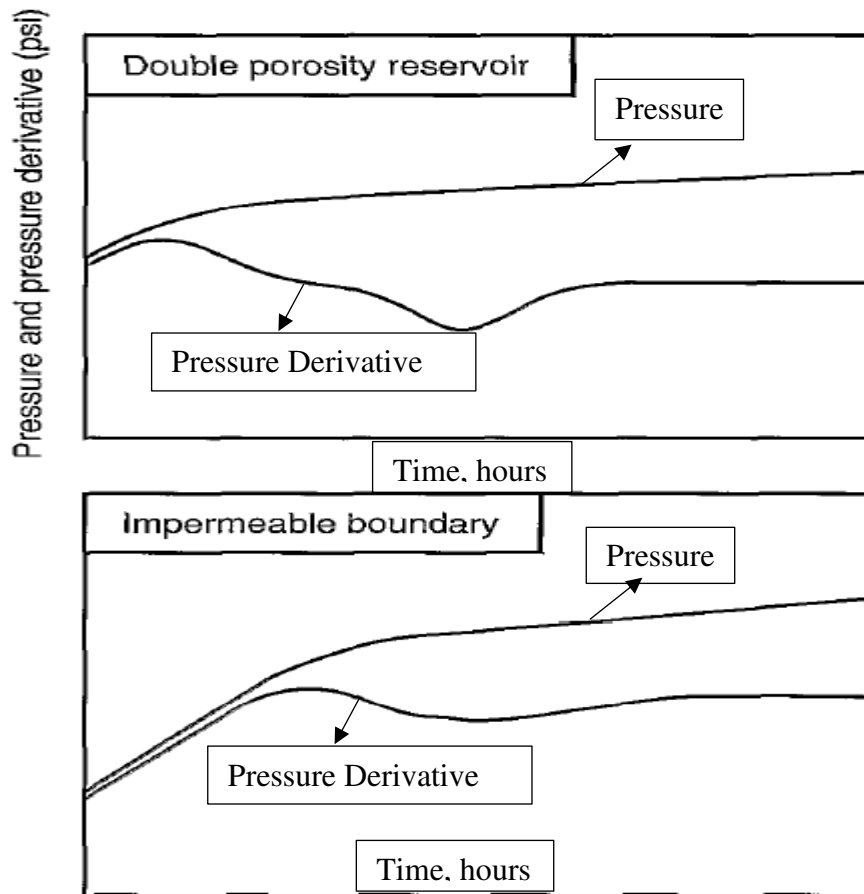


**Figure 2-1.** Characteristic Pressure Transient graphs yielding different reservoir characteristics (Schlumberger, 1994)

These plots are log-log graphs with pressure differential and its derivative. For instance, the top curve represents double-porosity reservoir, because derivative-pressure plot results in V-shaped curve. So, by carefully examining pressure-derivative curve, an engineer becomes informed about the fact that 2 different media (or layers) are involved in the flow process (Streltsova, 1984). One layer is responsible for delivering fluid to the well-bore, another one is recharging the preceding “productive” layer, if it's multi-layer reservoir. Naturally fractured reservoirs can also exhibit similar behaviour (Gringarten, 1972).

The bottom plot yields the information about impermeable boundary effect. Once the pressure transients have reached the boundary, it'll be reflected back and consequently the pressure derivative curve will rise upwards from theoretical straight trend line indicating the existence of boundary and its effect (Robert C., 1997).

It's clear from these 2 mere examples that the derivative curve alone can give a lot of valuable information about reservoir, making it the most effective tool. However, it's always used and interpreted together with the pressure change curve in order to quantify skin factor effects that can't be estimated by taking derivative curve alone into account.

Drawdown Test: The FBPH is recorded for interpretation. Theoretically, the well needs to be produced at a constant rate for the drawdown testing, but in reality it opposes huge challenge. That's the reason why sometimes the data can be noisy with less quality. The conclusions derived from drawdown testing may be misleading, and it needs to be validated with other well tests or with a 3D-dynamic reservoir model (Figure 2-1).

Build-up Test: As the well is closed, the FBHP gradually increases, and corresponding pressure response is used for the interpretation. In order to reach the stabilized production rate, the well needs to flow for a quite amount of time. However, in reality the stabilized production rate is difficult to achieve, in fact it can even fluctuate during the test. Therefore, build up tests predominates over drawdown testing from the quality of the data point of view.

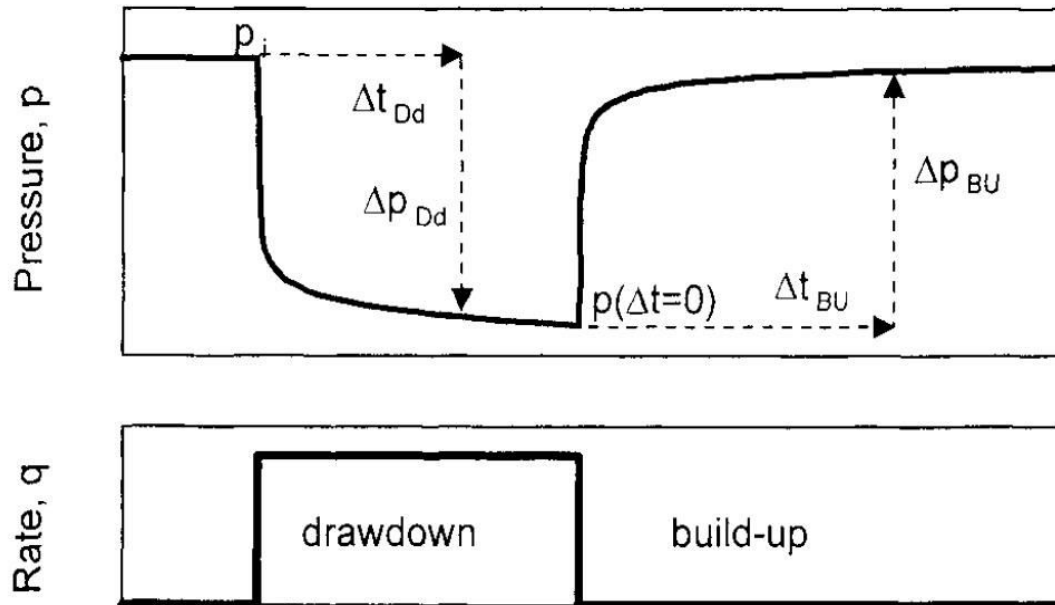


**Figure 2-2.** Drawdown and build-up well testing (Steward, 2011)

*Injection/fall-off test:* The nature of injection test is somewhat similar to build up tests, because in this test also the flowing bottom-hole pressure is measured after closing the well. But, with the difference that, this time some amount of fluid is injected to the reservoir to increase the FBHP, after shut-in this pressure decreases. The parameters of injected fluid is not compatible with the reservoir fluid properties, that's why it requires an additional careful approach for proper interpretation, and hence conclusions (Figure 2-3).

*Interference test/Pulse testing:* Interference tests are designed to assess the extent of the communication among wells. Special observation well is drilled away from the producers. Producer wells are flowing in a specific production rate, since then the observation well is shut-in, and its FBHP is accurately detected. In a pulse testing methods, producer well is flowing with a pair of short flow/shut-in repetitions, and then its pressure frequencies in the observation well are interpreted.

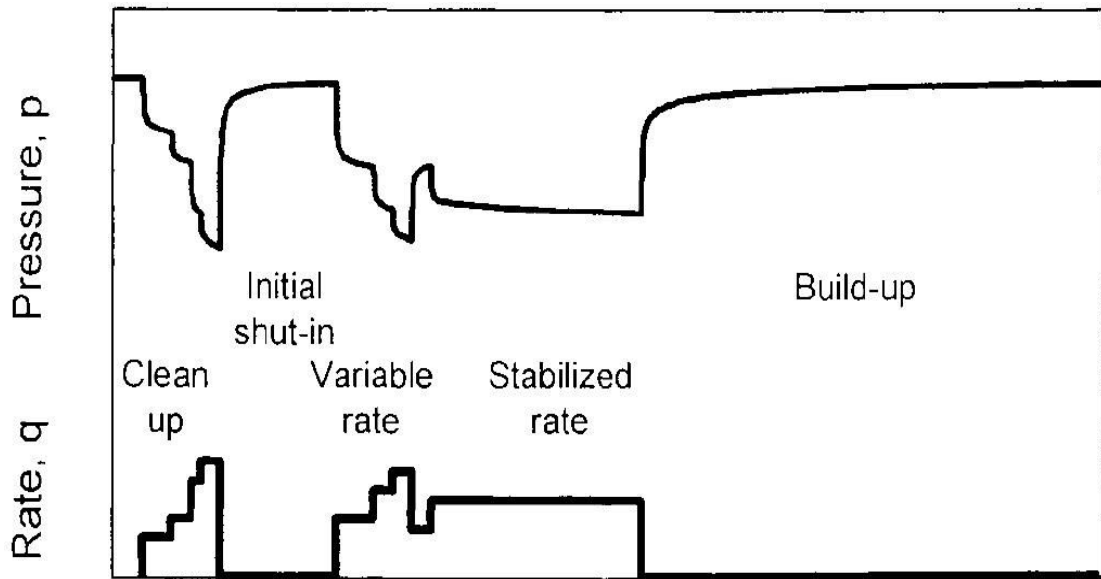


**Figure 2-3.** Common test sequence in oil wells (Schlumberger, 1994).

In this Figure 2-3, typical representative graph is depicted for an exploration oil well. Initially, the well is forced to produce in a step-rate fashion just to clean up the well when from the mud filtrate particles. This step-rate production continues until the surface production reservoir fluids are all from the reservoir. Since then, the well is closed to lower the downhole pressure, and well is brought to production that lasts for a quite amount of time. The orifice located within the choke is used to keep the flow rate in a normal value matching the best operational requirements. Throughout the whole main flow period, a number of choke diameters may be employed until stabilized, non-interrupting flowing conditions are acquired. After some production time, the well is closed for the final build-up analysis.

**Data to be introduced during well testing:**

Test data: Production flow rate combined with the corresponding flowing bottom-hole pressure as a function of time form the test data. Conclusion derived from results is entirely a function of the precision of the well test data. If the flow rate value is absent at the time when the well was producing, then it must be precisely calculated.

Well Data: Radius corresponding to the wellbore denoted as  $r_w$ , well geometry being whether inclined or horizontal, and depth of the well.

Reservoir and fluid properties: formation thickness denoted as  $h$ , porosity value  $\Phi$ , compressibility of oil and water depicted respectively  $c_o$  and  $c_w$ , water saturation  $S_w$ , oil viscosity  $\mu$ , and formation volume factor  $B_o$ . The total system compressibility can be calculated as following:

$$c_t = c_o * (1 - S_w) + c_w * S_w + c_f \quad (2-1)$$

In order to calculate the results, equation (2.1) is used along with the reservoir and fluid properties. If it's needed to validate the results after several interpretations, this first result may change or re-modified for the given theoretical interpretation model.

## 2.1 Well Testing Objectives

Reservoir characterization and interaction information between the well and the reservoir can be adequately acquired by well testing analysis. Because, well testing gives information about the dynamic response of the reservoir which can greatly improve the accuracy of the dynamic reservoir model (Matthew, 1975).

The data points that can be obtained from PTA can be encapsulated as following:

- To depict quantitatively produced petroleum products and to identify the nature of these produced oil and gas;
- Identification of (k\*h) product, the average relative permeability (k), and static reservoir pressure;
- Identification of the permeability damage around the wellbore as a result of drilling mud invasion, clay swelling, etc. and major skin constituents;
- To test the Productivity Index of wells;
- To get the overall information about heterogeneity distribution in an areal and vertical fashion;
- To validate the permeability barriers occurrence (faults, presence of discontinuity in flow units) in the reservoir;

- To identify the reservoir volume (Reservoir Limit Test);
- To validate any communication among producing/injecting wells (Interference Test).

The purpose of identification of these factors shown above should be accurately determined based on the expense and operational demands-conditions prior to carrying out the actual test.

The purposes of well test can actually vary based on the well type or phase of the reservoir management. It's for sure that well test is carried out in every stages of reservoir life. To summarize briefly, the following purposes can be stated on each phase depending on the life cycle of reservoirs:

- **Exploration and Appraisal Wells**

Exploration wells are the first wells that are drilled in order to prove the presence and feasibility of further reservoir management process from economic viability standpoint (Robert, 1997). In these wells, tests are conducted with an open-hole wireline tester for initial pressure estimation and for fluid collection purposes. Wireline tester is used to identify the initial reservoir pressure of all permeable layers. Formation fluid gradients and fluid contacts are identified from pressure versus depth plot.

A conventional DST is also important because the producer of the field needs to know whether the field is economic viable field or not. The purpose is to find out a production rate combined with the volume of the entire reservoir. If production rate appears to be low, the question arises whether it's due to low reservoir deliverability or high skin factor is involved. If high skin factor is the case, then the reservoir deliverability can be greatly improved by decreasing the skin factor through some acidizing work. But if the volume of hydrocarbons are not economical advantageous, then the field can lose its future perspectives, even high production rate is observed.

An essential objective for exploration well testing is the collection of formation fluid samples (Amanat, 2004). This is the best stage to characterize the reservoir fluids, because the reservoir has not been produced yet, the fluid compositional change has

not been observed. Since in later stages the fluid samples at the surface may not be the representative for the downhole fluids because of ongoing production operations (especially when there're two-phase situations in the reservoir).

Other ubiquitous purposes can be pointed out as the estimation of  $(k \cdot h)$  product and skin, as well as to test the well productivity. Apart from that, the discontinuity in flow units and the distribution of reservoir heterogeneity are also the targets for exploration well tests.

Once the presence of hydrocarbons are proven, appraisal wells are drilled in order to identify the extent of hydrocarbon accumulation, approximate estimation of reserves, and assessment of production rate to some extent. So, the geology of the reservoirs can be known by testing appraisal wells. Again, it will enable us to detect the PI rate, heterogeneity distribution, and occurrence of boundaries with the addition of drive mechanism, if possible.

- **Development Well Tests**

Once the phase has reached to Development stage, the objectives are quite different than those of exploration and appraisal stages. Most likely, reservoir deliverability has been analysed and reservoir fluid has been identified (Amanat, 2004).

Formation testing at this stage is essentially composed of using openhole wireline pressure testing. For the validation of fluid contacts and fluid density gradients, static reservoir pressure is on the emphasis. From this basis, various hydraulic compartments of the reservoir can be identified and introduced to the geological model. Sometimes, field production may already start while development well drilling proceeds. So, in these new wells, pressure gradients can also reflect the impact of production on the reservoir pressure. On those wells, the reservoir simulator can forecast vertical pressure profiles to be compared with wireline tester measurements. Any difference can be used to elaborate the geological model and inform about possible compartments to the dynamic model.

The main purpose of conventional testing on the new development wells is to estimate skin factor and to find out to what extent the formation is damaged. If no skin appears, the wells can be produced unimpeded, if skin factor appears to be high, firstly it must be removed prior to producing those wells.

Another reason for conducting formation testing on development wells is to prepare them for stimulation operations (Gordon, 1998). These operations can be inevitable later on to enhance the production. By these tests, fracture lengths and its hydraulic conductivity, financial risks can be assessed (Gringarten, 1972).

The producing life of a well needs to be procrastinated even further through modification of 3D-dynamic reservoir model, well workover operations, stimulation works such as to reduce the skin factor, etc. All of these purposes are also the target for development well testing.

Apart from that, communication between producer and observation wells can be also validated through interference well testing. So, well testing plays a significant role in development wells to make them more productive and advantageous.

- **Production and Injection well tests**

When it is the production phase, the objectives of well testing become the monitoring of reservoir, data collection to perform history matching of simulators, and productivity tests to judge the necessity for stimulation. Well tests are carried out to define the skin factor as a result of invasion of fines to well-bore region and to check the importance of acidizing work to decrease the skin.

The complexity of these tests is a function of the well condition and may range from a conventional build-up up to step-rate tests for determination of dynamic performance of multilayer systems.

## **2.2 Typical Flow Regimes**

Based on the nature of the pressure change with respect to time, there are 3 different flow regimes in a reservoir (Tarek, 2001).

- **Steady State**

During steady-state flow regime, the rate of pressure change with respect to time is zero, in other words the pressure is the same in every points of the reservoir. This constant pressure maintenance maybe a result of aquifer encroachment into the reservoir contributing the pressure maintenance or may be a result of water injection into the reservoir (Dake, 1972). This is the third flow behaviour that's encountered in the reservoir.

$$\frac{\partial p}{\partial t} = 0 \quad (2-2)$$

- **Pseudo Steady State**

Pseudo-steady state (PSS) flow happens during the late time region. This flow regime is applicable only when the outer boundaries of the reservoir are all no-flow boundary. That's why, this particular flow regime depicts a closed system response. Pressure differentials have reached to outer boundaries, and its effect starts to be noticed. This regime happens in late time region. The pressure changes linearly with respect to time with the constant rate value:

$$\frac{\partial p}{\partial t} = \text{constant} \quad (2-3)$$

- **Transient State**

Transient state sometimes referred as *unsteady-state flow* states that the rate of change of pressure as a function of time neither zero nor constant. This points out that the rate of pressure change w.r.t. time is dependent upon both position  $i$ , and time  $t$ . In this flow regime, pressure differential have not yet reached to the boundaries, so reservoir appears to be mathematically infinite. It also befalls during the middle time region (Figure 2.3).

$$\frac{\partial p}{\partial t} = f(i, t) \quad (2-4)$$

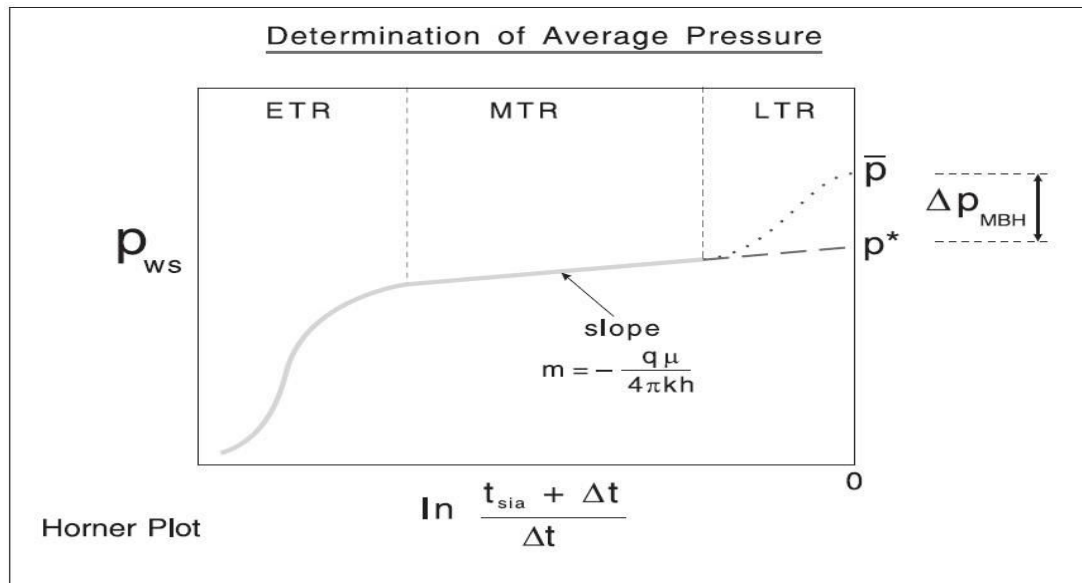


**Figure 2-4.** 3 flow regimes in a reservoir (Schlumberger, 1994).

### Wellbore Storage

When the well is brought to production after the shut-in, it's the hydrocarbons accumulation in the well-bore that contributes to the production observed in the surface rather than reservoir contribution. Because, when the well is closed in the surface, petroleum products will still migrate from reservoir towards wellbore (Steward, 2010). This effect is also named as *wellbore storage effect* in literature, and can continue from a few seconds to a few minutes. Once the wellbore contribution has ceased, the production in the surface is all a result of reservoir deliverability. After this stage, wellbore storage loses its efficiency, and the result can be used in PTA interpretation, since it describes reservoir behaviour. Starting from the time when the well is closed, the wellbore storage effect sometimes is referred as *afterflow*: After closing the well, reservoir still continues to deliver hydrocarbons to wellbore (Steward, 2010). This has an obvious effect on well test interpretation results in terms of wellbore pressure response, therefore it must be cautiously used in pressure transient analysis.

When the wellbore storage contribution predominates in the initial period of production time, the nature of pressure change with respect to time is calculated based on wellbore storage coefficient. When the well is filled with one single-phase fluid, wellbore storage coefficient is estimated on the basis of compressibility term:

$$C = - \frac{\Delta V}{\Delta P} = c_o * V_w \quad (2-5)$$

$c_o$ – liquid compressibility;  $V_w$  – wellbore volume in bbl.

## 2.3 Well Tests

### 2.3.1 DRAWDOWN TESTING

Pressure Drawdown test is just a sequence of bottom-hole pressure observations as a result of constant producing rate. In general, before the constant flowing rate, the well is closed for a sufficient amount of time in order to make the pressure prevailing in the reservoir to reach static reservoir pressure. The graph illustrating this phenomena is depicted by Figure 2-4.

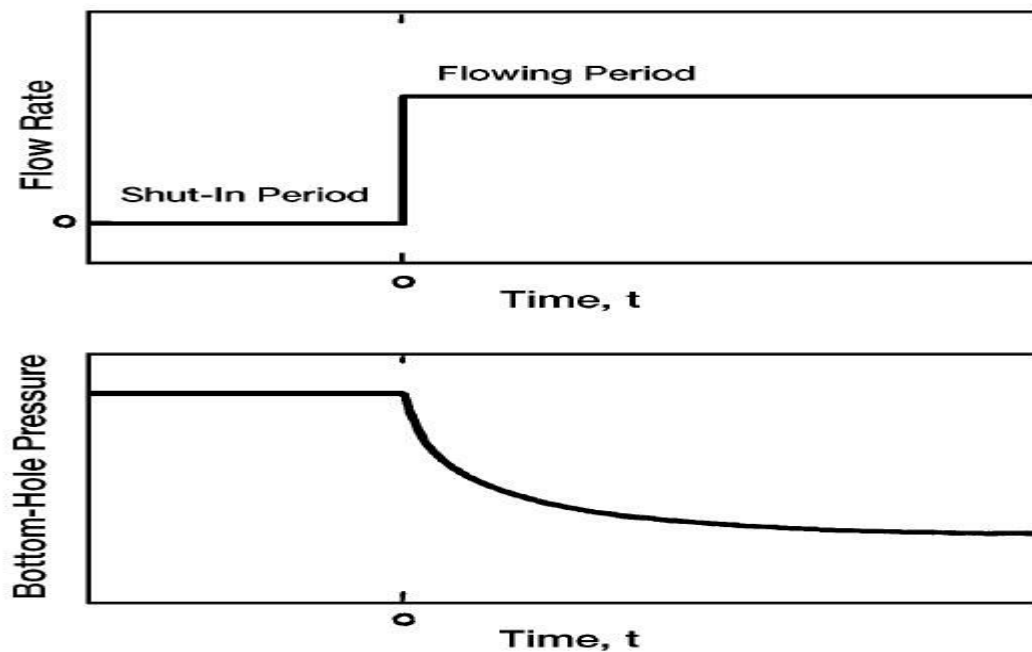


**Figure 2-5.** Drawdown Test (Tarek, 2001).

The key purpose for the implementation of drawdown testing is to estimate the  $(k \cdot h)$  product, and the degree of the damage around the wellbore as a result of drilling mud invasion, i.e. *skin factor*. Other targets can be exemplified as the estimation of hydrocarbon pore volume, and to identify the extent of reservoir heterogeneity.

Figure 2.1 adequately depicts the production and pressure variation when drawdown testing is performed. As it's already been noted above, generally the well is closed for a significant amount of time until it coincides with the static reservoir pressure.

However, sometimes it opposes another challenge, because not all of the reservoirs this accomplishment can be obtained. This initial shut-in to reach static reservoir pressure requirement can be met in a relatively new reservoirs. It's in general quite a big deal to get this condition met in old reservoirs. The drawdown testing is just observing the bottom-hole pressure during the constant production rate period. Despite of the fact that, the information acquired from the drawdown testing can also be reached through build-up, there's an economical inclination to perform drawdown testing, since the well is producing during the test. But naturally, there are also some challenges entrenched within this test. For instance, it's not easy to keep the well producing at the same production rate. Skin factor can also fluctuate throughout the production. One of the essential advantage of drawdown over build-up is the possibility of identification of hydrocarbon pore volume.

The bottom-hole pressure in an infinite acting reservoir can be calculated as following:

$$P_{wfD} = \frac{1}{2} * [lntD + 0.80908 + 2S] \quad (2-6)$$

Or to represent in terms of variables:

$$P_{wf} = P_i - \frac{q_s * B * \mu}{2\pi kh} * \frac{1}{2} \left[ \ln \frac{kt}{\phi \mu c_t r_w^2} + 0.80908 + 2S \right] \quad (2-7)$$

Logarithmic expression can also be shown as a sum of 2 logarithms as following:

$$P_{wf} = P_i - \frac{q_s * B * \mu}{2\pi kh} * \frac{1}{2} \left[ \ln t + \ln \frac{k}{\phi \mu c_t r_w^2} + 0.80908 + 2S \right] \quad (2-8)$$

In the equations written above initial reservoir pressure is denoted as  $P_i$ , hence  $t$  shows the *elapsed* time starting from production. So, theoretically if to plot a graph of flowing bottom-hole pressure versus natural logarithm of an elapsed time, this will yield a linear trend with the downwards direction. This kind of graph is called *semilog plot*. The slope of this line is denoted as  $m$ , the intercept of  $y$ , in our case bottom-hole pressure corresponds when  $\ln t$  equals to zero, when  $t = 1$  (Figure 2-5). Corresponding pressure value is often written as  $p_{t=1}$ . So, taking into account of these procedures, the equation is simplified as:

$$p_{t=1} = m \ln t + p_t \quad (2-9)$$

Where,

$$m = -\frac{q_s B \mu}{4\pi k h} \quad (2-10)$$

The intercept of this line with the y axis (bottom-hole pressure axis) corresponding to the value of pressure when t equals to 1 is:

$$p_{t=1} = p_i + m \left[ \ln t + \ln \frac{k}{\phi \mu c_t r_w^2} + 0.80908 + 2S \right] \quad (2-11)$$

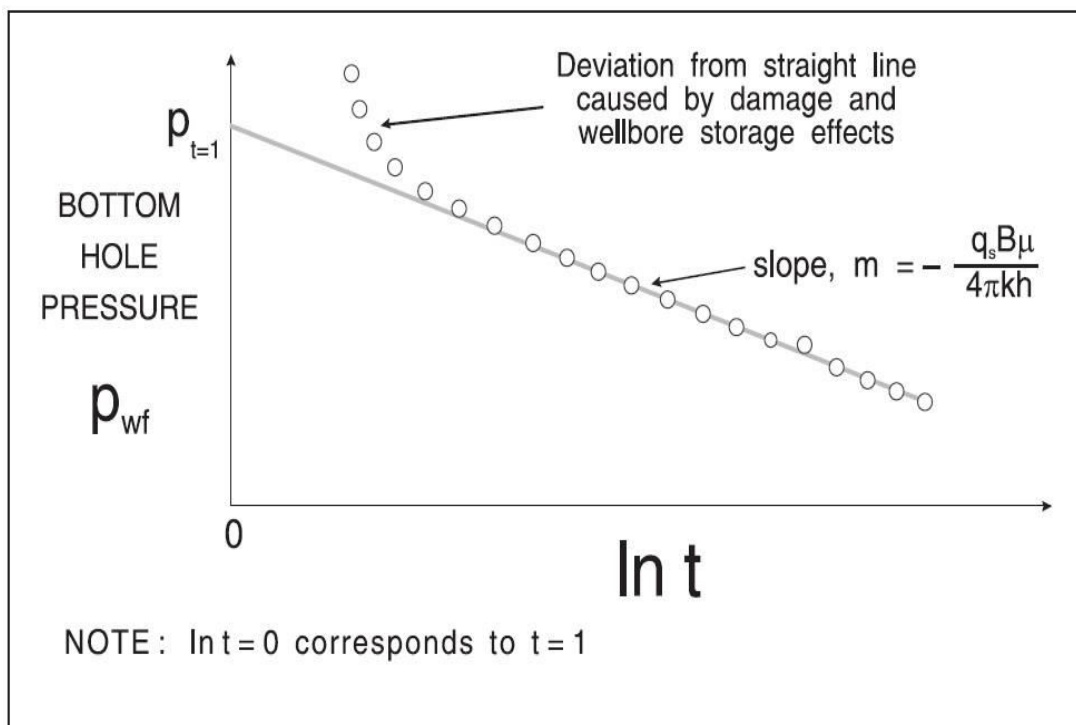


**Figure 2-6.** Drawdown semilog plot (Schlumberger, 1994).

From equation (2-5) it is apparent that if the slope - m is known, the permeability-thickness ( $k \cdot h$ ) can be determined. This approach of course necessitates the availability of accurate determination of well flow rate along with oil formation volume factor and viscosity (Dake, 1977). The last two factors can be accurately determined from fluid PVT tests. However, if the hydrocarbon bearing thickness of formation is available from log evaluation, k can be precisely identified. So, in order to adequately determine skin factor, equation (2-6) can be re-written as following:

$$s = \frac{1}{2} \left[ \frac{p_{t=1} - p_i}{m} - \ln \frac{k}{\phi \mu c_t r_w^2} - 0.80908 \right] \quad (2-12)$$

So, if initial reservoir pressure, total fluid compressibility, porosity, and well-bore radius are known, by virtue of slope (m) and  $p_{t=1}$  values, the damage around the

well-bore can be identified. As it can be deduced, the first term in brackets is negative.

As it can be observed, the initial data points are not set on the theoretical idealized line. Moreover, from theoretical point of view, early data points should fall below the linear portion of the semi-log plot as opposed to being located above from the line (Robert, 1997). This deviation happens due to the combined contribution of well-bore storage and damage effects. The theoretical model involves a flow rate change at the well-face when  $t$  equals to zero. Nevertheless, it is impractical to get the flow rate from zero to desired value in the sand-face despite of the fact that the surface rate can be abruptly changed to any value. This because of the fact the compressibility of the accumulated hydrocarbon around the well-bore will provide the initial production when the well is closed, and therefore the surface production rate should not be considered as the contribution from the reservoir. This phenomenon is called as *well-bore storage*.

The effect of well-bore storage is becoming more complicated due the occurrence of skin factor (Tarek, 2001). In theory, starting from the time when the well is opened, the flowing bottom-hole pressure should fall by the amount of  $\Delta P_s$ . However, because of the additional pressure drop associated with the skin factor, it becomes difficult to obtain initially presumed  $\Delta P_s$ . So, because of the joint combination of well-bore storage and skin factor, the initial data points fall above from the theoretical straight line. In order to adequately estimate the slope and intercept of the straight line, it's crucial to eliminate these two effects. Otherwise, the results may be misleading. For doing this, log-log plot is generated. After the well-bore storage and skin factor contribution have been avoided, the best way of identification of slope and intercept is using least-squares linear regression method.

But nowadays because of being consistent with oil-field units, these equations have undergone some changes. So re-writing these equations in oil-field units, the above equations will take the form as following:

$$m = -\frac{162.6 \times q_s \times B \times \mu}{k \times h} \text{ psi/log cycle} \quad (2-13)$$

$$P_{t=1} = P_i + \mu \left[ \log \frac{k}{\phi \mu c_t r_w^2} - 3.2275 + 0.86859s \right] \quad (2-14)$$

$$s = 1.1513 \left[ \frac{P_{t=1} - P_1}{\mu} - \log \frac{k}{\phi \mu c_t r_w^2} + 3.2275 \right] \quad (2-15)$$

Again from equation (2-10),  $P_{t=1}$  value must be referenced from the semi-log straight line. If the pressure value at  $t = 1$  hr is not on the straight line, then the line should be stretched up to the intersection point with the Y axis and corresponding intersection value should be used (Tarek, 2001). This technique is extremely crucial to use in order to avoid the incorrect value of skin through using wellbore storage pressure value from inclined curve deviated from the straight line.

If the duration of the drawdown test is long enough, the BHFP will depart from the infinite acting straight line and will reach to the Semi-steady-state flow regime.

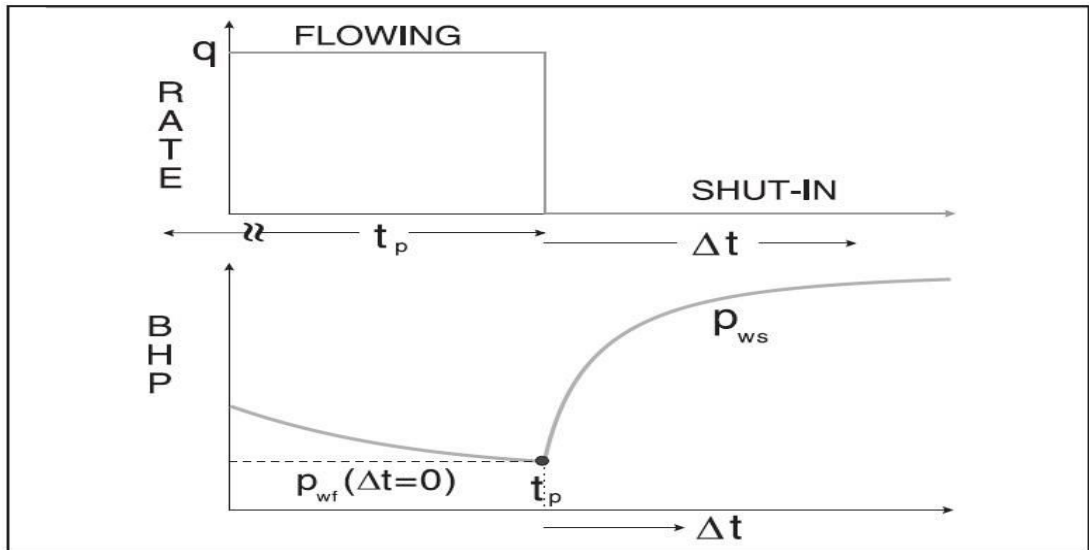
Despite of the fact that, the drawdown test may be quite informative in terms of identification of reservoir parameters, at the same time it poses a challenging task to the engineer to keep the production rate flat. The reason of this difficulty is due to the fact that it's flowing test. If a constant production rate can no longer be sustained, the technique used here is not valid, instead variable rate procedures are used.

### 2.3.2 BUILD-UP TESTING

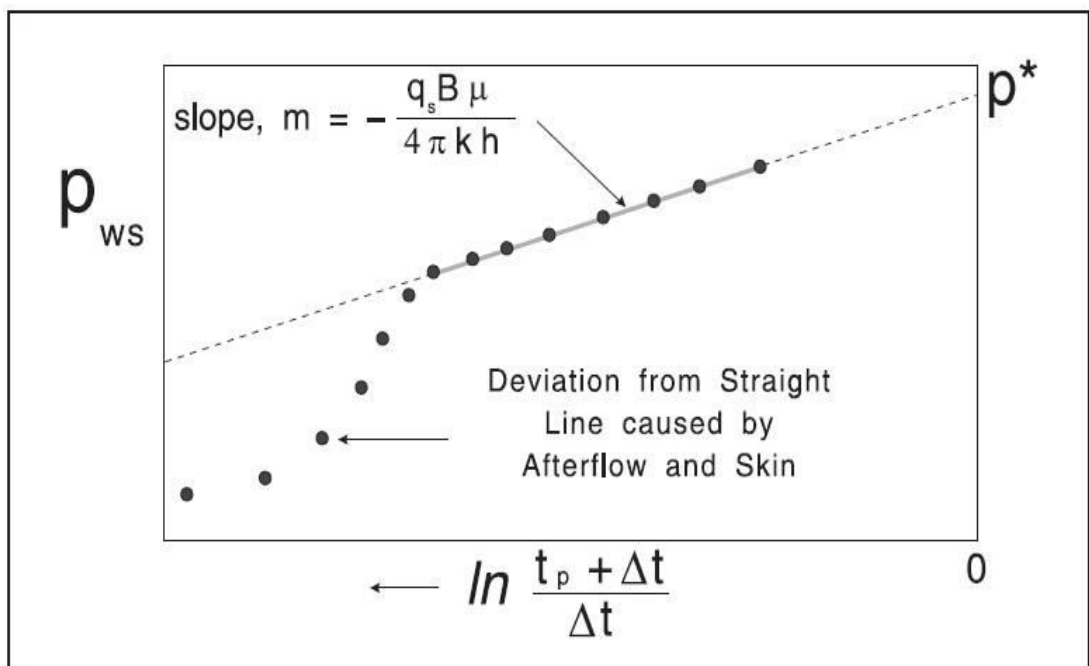
The most frequently employed method of transient well testing is build-up technique. Pressure build-up analysis involves shutting the well and measuring the corresponding bottom-hole pressure. But it's also crucial to have the constant production rate profile before closing the well. This can be procured either from the start of the production or after the continuous production profile from the well to initiate constant pressure variation (Streltsova, et. al., 1984). If the purpose is also measurement of skin factor, then recording the pressure value before the shut-in becomes necessary.

Figure 2-7 and 2-8 illustrate the production rate and bottom-hole pressure profile corresponding to the build-up test. In plots, production time is denoted as  $t_p$ , whereas the elapsed time from the shut-in is denoted as  $\Delta t$ . Prior to the shut-it the pressure is recorded, and once the well has been closed, the corresponding wellbore pressure is quantitatively identified in order to get the reservoir parameter values and wellbore condition.

As in all transient well testing, prior to embarking on an interpretation, all the choke size, tubing with casing sizes, well penetration depth and all other information need to be measured accurately, since these measurements have a huge impact over the interpretation method (Tarek, 2001). Well stabilization at a constant rate is also essential, otherwise using conventional techniques to interpret the test may lead devilishly erroneous result.



**Figure 2-7.** Flow-rate and pressure behaviour for an ideal buildup (Schlumberger, 1994).



**Figure 2-8.** Horner Plot for a buildup (Schlumberger, 1994).

Several techniques are available for the interpretation of the build-up test, but in most cases Horner plot is widely employed method. This method presupposes that the reservoir is infinite in extent and very limited amount of hydrocarbons have been extracted from the well during the production profile prior to shut-in of the well (Dake, 1977). During an infinite-acting period, the pressure profile can be pointed out as follows:

$$p_{ws(\Delta t)} = p_i - \frac{q_s B \mu}{2\pi k h} \times \frac{1}{2} (\ln(t_p + \Delta t_D) - \ln \Delta t_D) \quad (2-16)$$

or

$$p_{ws(\Delta t)} = p_i - \frac{q_s B \mu}{2\pi k h} \ln \frac{t_p + \Delta t}{\Delta t} \quad (2-17)$$

This is the Horner plot in which a linear correlation is described between  $p_{ws}$  and  $\ln((t_p + \Delta t)/\Delta t)$ . This equation also implies that closed-in bottom-hole pressure can reach the initial reservoir pressure –  $p_i$ .

$$p_{ws} = m * \ln \frac{t_p + \Delta t}{\Delta t} + p^* \quad (2-18)$$

With slope

$$m = - \frac{q_s B \mu}{4\pi k h} \quad (2-19)$$

And intercept

$$p^* = p_i \quad (2-20)$$

For (2-20) equality, logarithmic expression must be set to zero. In other words,  $((t_p + \Delta t)/\Delta t)$  needs to equal to unity. But for this,  $\Delta t \gg t_p$ . This equality implies that closure time of a well must be very long in comparison with the production time.

From equation (2-19) permeability can be defined as follows:

$$k = - \frac{q_s B \mu}{4\pi m h} \quad (2-21)$$

With the condition that all of the factors on the right side is accurately determined. Applying oil-field units, equation (2-17) will take the following form:

$$p_{ws(\Delta t)} = p_i - \frac{70.6 q_s B \mu}{k h} \ln \frac{t_p + \Delta t}{\Delta t} \quad (2-22)$$

Or

$$p_{ws(\Delta t)} = p_i - \frac{162.6q_s B \mu}{kh} \log \frac{t_p + \Delta t}{\Delta t} \quad (2-23)$$

One of the most helpful aspect of using semilog plot is that it enables to measure the (k\*h) product through the slope of the build-up (Ronald, 1990). This value is much more accurate and reliable value in comparison with the permeability value derived from core measurements from the entire range of producing interval.

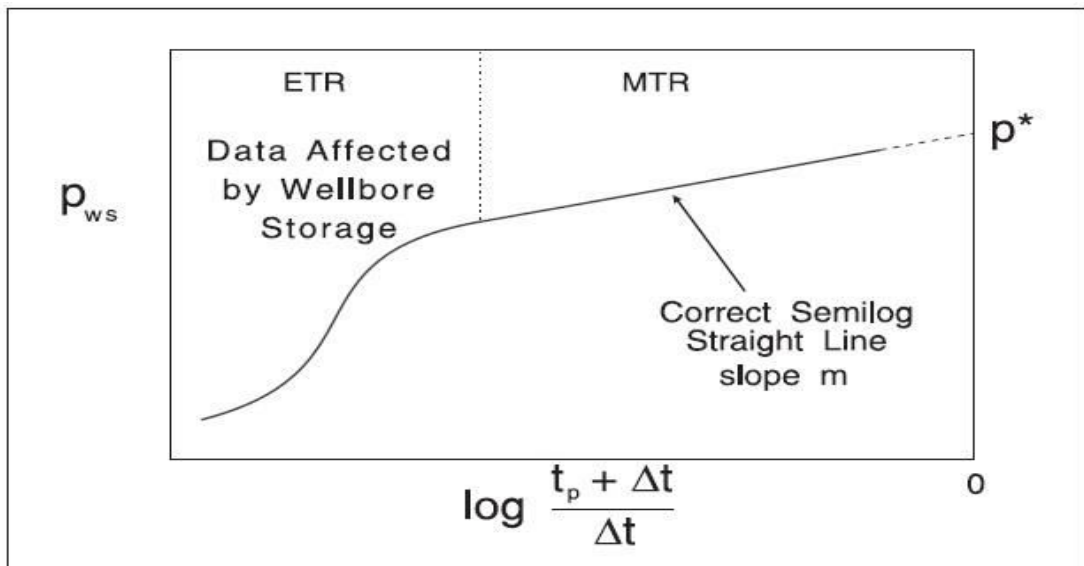


**Figure 2-9.** Impact of wellbore storage on a build-up (Schlumberger, 1994).

Figure 2-8 illustrates the concept of after production. It means that, right after the constant production rate when the well is shut-in, the wellbore pressure increase necessitates the influx of hydrocarbons from formation into the wellbore and compressing its existing contents. But due to insufficient pressure at the wellhead, it can't flow from the wellbore to the well-head. Figure 2-8 describes that the pressure values are located below from theoretical straight line in which wellbore storage contribution is important.

The most frequently employed technique for the interpretation of the build-up data in an infinite acting reservoir is the Horner plot in which closed-in bottom-hole pressure is plotted against  $\ln((t_p + \Delta t)/ \Delta t)$  (Tarek, 2001). It's worth to emphasize that this "infinite-acting" behaviour is referred to both before and after shut-in. It's also worth to highlight that that this graph should be plotted on a normal paper:

Bottom-hole pressure as an ordinate, logarithmic expression as an abscissa. The pressure data points influenced by the well-bore storage are eradicated from the interpretation. This technique gives a slope value, i.e.,  $m$ , and the intercept of  $p^*$ .

Permeability-thickness product,  $(kh)$  is computed as usual from the straight line in the graph using the following formula:

$$kh = -\frac{q_s B \mu}{4\pi m} \quad (2-24)$$

Applying oil-field units, equation (2-24) becomes as following:

$$kh = -\frac{70.6 q_s B \mu}{4m} \quad (\text{natural log}) \quad (2-25)$$

$$kh = -\frac{162.6 q_s B \mu}{m} \quad (\text{log base 10}) \quad (2-26)$$

And for the correct estimation of average permeability value, the net zone thickness must be adequately known.

Using only build-up data does not yield and skin related well-bore damage, since only pressure values prior to shut-in are influenced by the skin. The flowing pressure in an infinite-acting reservoirs before the shut-in is described as following:

$$p_{wf}(\Delta t=0) = p_i - \frac{q_s B \mu}{4\pi kh} \left( \ln \frac{kt_p}{\phi \mu c_t r_w^2} + 0.80908 + 2s \right) \quad (2-27)$$

In which the initial pressure value replacement- $p_i$  by the extrapolated pressure value- $p^*$  is valid for the infinite-acting reservoirs. So, re-writing equation (2-27) by using extrapolated pressure value, the following equation is derived:

$$p_{wf}(\Delta t=0) = p^* + m \left( \ln \frac{kt_p}{\phi \mu c_t r_w^2} + 0.80908 + 2s \right) \quad (2-28)$$

In which  $-\frac{q_s B \mu}{4\pi kh}$  is replaced by the slope of a straight line,  $m$ . Skin factor can be estimated from the equation (2-28) as described below:

$$s = \frac{1}{2} \left( \frac{p_{wf}(\Delta t=0) - p^*}{m} - \ln \frac{kt_p}{\phi \mu c_t r_w^2} - 0.80908 \right) \quad (2-29)$$

Where the slope value is negative. To modify equation (2-29) by using oil-field units, the following equations are derived:

(a) By using natural log:

$$s = \frac{1}{2} \left( \frac{p_{wf}(\Delta t=0) - p^*}{m} - \ln \frac{kt_p}{\phi \mu c_t r_w^2} + 7.43173 \right) \quad (2-30)$$

Where,

$$m = -\frac{70.6q_s B \mu}{kh} \quad (2-31)$$

and (b) log based 10

$$s = 1.153 \left[ \frac{p_{wf}(\Delta t=0) - p^*}{m} - \log_{10} \frac{kt_p}{\phi \mu c_t r_w^2} + 3.2275 \right] \quad (2-32)$$

Where,

$$m = -\frac{162.6q_s B \mu}{kh} \quad (2-33)$$

When relatively few data points are available, extrapolating the line too far to get  $p^*$  may not be so accurate. However, it's possible to determine the pressure just one hour after shut-in. Shut-in pressure is simply described as:

$$p_{ws} = p^* + m \log \frac{t_p + \Delta t}{\Delta t} \quad (2-34)$$

And so,

$$p_{wf}(\Delta t=0) = p_{1hr} = p^* + m \log(t_p + 1) \quad (2-35)$$

From which,

$$p^* = p_{1hr} - m \log(t_p + 1) \quad (2-36)$$

Substituting equation (2-36) of one hour after shut in pressure into equation (2-32) will yield:

$$s = 1.153 \left( \frac{p_{wf}(\Delta t=0) - p_{1hr}}{m} + \log \frac{t_p + 1}{t_p} - \log \frac{k}{\phi \mu c_t r_w^2} + 3.2275 \right) \quad (2-37)$$

In which the logarithmic expression being  $(\log \frac{t_p + 1}{t_p})$  is quite small, that's why not considered. This skin factor equation is frequently encountered in literature, and the subsequent plot for the determination of  $p_{1hr}$  is illustrated as following:

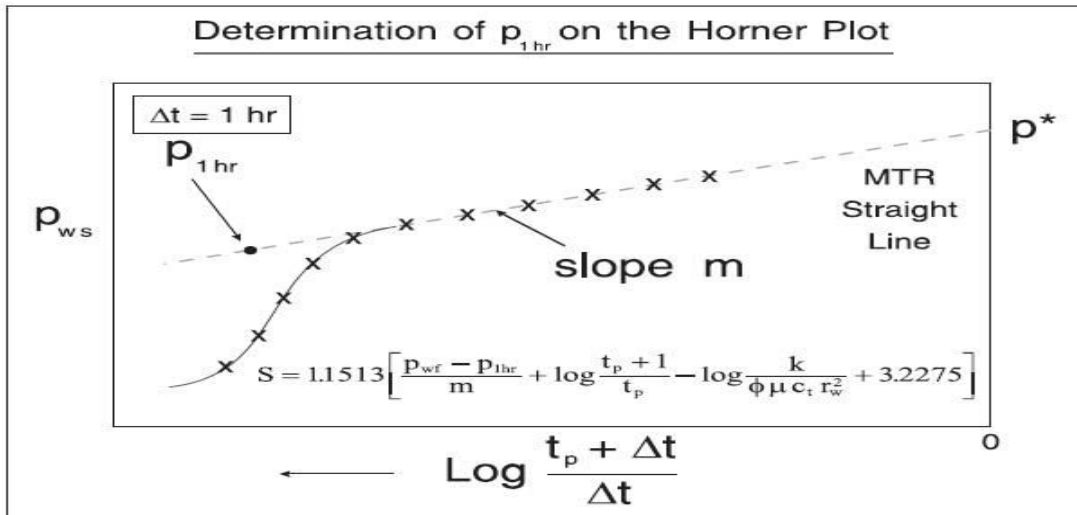


**Figure 2-10.** Procedure for determination the Middle Time Region pressure at 1 hour (Schlumberger, 1994).

### 2.3.3 INTERFERENCE TESTS

When flow rate is deliberately altered in one well and its impact is measured in other wells, this type of well test is called multiple-well tests (Streltsova, et. al., 1984). For instance, interference and pulse tests can be shown as an example for these tests. Multiple well tests are conducted in order to find out the communication between 2 points or wells located in the same reservoir. If there's communication, vertical formation permeability-thickness and porosity-compressibility product can also be estimated by these tests. Interference tests are carried out to by injecting or producing from one well and defining the pressure responds in another well. The active well – that's producing at some uniform pressure at zero time and the corresponding pressure response is recorded in another observation well located in  $r$  distance from active well after some time tag (Figure 2-11).

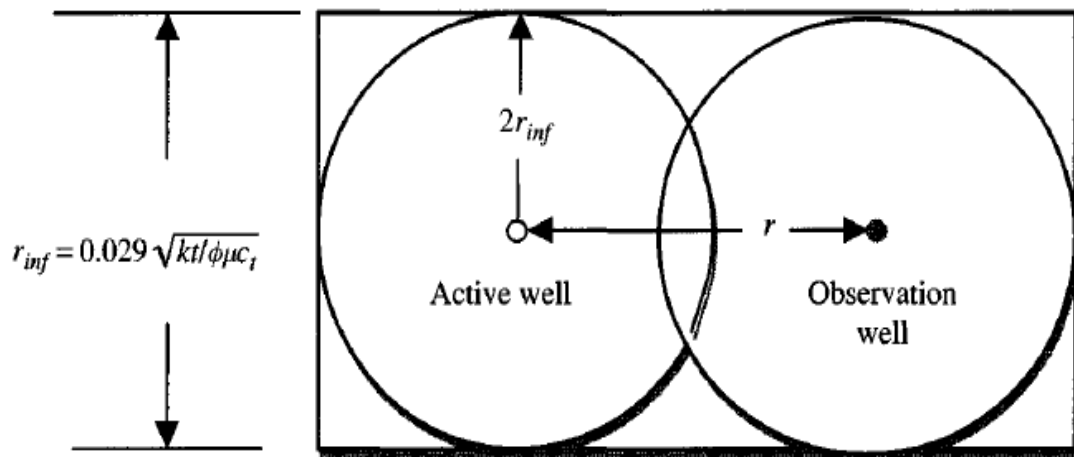


**Figure 2-11.** Influence region for interference or pulse testing, (Chaudhry, 2004).

In homogenous anisotropic reservoirs adequately designed multiple-well tests can yield information about permeability variation through major and minor axes, orientation of these axes, and the value of  $(\Phi\mu c)$  product. Multi-layered reservoirs also exhibit similar responses to multiple-well tests.

When dealing with naturally fractured reservoirs, the orientation of fractures and the ratio of porosity-compressibility product of fracture to matrix can also be identified by multiple-well testing. It was found that multiple-well tests are more sensitive to reservoir heterogeneity than single-well tests. That's why for the accurate reservoir heterogeneity description the use of multiple-well tests are more encouraged.

#### 2.3.4 PULSE TESTING

Pulse tests will yield the same information acquired from interference tests. But there are some advantages of pulse tests over interference tests such as the time required for these tests are less resulting in normal disruptions to ongoing operations, and less complex interpretation is involved because of random noise in reservoir pressure.

The test is performed by sending pressure transients to observation well by producing or injecting for some time, and then shutting it in. This sequence is repeated for some time in a regular fashion to get different pulses. Corresponding pressure responses which are quite small are recorded in observation well with very sensitive pressure gauges. These gauges were utilized for the first time to detect very small changes in pressure profile (Figure 2-12).

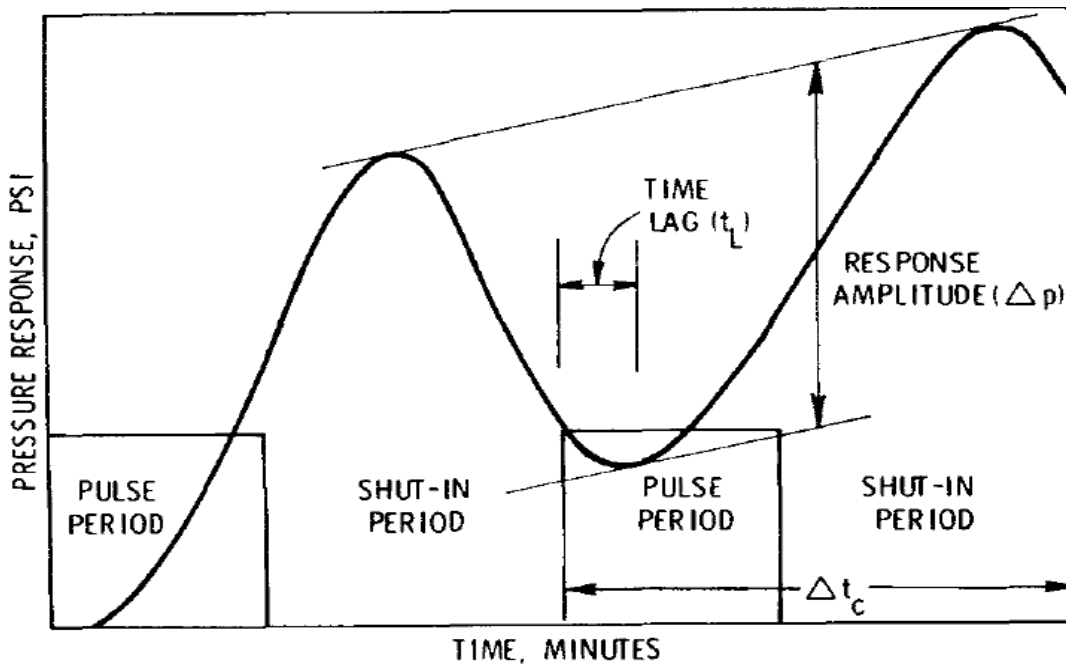


**Figure 2-12.** Pulse Test methodology (SPE, 1983).

The parallel lines drawn in above graph helps to cancel any unknown linear trends, and hence contributes the correct estimation of  $kh/\mu$  and  $\Phi c_t \mu$ . This method is called tangent method and it appears to be one of the best advantages of pulse tests over interference tests (Robert, 1997).

## **CHAPTER 3**

### **WELL TEST DESIGN**

As described before, well test is carried out in order to get reservoir parameters value through which dynamic reservoir performance can be adequately described. For the accomplishment of this, the test needs to be properly designed. Inappropriate design can lead to erroneous results and all of the efforts, money and time would go haywire (Steward, 2010).

Well test consideration is centred on answering the several questions such as which variable is the highest priority to be known firstly, what kind of transient test is more appropriate for the particular case, flow rate determination as well as how long the test should last. Some of these operational variables are under engineer's control (Steward, 2010). These are flow rate determination, and the test period duration.

In general, well test design starts from the specification of the objectives for the well testing. Based on these objectives, proper well test type is selected for the satisfaction of demands. Well test purposes can be different in each case. It can span from correct identification of transmissibility, well productivity assessment up to the boundary distance from the well as well as its location. But, by and large, in petroleum engineering the most frequently employed well test techniques are build-up and fall-off for producing and injecting the wells accordingly. Drawdown testing is also widespread well test type to carry out. These well tests are usually performed to assess the wellbore storage effect, to judge skin effect and perform further acidizing if necessary to reduce it as well as to find out permeability value combined with transmissibility. Apart from that, faults, pinchouts or other geologic elements, and average reservoir pressure can also be determined through these tests.

Less frequently employed well tests are pulse or interference tests to find out the communication of two or more points in the same reservoir to assess whether geologic barrier or other features are present or not.

Once the well is drilled, its productivity is assessed by drillstem testing. However, repeated formation tester (RFT) can also help to adequately describe the well productivity by interpretation of reservoir characteristics.

### 3.1 Variable Dependency

In designing the well test, 2 crucial factors need to be taken into account: (a) Will the reservoir parameter to be identified from well test have an impact on the well pressure, if so, can these effects be identified by available tools, and investigate the possible response, and (b) will the test duration be long enough for this response to be observed and noticed (Streltsova, et al., 1984).

It's apparent that, different sections of pressure behaviour start and terminate at some certain time period.

For instance, wellbore storage influence terminates at:

$$t_D = C_D(0.041 + 0.02s) \quad (3-1)$$

Beginning point of semi-log straight line is:

$$t_D = C_D(60 + 3.5s) \quad (3-2)$$

Final point of semi-log straight line (secondary porosity) for the double porosity reservoir:

$$t_D = \frac{\omega(1-\omega)}{6.6\lambda} \quad (3-3)$$

Termination of double porosity transition:

$$t_D = \frac{1.2(1-\omega)}{\lambda} \quad (3-4)$$

End of infinite-extent reservoir behaviour is a function of both reservoir shape and boundary configuration. However, for circular bounded reservoir:

$$t_{DA} = 0.1 \quad (3-5)$$

Like infinite-acting reservoirs, starting point of pseudo-steady state type behaviour is also a function of reservoir shape and boundary configuration. Again the corresponding equation pertains to circular bounded reservoir:

$$t_{DA} = 0.1 \quad (3-6)$$

The essential point about start and end times is that, they can also be pointed out in terms of dimensionless time being  $t_D$  or  $t_{DA}$ . The transition time is not dependent upon the flow rate, this time is affected by mobility  $k/\mu$ , storativity  $\Phi c_t h$ , and transmissivity  $kh$  factors. So, for the given reservoir transition time will occur at a specific time irrespective of the flow rate.

The pressure behaviour in an infinite-acting reservoir can best be shown as:

$$p_{wf} = p_i - 162.6 \frac{qB\mu}{kh} \left[ \log t + \log \frac{k}{\Phi c_t \mu r_w^2} + 0.8686s - 3.2274 \right] \quad (3-7)$$

It's obvious from the equation that, pressure drop around the wellbore is mostly a function of  $qB\mu/kh$ . So, based on the above expression, it can be deduced that pressure drop is directly dependent on the flow rate. On the other hand, storativity  $\Phi c_t h$  will have an indirect impact on the pressure change. This speculates the fact that reservoirs having higher storativity will exhibit the same (or quite close) pressure drop compared with other reservoirs with low storativity. Nevertheless, the time scale attached to the pressure drop will be quite different.

### 3.2. Test Duration

The overall test duration should be sufficient enough to make sure that effective reservoir response has been obtained and proper interpretations can be made. But sometimes this may pose some practical and economical challenges for the flow period to be proceeded long enough for proper interpretations. For instance in build-up testing production loss can be a severe constraint or in drawdown testing the engineer may not be able to sustain a constant rate flow of fluid (Lee, 1997). These are some of the common issues that may counteract long duration of tests. However, the analyst is expected to be able to track down 3 flow regimes in the reservoir. These are early, middle, and late times. In practise, well tests can last from a few hours to a few days depending on the formation parameters. For example a formation

with very low permeability necessitates a relatively long transient test duration so that an engineer can track and interpret late time region (Lee, 1997). For instance, if one needs the whole log cycle of infinite-acting reservoir, then the test needs to be continued for a time of at least:

$$t_D \geq 10 \times C_D(60 + 3.5s) \quad (3-8)$$

For correct estimation of drainage radius of a well, one needs the well to flow for a sufficient amount of time in pseudo-steady state regime. If to make such an assumption that the drainage radius is circular in shape, then:

$$t_{DA} \geq 1 \quad (3-9)$$

Another key parameter concerning the test duration is acknowledging the fact that sometimes reservoir pressure response can be masked by a less diagnostic effect. For instance, if reservoir is quite small with a large wellbore storage effect, the pressure distribution profile can be shifted from wellbore storage effect (for example due to liquid level reduction in annulus) to directly pseudo-steady state. It could be valid if the following condition is satisfied:

$$C_D(60 + 3.5s) \geq 0.1 \frac{A}{r_w^2} \quad (3-10)$$

Estimation of permeability and skin factor through well test interpretation in this reservoirs become quite challenging, especially if wellbore storage coefficient outstrips this value:

$$C_D \geq \frac{A}{r_w^2} \frac{0.1}{(60+3.5s)} \quad (3-11)$$

In real units, the wellbore storage coefficient  $C$  measured in STB/psi units, should be less than:

$$C \leq \frac{2\pi\Phi c_t h A}{5.615} \frac{0.1}{(60+3.5s)} \quad (3-12)$$

If the wellbore storage appears to surpass this value, it becomes waste of time to operate well test in this type of reservoirs with one exception that the wellbore storage is diminished or overcome by some techniques.

Similar approach can also be introduced to double-porosity reservoirs to check the wellbore storage effect and to assess the likelihood of operating well test. Thus, if the following condition is met, then there's no need to conduct well test:

$$C_D(60 + 3.5S) \geq \frac{\omega(1-\omega)}{6.6\lambda} \quad (3-13)$$

Testing of horizontal wells necessitates quite long time for the radial flow to be established. But this might not be technically possible due to excessive production lost.

### **3.3. Flow Rate Consideration**

As have already been discussed previously, the amount of pressure drop encountered around the well-bore is a function of the production rate that the well is flowing.

The rate should be elected as optimally as possible to prevent the gas coming out of the solution. So, it's crucial to take into account of production rate in terms of deciding whether this rate can yield sufficient amount of pressure response from the reservoir to acquire the required reservoir data or not (Kamal, 1992). Giving the fact that pressure change depends upon the reservoir permeability, fluid viscosity and acknowledging the fact that it's also common to observe measurement noises due to the instrument used, there's no exact set of equations to assess whether that particular production rate is enough for reservoir parameter estimation (Robert , 1997).

By and large, design of well test focuses on the answer of the question as how long the major flow should proceed for constant production rate (in build-up for instance) and for reservoir parameter identification. For example, in offshore environment where rig time expenditure is a crucial point, there's an obvious inclination to reduce the flow time. The major decision is based on the analysis between the cost and value of acquired additional data obtained from extension of flow time. The duration of final build-up should last 1 ½ times more than previous flow time (George S., 2010).

The case for exploration (or appraisal) well test is not the same, in fact the decision of flow-rate is dependent upon several key parameters. Concerning the oil well, the important factor to be considered is the capacity of the separators. However, for gas wells the key parameter is the flare system. For the reservoirs with very low

permeability value, the flow rate choice is a function of reservoir deliverability. In some cases it becomes technically impossible to operate any transient well tests, because no constant production rate can be maintained. In general, it's also important to take an advantage of production engineers' nodal analysis in which flow behaviour is simulated through some modifications on tubing size, choke size etc.

### **3.4 Computer Aided Well Test Interpretation**

As it's already been mentioned before that transient pressure tests have become an indispensable technique for dynamic reservoir performance identification and reservoir parameters' estimation. The analytic methods described above require some severe restrictions (Ronald, 1990). For example, constant oil/gas property throughout the production, single phase, homogeneous isotropic property which implies that permeability, porosity and thickness remain fixed in all directions and so on. However, in reality, such kind of reservoirs are rare. In these cases, analytic methods described above can't be used and instead numerical solutions can yield the required solution with a high accuracy.

The use of numerical models to differentiate the physical effects, such as skin factor and other complex heterogeneities have become quite useful tool over the last years. The level of accuracy of complex geologic features description are usually either non-satisfactory or unavailable to rely on. Numerical solutions use finite difference grids to discern various complex features in a reservoir.

Grids through Cartesian co-ordinate system are generally more common but also provide some drawbacks such as inflexibility for representation of faults, pinch-outs, compartments, well locations as well as it may exhibit errors generated from grid orientation effects (Palagi, 1992). To fix these issues several solutions have been provided such as local grid refinement, nine-point and etc (Gordon, 1998). However, with the advent of applicability of Voronoi gridding or PEBI (Perpendicular Bisection) engineers have become more confident in their models from flexibility and accuracy point of view (Robert, 1997). This can be accomplished only through numerical grid generation. It's interpreted as the space that is closer to its grid points in comparison with other points.

Accurate well test analysis depends on the preciseness of the match between actual reservoir performance and the chosen reservoir and boundary models with the description of any geological features (Perrine, 1994). Therefore the first step in computer-aided interpretation is selecting the correct mathematical model. This stage is often called *model recognition*. Model recognition can be accurately selected by using both graphical Horner analysis and computer-aided methods. In conventional analytical methods the reservoir model can be picked through interpreting its responses in log-log or Horner Plot. Nowadays as the latest graphical analysis, *pressure-derivative* curves are used especially due to its informative nature about skin factor, boundaries effect, flow pattern, permeability-thickness product and so on. However, even use of pressure-derivative curves is somewhat limited, because it requires step change rate from constant flow rate to another stabilized rate. In practise it's rarely possible to shift from one constant rate to another, so it necessitates to modify the variable-rate pressure data into constant-rate pressure data which is called *deconvolution*.

So, once the compatible reservoir model has been approved, the sought reservoir parameters can be estimated through matching the actual and model performances. In a conventional testing, this can be succeeded by matching either a portion of the response or by matching the whole response. However, thanks to advancements in computer technologies, now it can be performed by taking an advantage from *non-linear* regression. It also should be emphasized that just like type-curve matching a whole set of response can be matched. But its preference over type-curve matching is eliminating the necessity of having step change rate between stabilized flow rates.

Another advantage in using non-linear regression is that it's capable of calculating *confidence intervals* for the model outputs. This interval is quite useful in terms of judging how precise the model estimations are based on quantitative estimates and also discerns both strengths and inaccuracies in the interpretation process.

The advantages of using the analytical method over the numerical method is that, in analytical methods no complex interpretations and/or analysis are involved and the time scale attached to interpretation is considerably less (Robert, 1997). However, as described above there are some drawbacks concerned with the use of analytical methods. Because, analytical methods assume homogeneous and isotropic reservoirs

with simplified and ideal shapes, and simple fluid flow patterns. Nowadays with the advent of technological advancements in drilling and completion makes it feasible to drill slanted wells with complex completion techniques with individual skin effects, especially in multi-layered tight reservoirs in which horizontal well drilling and completion allow various perforations to lead oil/gas to wellbore from reservoir from different layers. In such cases use of analytical methods alone can yield considerably misleading results to engineer. However, it's still believed that even in complex reservoirs analytical methods can guide the numerical simulations when both of them are used to generate valuable results.

### **3.5 Optimization of Well Test Design and Steps for Workflow**

Full Field Development Plan and production strategy are defined based on reservoir parameters and geologic description of formation (Kumar et al., 2010). This information can be best acquired from the field data collected during exploration and appraisal phases. The key factors that define the well and reservoir deliverability are permeability-thickness factor, fluid properties and reservoir extent (Kumar et al., 2010). To acquire the information about these parameters flow tests along with the fluid analysis and fluid samples are employed. Flow tests that are often times employed by engineers are Wireline Formation Tester and Drill Stem Tests depending upon the scale of flow tests.

Experience with the applicability of DST's has exhibited the fact that optimal value is often not acquired (Kumar et al., 2010). Examples of DST's application with suboptimal values to formations can be exemplified as following:

- Only water is produced or oil production is accompanied with the large amount of water cut from existing aquifer;
- Because of low bottom-hole pressure or other technical well-related problems fluid flow to surface ceases;
- Lower production rate of fluid preventing clean-up procedure of the formation;
- Reservoir Limit Tests with limited radius of investigation (Kumar et al., 2010).

The results of DST's can be properly forecasted based on initial estimation of reservoir pressure, fluid properties and permeability by using WFT together with the

usage of software package. These simulations can yield informative description to engineers which zone is more affected and requires clean-up or other workover operations. In formations where the production rate is not so desirable, as an alternative solution commingled layer testing may be performed.

During the conventional DST procedure, the zone of interest to be tested is isolated with a packer and fluid flow from the reservoir to surface through well-bore is initiated. Having reached the surface, oil, water, and gas are separated and individual flow rates are recorded with different level of preciseness.

In general well testing objectives can be best classified as the evaluation the need for workover operations through skin factor identification, permeability-thickness product, reservoir boundaries and fluid properties (Elshahawi, 2008). Initial reservoir pressure is also the target for well testing objectives. To meet the aforementioned objectives some sort of optimization and planning are required.

Permeability and skin factor can be directly acquired by using permeability-thickness product from the precise identification of Infinitely Acting Radial Flow (Kumar et al., 2010). There should not be any additional pressure disturbances that can disguise this zone.

It's crucial to maintain the bottom hole flowing pressure higher than saturation pressure so that representative fluid samples can be obtained and investigated (Kumar et al., 2010). This necessitates the knowledge of hydrocarbon phase behaviour. In order to be able to get the representative downhole fluid samples, stable flow must be initiated with the effective surface separation and accurate recording of oil, gas, and water. However, in order to be able to detect the reservoir boundaries longer tests are performed so that log-log plot can exhibit information about Late Time Region. Precise forecasting of flow rates along with the rock and fluid reasonable estimates are crucial factors to detect distant boundaries in given well test schedule (Kumar et al., 2010). Any overestimation or underestimation of flow rate data, rock and fluid properties will cause to produce unreliable and incorrect results. Common errors in pressure transient stem from the phase redistribution within the wellbore, i.e. in condensate reservoirs, condensate may evolve below the shut-in valve leading noise in pressure measurements. This kind of problems even lead to incorrect recording of oil, gas, and water at surface. In tight

reservoirs where the permeability is very low allowing to maintain high production rate, decreasing the flowing bottom-hole pressure can be an option provided that dew point pressure is not reached, otherwise due to condensate accumulation flow rate can be further decreased through condensate blockage.

In order to be able to predict all these problematic issues in well test design, a workflow is required that can allow proper test design (Kumar et al., 2010).

#### *Well Test Design Optimization Workflow*

In this part several steps are introduced in a workflow that should be followed to generate a reasonable result.

##### *Step 1: Single Well Model for Flow Rate Forecasts*

The workflow begins with the construction of Single Well Predictive Model (SWPM) that will be employed to anticipate flow rate. Rock and fluid data from well logs, cores, and cuttings are used to build the geological framework of the model (Kumar et al., 2010). Dynamic parameters of the reservoir such as relative permeability data, capillary pressure, and permeability are obtained either from SCAL results or from Nuclear Magnetic Resonance logs results. In either case the results are validated by utilizing WFT data results. Rock classification and flow units are detected by using SWPM model. Before embarking on 3-D model construction, firstly 1-D model is built and validated, then after validating its results, 3-D model is built.

Flow Simulation model is then generated which accounts for validated SWPM Model within ECLIPSE software. Down-hole representative fluid sampling data along with PVT information is introduced to specify fluid properties in a model. Flow Simulation Model runs from ECLIPSE software are used to forecast oil, gas, and water rates under various perforation and well scenarios. These forecasted production rates for the oil, gas, and water are later used in the workflow to assess the likelihood of meeting the DST objectives.

##### *Step 2: Determine the Intersection Point of IPR and TPR*

Having performed the ECLIPSE simulation runs to predict the flow rate, the following step is to employ Nodal Analysis to find the intersection point of Inflow

Performance Relationship (IPR) and the Tubing Performance Relationship (TPR). All tubing and perforation types that are available need to be considered in this analysis. If no intersection point is achieved, the stimulation can be initiated to increase IPR under favourable economic circumstances. Otherwise, the zone that is selected for DST appears to be unsuccessful candidate.

If however, the intersection point is achieved between IPR and TPR, then the ability of reservoir is determined. The workflow steps are depicted in Figure 3-1.

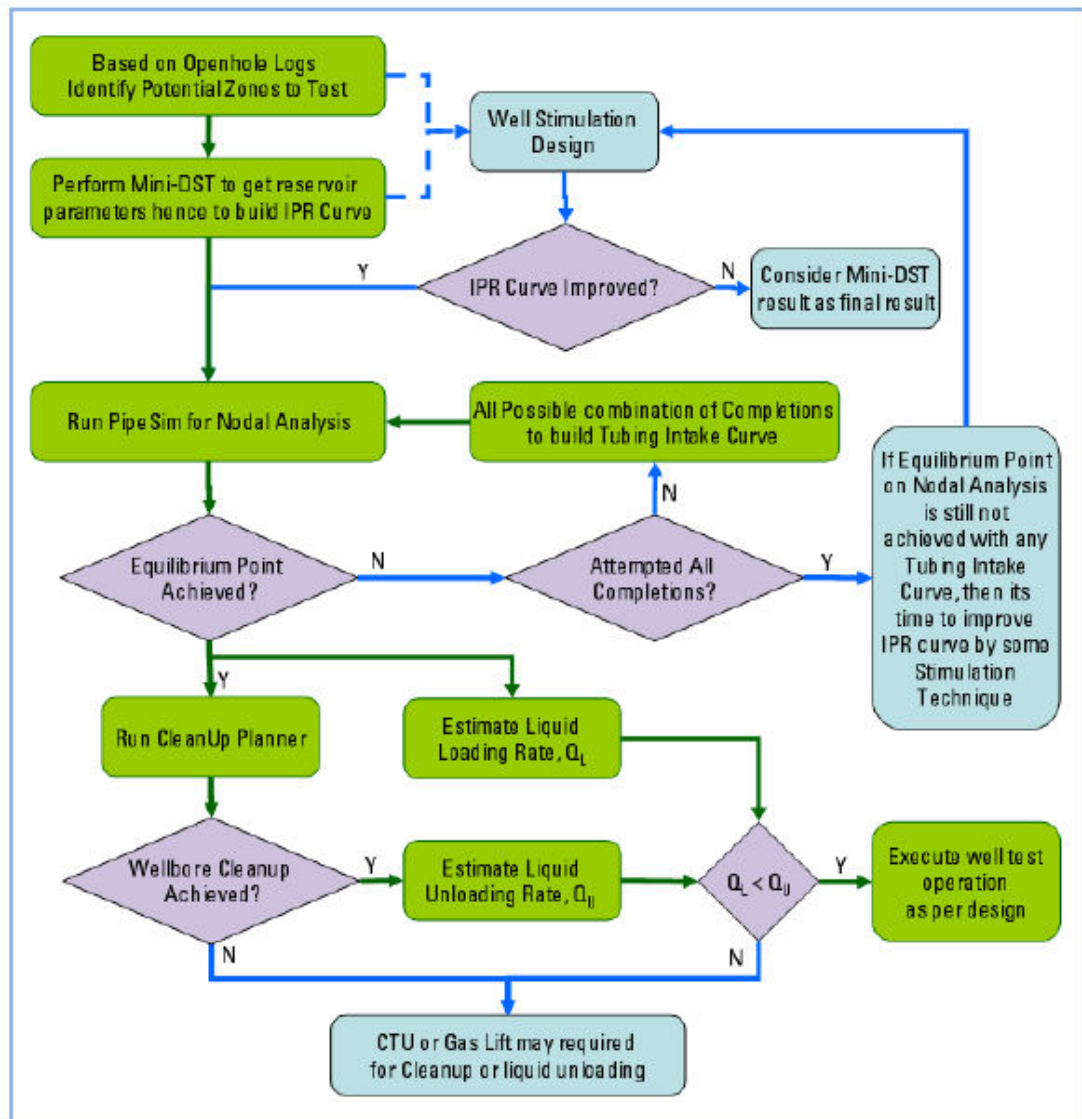


Figure 3-1. Well Test Design Optimization Workflow (Kumar et al., 2010).



## CHAPTER 4

### RESERVOIR SIMULATION

#### 4.1 Introduction to Reservoir Simulation

Hydrocarbons are trapped structurally or stratigraphically in underground medium named as reservoirs (Gordon, 1998). The flow of these hydrocarbons are quite difficult phenomena. In order to be able to solve analytical solutions to mathematical models, some assumptions are made to simplify the process with respect to reservoir geometry, properties and boundary conditions. This in turn poses some challenges especially when these assumptions are not valid for some fluid flow models. Most of time, it becomes impossible to find some analytical solutions for the mathematical models because of non-linearity equations nature, reservoir heterogeneities, complex multi-phase flow of fluids through the reservoirs, and so on (Gordon, 1998). As a consequence, these kind of models can be solved through numerical methods such as finite difference or finite element. Reservoir simulation provides a numerical solution for the reservoir-well system from which fluid flow problems can be solved. Now, it's become a ubiquitous method for the solution of complex multi-phase flow equations in Petroleum Engineering discipline aimed at simplification of oil and gas recovery from the system.

Essentially, reservoir simulation method is used to predict the reservoir performance and production rate for the correct and accurate reservoir management decisions (Sattar, 2008). Apart from that, it can also be used to get some reasonable information about the drive mechanism.

Most often, reservoir simulators appear to be the only way to offer most accurate and reliable solution to reservoir models through numerical solutions because of complex

reservoir heterogeneities and multi-phase fluid flow (Gordon, 1998). For the correct reservoir simulator development for various reservoir-well systems and production processes some mathematical and applied science knowledge is required. This starts with the generation of finite difference equations of mathematical model for the hydrocarbons flow in a reservoir-well system, being followed with numerical modelling combined with computer programming and yields simulation software as a result. A typical graph of this process is shown in Figure 4 – 1.

Nowadays numerical simulation has received a great application almost in all reservoir life cycles, because it's capable of representing the actual reservoir if designed and built properly. Prior to applying production or injection changes to the actual reservoir, firstly these changes are introduced to the model from which similar response of model can be identified and interpreted. If response becomes efficient and economical, then changes can be made to actual reservoir.

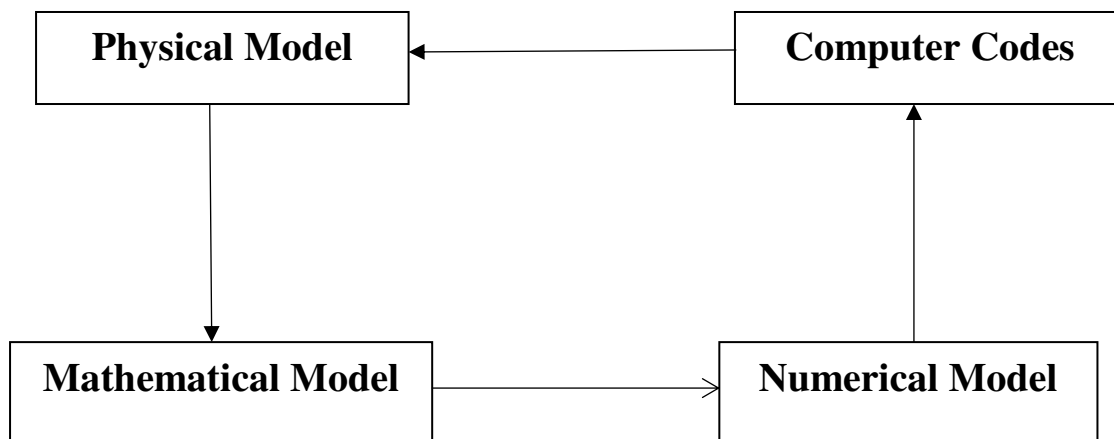


**Figure 4-1.** Reservoir Simulation Workflow (Cheng, 2011).

### *Motivation for Simulation*

As it's mentioned above, the simulation model is quite useful in describing and predicting the reservoir dynamic performance under the ongoing operation circumstances; to assess its sensitivity to water, gas, steam injection; to detect the possible reservoir reactions to the change in operating circumstances such as shifting production rate from one to another or drilling infill wells; forecasting production profile from slanted or horizontal wells and so on.

There are always a set of economic considerations that need to be taken into account when performing simulation and realizing its results. For example, where could the wells be drilled for best economic perspectives? How many wells are needed to meet the contract demands and to get maximum hydrocarbons available out of the ground? Should the operator perform some sort of EOR techniques or secondary recovery mechanisms to boost the reservoir energy? All of these questions define the complexity and elaboration of the model so that accurate results can be acquired. The result yielded from the model may necessitate the infill drilling or change in production rate as well as the secondary recovery or EOR mechanism technique implementation. Having determined the objective of simulation which is the accurate representation of the actual reservoir, the next stage is to portray the reservoir accounting for its oil and gas reserves, producible reserve estimation and the rate that the reservoir will be produced. For the accurate estimation of producible hydrocarbons from the reservoir, its framework being comprised of layers, flow units with geological elements such as faults and pinch-outs need to be properly built. This is called stochastic model which is established by the co-operation of reservoir engineers, petrophysicists, geophysicists and geologists (Peaceman, 1977).

Fluid flow equations are calculated by the simulator itself. The mechanisms underlying the simulator are quite straightforward. Firstly, fluid flow equations are described as a partial differential form corresponding to each phase present. These equations are derived from the combined equations of conservation of mass, fluid flow equation, and equation of state. Fluid flow equations by and large are referred as Darcy's law. But in gas reservoirs, to make this equation applicable, it takes account of turbulence terms as a result of higher production rate. Equation of state indicates each fluid's volume or density change as a function of pressure. In order to come up with the partial differential equation, these 3 equations are combined. After that, for the numerical solution of these equations, they are written in the form of finite-difference in which the reservoir is described as the congregation of imaginary blocks. Each of these block is an indicative of actual corresponding reservoir volume and must include rock and fluid properties at that specific place. The simulator models the fluid flow by solving the equations at the interface of each block, since fluids flow from one grid block to another. For the solution of these equations some parameters are required such as permeability, porosity, layer or wall thickness,

pressure and so on. Required fluid parameters are viscosity, density, solution GOR, and compressibility. Rock parameters are compressibility, and relationship of capillary pressure with relative permeability. Splitting the reservoir into grid blocks and then appointing the fluid and rock properties to each of them is quite long procedure and takes some effort and time. Reservoir production time scale is further split into a different time scale. A grid or sometimes referred as a mesh is a block unit that corresponds to actual reservoir volume. Based on the classification of topological and geometrical properties of grids, they are classified as *structured* and *unstructured* grids.

#### **4.2 Structured Grid Simulation**

For building accurate representative model to imitate the actual reservoir, structured Corner Point Geometry grids (CPG) are ubiquitously used in reservoir engineering industry (Brand, 1991). Because of inherent complexity of reservoirs being even more compounded with geological elements such as with faults, pinch-outs and etc. it generally poses quite technical challenge to construct a model with regular grids, even in some cases it becomes impossible. Generally speaking, sometimes large-scale elements including faults and other features are simplified and undergo some alterations in order to make it technically feasible to construct the grids. The primary objective of the simulation is to represent the actual reservoir as accurately and adequately as possible. So, if large-scale elements such as faults, pinch-outs are modified and simplified, it puts the model applicability under the question.

Most often structured grids are specifically portrayed as hexahedral Cartesian grids as shown in Figure 4 – 2. For grid geometry and its topology identification, one would simply need to know the origin, and the number of grid-blocks in three (x, y, z) coordinates. Especially this kind of gridding is quite handful in geophysics. Its application in reservoir engineering for the simulation purposes in the spotlight even earlier than that. Their primary advantage of using this kind of gridding is the simple discretization of partial differential equations for the simulation in block interfaces. However, when complex reservoir geometries and geological elements are involved, using regular structured gridding can lead to erroneous results, since some features such as faults or fractures are simplified for the sake of its applicability. To put it differently, less flexibility is involved in this gridding.

#### 4.2.1. CORNER-POINT GEOMETRY GRIDS

For improvement of accuracy of regular gridding simulation, some techniques were introduced such as distorting Cartesian gridding especially to account for the complexity of the reservoirs with geological features. After that, the industry was introduced with the corner-point geometry (CPG) gridding, and this gridding method in fact are the most employed technique because of simple fulfilment in standard simulators and considerably less time-scale attached to implementation due to regular grid structure. It can manifest the actual reservoir geometries by appointing the corners of each grid block in grid construction. Another benefit of using this gridding is its flexibility for well modelling. Nevertheless, some scientists stressed the caution of using CPG grids for this purpose, especially when radial fluid flow is not perfectly approximated. Initially CPG gridding was constructed for the sake of accurate representation of reservoir layering by adding some “dead” cells.

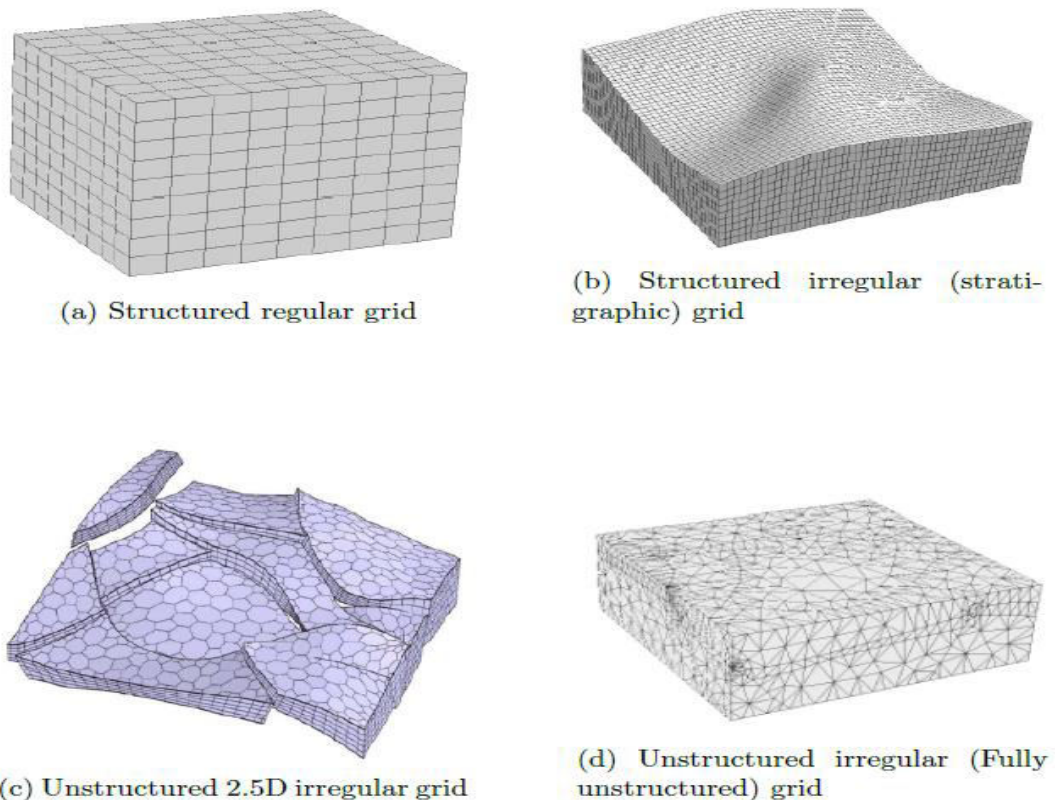


**Figure 4-2.** Reservoir Simulation Grids (Souche, 2003).

These dead cells are not active during the simulation, hence used only for reservoir flow unit description. Faults can be manifested through the distortion of Cartesian grid blocks by orientation of their corners. Large network of fractures or other

complex geological features can necessitate the large number of inactive cells or grid blocs which obviously can reduce the efficiency of simulator computation and will make it more difficult to calculate the transmissibilities. With the presence of complex reservoir heterogeneity and geological features, use of CPG gridding is not preferable, since this kind of reservoir system requires elaborated handling in grid construction.

### **4.3 Unstructured Grid Simulation**

Unstructured gridding provides much more flexibility to account for the geological complexity of the reservoir. They can be used with more confidence when extremely heterogeneous reservoirs are involved. However, even in unstructured reservoir gridding simulations, engineers tend to sustain a regular pattern or structure so that the construction of grids and consequently their discretization can be simplified. In fact, when stratigraphic flow units, fracture networks or wells are involved, some certain types of unstructured grids could be utilized.

When stratigraphic layering is involved, for the representation and modelling purposes 2.5 dimensional models are used as a substitute of the stratigraphic gridding (Figure 4-2). Given the fact that many geological environments are comprised of layers, 2.5D Delaunay or 2.5D Voronoi grids can account for these layers. They also make it feasible for the vertical geological elements to be manifested.

To model the complex faults and wells, hybrid grids being essentially comprised of different types of gridblocks are frequently deployed. Some scientists introduced a new technique in which structured grids are ubiquitously used throughout the reservoir, only faults and wells are modelled through use of unstructured grids. Other engineers introduced structured coarse gridding blocks which are further split into structured finer blocks, and around wells radial structured grid-blocks are employed.

One of the most employed fully unstructured grids is *tetrahedral* grids (Forsyth, 1986). This grid is in the form of three dimensional Delaunay grid. What makes them attractive to use is the existence of decent algorithm and mechanism for implementation. This gridding is especially useful for geophysical interpretation and geomechanical simulation. However, in reservoir engineering industry their

applicability is not so widespread mainly because of difficulty on construction of these grids (huge number of elements are prerequisite) although they can represent quite accurately almost any reservoir geometry.

Another type of unstructured gridding simulation is *polyhedral* grids. These grids also can be used as a substitute for any other gridding types, especially it's beneficial to use them when complex fracture network or wells are involved. When it comes to their applicability, again it is not generally utilized in the industry due to reason that these grids necessitate sophisticated discretization handling for simple two-point flux approximations (TPFA) which is quite challenging. Apart from that, development of data setting in 3D framework poses another technical difficulty.

#### **4.4. Use of Voronoi Gridding on Reservoir Simulation**

For the modelling and simulation of actual reservoirs, the domain is constructed and split into imaginary grid blocs in which then fluid and rock properties are assigned. The fluid flow in actual reservoir is manifested as the flow from one block to another and is computed through use of discretized Darcy's law. Apart from that, PVT estimations and relative permeability values are also taken into account for the sake of accuracy of the model. The outcome of the simulation is strongly dependent upon the scheme of how the reservoir is divided and flow equations are computed.

Recently out of plethora, Voronoi gridding has subjected itself to the kinds of attention and in fact offers great convenience and flexibility. The merit of using Voronoi gridding is the fact that individual imaginary grid blocks can be distributed anywhere throughout the domain being independent of other blocks placement and location. Giving the fact that its usage offers great convenience, this gridding incurred its applicability not only in Petroleum Engineering, but also in Physics, Electrical Engineering, Rock Characterization and so on. In some literature Voronoi gridding is interchangeably called as PEBI (Perpendicular Bisection) owing to its construction fashion.

Firstly, it was introduced from Heinemann and Brand to use Voronoi gridding technique for simulation purposes in reservoir engineering industry. These authors pointed out the discretization of flow equations in grid blocks by the help of any number of adjacent grid blocks which utilizes integral method of discretization.

Nevertheless, the actual execution lied on the algorithm method which maintains 7-point connection being a special modification of Voronoi gridding. Other engineers tended to use this gridding technique to increase the preciseness in the connection bonds between coarse and fine Cartesian blocks. This type of gridding is also a special modification of Voronoi gridding and is called control volume finite element (CVFE) technique of discretization.

A Voronoi grid block is portrayed as the region of space that appears to be closer to its grid point in comparison with any other points and Voronoi mesh is primarily comprised of this kind of blocks (Figure 4-3). Each block is assigned with a grid point and surrounds with other blocks.

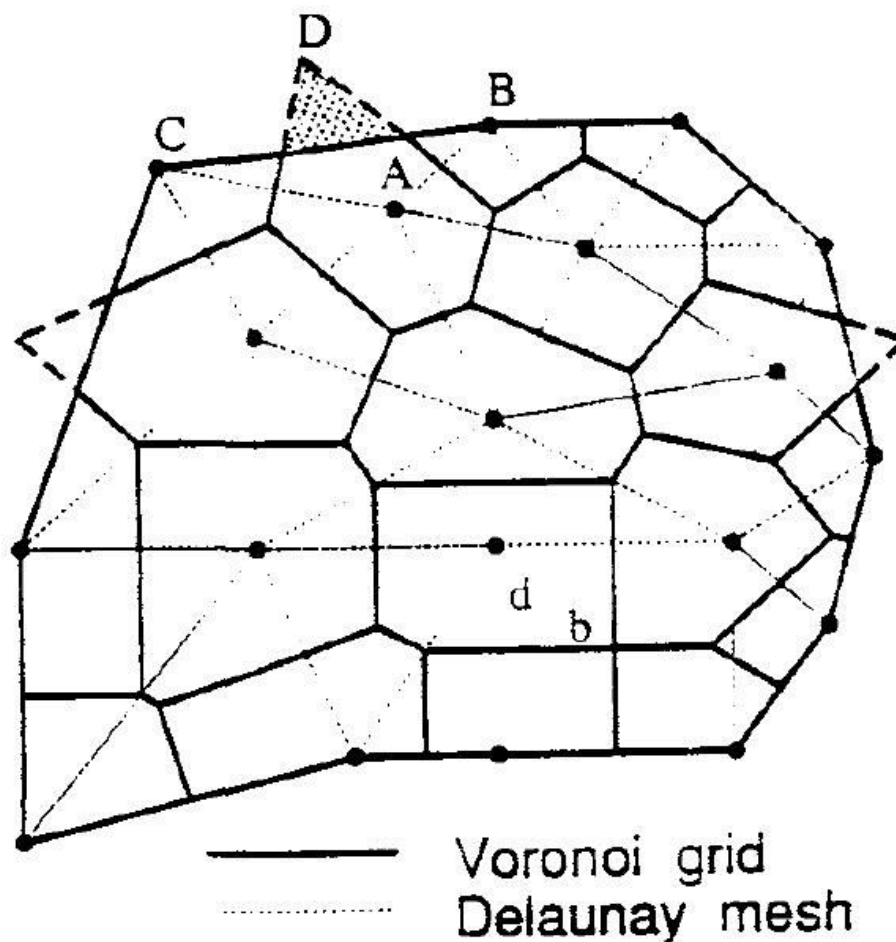


**Figure 4-3.** Voronoi Grid and Delaunay mesh (Palagi, 1994).

Material balance equations are computed for each of these blocks by taking into account of accumulation of fluids combined with the fluid flow by crossing the boundaries and wells. This method of discretization is often referred as the integral

method of discretization or control volume finite difference (CVFD) technique. Grid boundaries are perpendicular with respect to the grid points within the domain. That is the reason why sometimes this method is sometimes called as perpendicular bisection (PEBI) technique. Given the fact that the point sitting on the boundary that connects 2 adjacent blocks appear to be in the same distance from the grid points, this type of gridding technique is sometimes called as generalized point-distributed grid. So, in this case, when the grid points are connected and constructed, this type of mesh is called as Delaunay mesh provided that triangles are formed from this connection.

The line appearing in the Delaunay mesh is an indicative of possible fluid flow between the grid points in the domain. Voronoi and Delaunay meshes turn out to be duals for each other. Voronoi gridding appears to be in the realm of interest more than Delaunay mesh especially for reservoir engineers. Even though there are several gridding types that are frequently employed, but nearly all of them are some type of modification of Voronoi gridding to some extent, at least very close approximation exists. Figure 4 – 4 illustrates some of them.

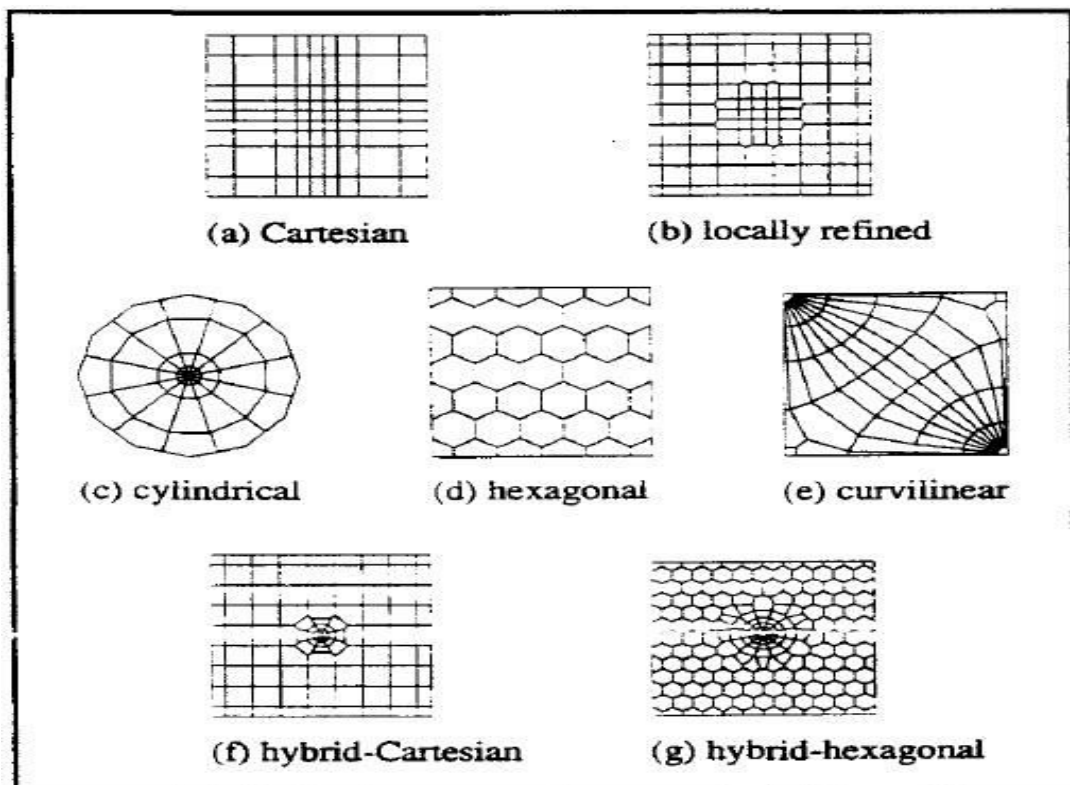


**Figure 4-4.** Special cases of Voronoi Gridding (Palagi, 1994).

#### 4.4.1 GRID GENERATION

The simulation of Voronoi gridding, as for all gridding starts from the grid generation. Firstly, in a local coordinate system easy-to-deal with modules are picked (Figure 4 – 5). For the construction of Cartesian and cylindrical modules, the input data are the number of grid points in each direction and the increase of points in each direction. Regarding to the Rectangular domains of hexagonal blocks, only number of grid points are enough for the establishment of module. Concerning the irregular modules, an engineer needs to know the accurate placement of each grid points. Figure 4 – 5 illustrates some of the most frequently used modules. In fact, complete unstructured or irregular domains are used to correctly describe the complex heterogeneity of the reservoir.

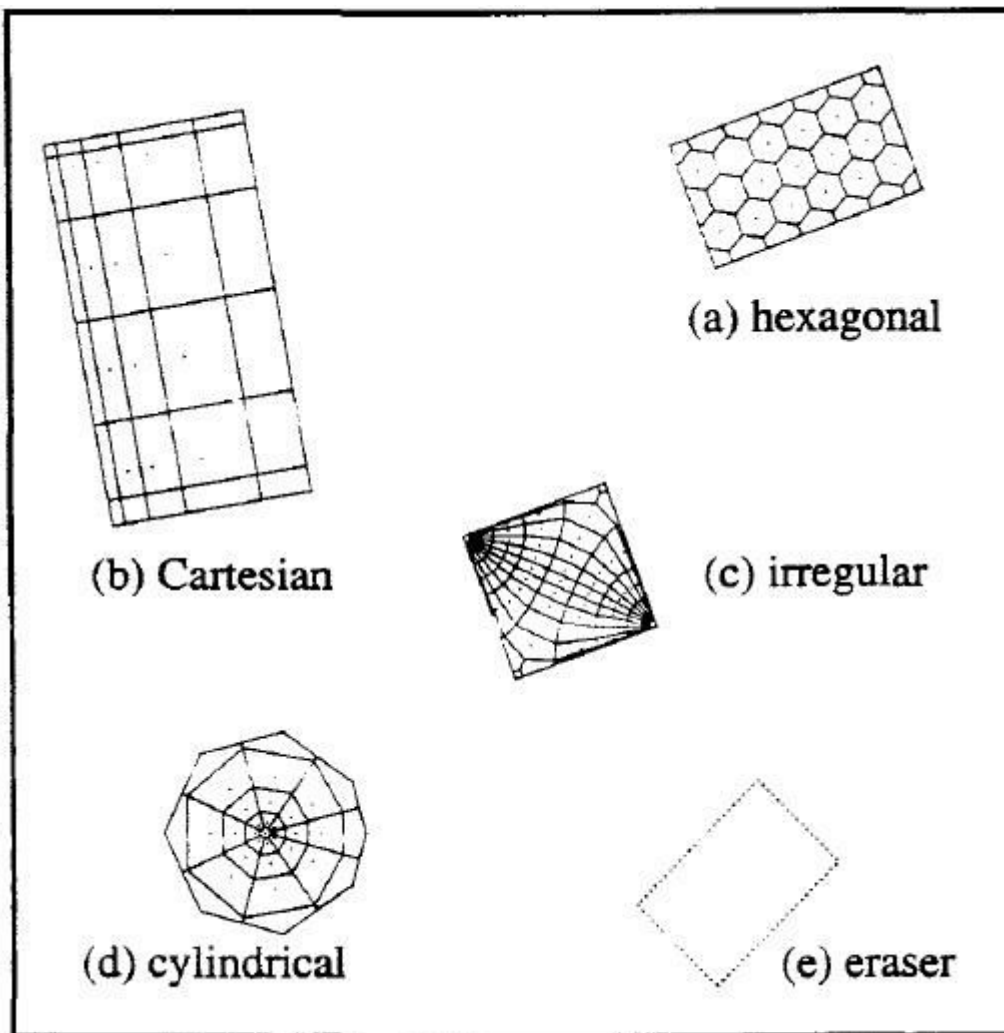


**Figure 4-5.** Different modules for grid generation (Palagi, 1994).

Having determined the modules, they can be adjusted in terms of being scaled or rotated within the domain. One of the modules illustrated above (eraser) is used to remove all the points inside the module. In this phase, only grid points have been generated, Voronoi grid blocks are generated automatically through use of final grid points.

Different modules can be incorporated simultaneously within the domain, and the same module can be repeatedly used for some time. Figure 4 – 6 depicts a hypothetical usage of this method.

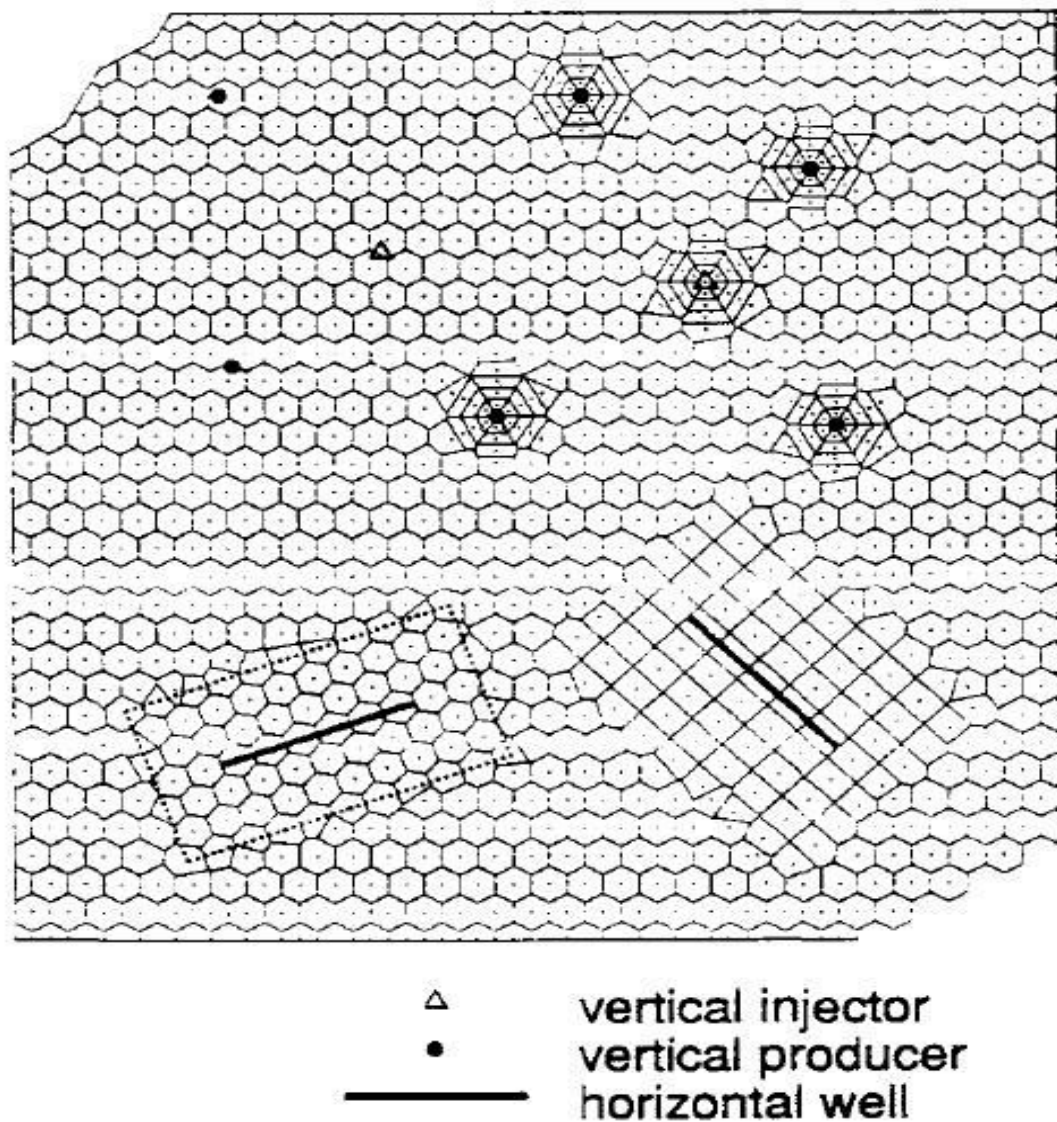


**Figure 4-6.** Hypothetical use of different modules (Palagi, 1994).

As it's illustrated above, within the same domain different modules can be used. For example, regular hexagonal Voronoi gridding is used to minimize the grid orientation effect, whereas cylindrical modules are placed inside the domain precisely where the wells locate, so that even unknown well patterns can be adequately represented. Hexagonal and Cartesian modules are utilized in order to be able to match the longitudinal orientation of slanted (or horizontal) wells. As it's pointed out, the domain have a kind of unconformities both in the top-left and in the bottom-right direction. This was done due to match the external boundaries of the reservoir. Bottom-right area of the domain consists of dead cells which are not active during the simulation period.

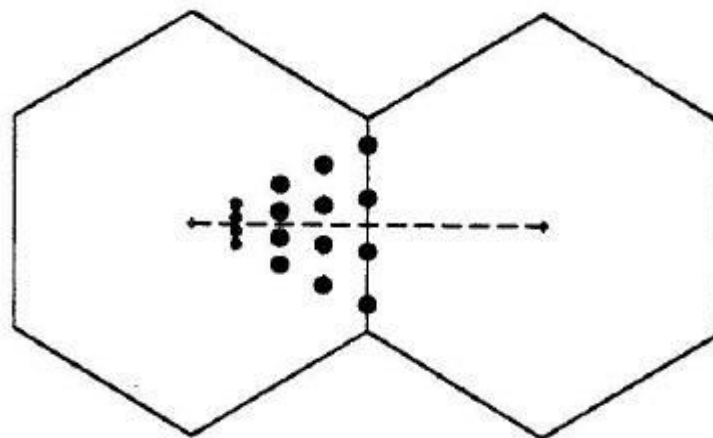
Traditional gridding technologies do not offer the same level of variability or flexibility to match the actual reservoir, particularly to match flow towards the wells.

#### *4.4.2 ASSIGNMENT OF PHYSICAL PROPERTIES*

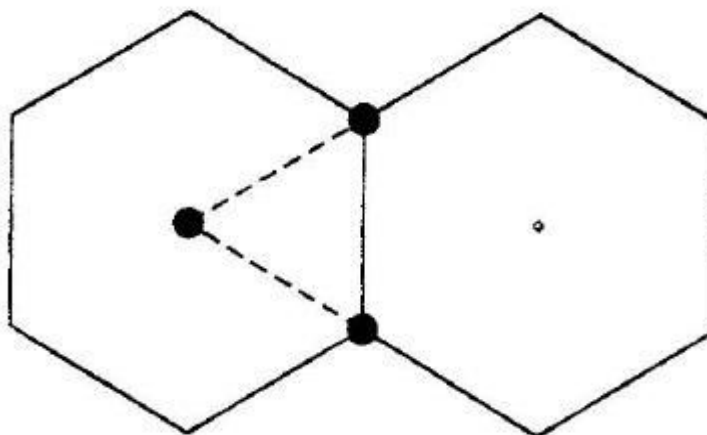
After the grid geometry identification, the next phase is embedding of physical properties to each block and its subsequent connections. Tradition gridding techniques require the exact estimation of each properties for each block which is obvious time-consuming. Some parameters are averaged between the neighbouring block boundaries, like transmissibility for instance. In this gridding technique, physical parameters are embedded at property-points irrespective of grid-points. These physical parameters are permeability estimation in both x and y direction, porosity value, thickness value, and depth for each flow unit. For the identification of property-point value, x-y coordinates and value of properties are utilized. As shown in Figure 4 – 7, each Voronoi block is split into triangles, and aforementioned physical parameters are evaluated for each vertices of triangles, and then they are averaged for the whole block by weighing factor corresponding to an area of the triangle. Special care should be taken when averaging these properties, because in this notation vertical permeability is computed and averaged, with the horizontal permeability, the case is different. In fact there's no reliable technique through which horizontal permeability can be calculated with confidence for each block at any time. However, this gridding seems to be more promising. For the estimation of horizontal permeability each of the triangle is split into points appointed by the user, and for

each of these points permeability value is calculated. After that, these values are averaged harmonically by use of some mathematical equations.

Naturally, after all the outcome of the model is all dependent upon the engineer's experience and the way how the work has been dealt with. Special attention needs to be paid when the reservoir contains some flow barriers and high permeability variation zones.



(a) average permeability of a connection



(b) average property of a grid block

**Figure 4-7.** Assignment of physical properties to each block (Palagi, 1994).

#### *4.4.3 USE OF VORONOI GRIDDING SIMULATION FOR HETEROGENEOUS RESERVOIRS*

The “effective permeability” of the connection between 2 adjacent gridblocks define the flow rate on this boundary (Ballin et al., 2002). Even though there are several techniques that have been described in literature to upscale the permeability values for structured Cartesian grids, these techniques have not been explored for unstructured flexible grids. Voronoi gridding technique offers to distribute the gridpoints throughout the reservoir freely without considering other gridpoints position, so its usage to simulate the reservoir and the well is more flexible and more accurate (Ballin et al., 2002).

As an assumption, permeability values have already been embedded for each grid-blocks, in a reservoir simulation sense, the connection of each blocks define the permeability values. In some complex cases, single grid-block can exhibit significantly different values for permeability based on its connection to other adjacent blocks. In this cases assigning a single permeability value for the whole block would omit this complexity and ultimately the results would not be as reliable as the engineer would like.

An upscaling process is essentially comprised of calculating average connection permeability values based on smaller scale representation of a real reservoir (Journal et al., 2000). The upscaling techniques used for reservoir simulation purposes that are available in literature can be classified into two types. One of these methods utilizes the correlation between the small scale reservoir representation data and the average permeability for gridblock or the connection with other blocks (Journal et al., 2000). Having generated and validated the correlation, block permeabilities are defined based on this correlation. Second method unlike from the first always necessitates the simulation for fine and coarse grids for each reservoir representation in order to define the average grid-block permeability (Journal et al., 2000).

From the two techniques that are aforementioned, first technique of them necessitates the validating the correlation based on comparison the numerical results for fine and coarse grids. Some authors in the literature offer the distribution of small scale permeability values for the block and then based on the geometric average of these values, the average permeability is derived for that block, while others came up

with the power law technique to compute the average permeability of reservoir blocks where sandstone layer is followed by shale layer. For this purpose the optimum power law coefficient is calculated based on the fine grid simulation of one single block with four closed and two constant pressure boundaries. Authors such as Journal came up with more sophisticated method that uses geostatistical techniques to calculate the average permeability on the interface based on the actual data. So, the authors concluded that their method is only applicable for the reservoir where the grid-blocks are equal in size.

Second technique for the estimation of average permeability on the connection of grid-blocks is based on the results of computing the permeability data for the coarse grids by making reference to fine grids results. Nevertheless, the results are not utilized for generating simple correlations. The transmissibility coefficients for the boundary of each block is calculated in a way that the error between the fluxes of actual and calculated is minimized for coarse grids.

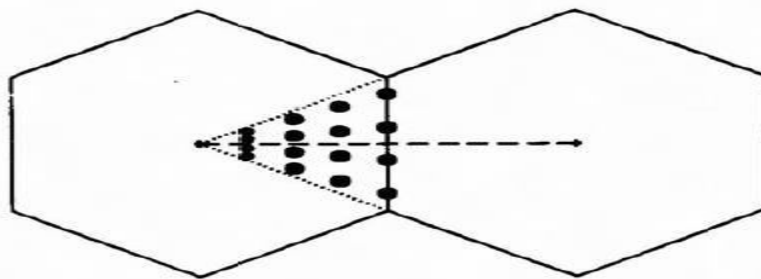
In this literature survey, the first type is introduced which is applicable to unstructured gridding, especially to Voronoi gridding. Giving the fact that there is no ideal tool that can allow to adequately determine the average permeability value for each boundaries at all time with very little error, this proposed technique is envisaged to cover the main steps to calculate the permeability value while keeping it easy to handle and accurate to rely on (Ballin et al., 2002). This suggested tool to determine the average permeability value on the interface between blocks of i and j, is as follows:

1. Based on parameters that have been introduced by the user, the connections forming internal triangles is divided in a pattern as shown in Figure 4-8;
2. Permeability is computed for each point in this pattern, from point (1) through point (16);
3. Power Law Average is determined based on the coefficient that is introduced to simulator from the user;
4. The same steps are applied for block j, and finally based on the following equation the permeability ij is computed like this:

$$k_{ij} = 2 / \left( \frac{1}{k_{ij,i}} + \frac{1}{k_{ij,j}} \right) \quad (4-1)$$

The optimum value for the power law average can be acquired from the pressure comparisons of fine between coarse grids. It has been pointed out by many authors that when there is only oil flowing through the reservoir the analytical results for the pressure values in grid-points is very similar with numerical results, it even works well when normal coarse grids are involved (Ballin et al., 2002). However, wellblock pressure does not comply with this practice, since it's been proved to be different from well pressure. So, excluding wellblock pressure, the analytical results are supposed to be identical to numerical results for the pressure values at grid point.

In literature, there are no analytical equations allowing to calculate the pressure points for the single phase in heterogeneous reservoirs. Nevertheless, numerical results generated from reasonably fine grid can be considered as a potential solution that is precise and reliable enough for practical purposes. Numerical results acquired from simulating coarse grid are supposed to yield overall pressure distribution in a reservoir that should be similar to pressure profile obtained from fine grid for the same reservoir system. But it requires to use elaborated averaging technique to estimate permeability value at each interface of adjacent grid blocks.



(a) average permeability of connection  $ij$ .

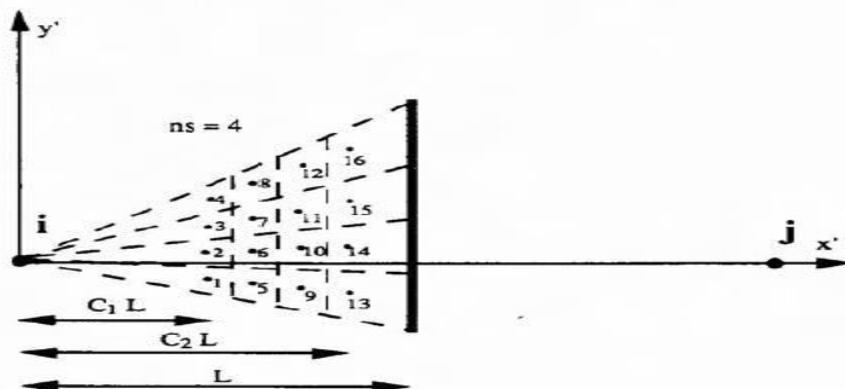


**Figure 4-8.** Specifying of physical properties to each Voronoi grid blocks and its connections (Ballin et al, 1993).

#### **4.5 Numerical Well Testing Using Unstructured Voronoi Gridding**

Numerical models offer great flexibility and accurate results compared with analytical equations that do not take into consideration of dynamic properties change with the depletion of the reservoir (Hui et al., 2011). Unlike analytical equations, numerical models can simulate simultaneous oil, gas, and water flow through the reservoir. In order to simulate this kind of multiphase flow and other complex reservoir systems, numerical models use gravity, capillary forces simultaneously together with the relative permeability functions (Hui et al., 2011). Nevertheless, even numerical models can be entrenched with inherent errors, so its results must be meticulously validated. One of the major challenging task is to simulate the near well-bore region, because pressure drop in this region is higher, and re-distribution of fluid phase sometimes becomes inevitable. The question is how to introduce an appropriate grid around this zone to match the pressure profile accordingly (Hui et al., 2011). Numerical well testing is a way to incorporate the dynamic well testing results into existing static model to make it more representative (Hui et al., 2011).

Heinemann (1994) pointed out the applicability of unstructured gridding in petroleum industry. He developed an equation that can produce this kind of irregular grids while maintaining Cartesian gridding and employ it wherever it's suitable. The so-called windows method was introduced that manifested any area of the reservoir grid. Updating of the existing static model is implemented by virtue of windows method. Fortunately, the results acquired from windows grid method are identical to the analytical methods results.

He and Chambers (1999) approached the problem by improving the history match procedure by using well test data. Well test results yielded a factor that is multiplied to each property around each well as a result the reservoir model was updated geostatistically. In-situ permeability data were introduced to the system so that any disagreement of pressure values (actual and simulated pressure values) are exceedingly diminished. This suggested technique was utilized in a real field and good match was obtained between historical pressure data and simulated pressure data.

Mlacnik and Heinemann (2001) developed a well windows method and it was employed in a full field simulation. This method runs a small block size in a

windows area. Real field model was constructed by using Voronoi gridding and a good match between actual and simulated data proved this windows technique together with Voronoi gridding to be accurate for field simulation purposes.

Escobar and Djebba (2002) explored the investigation of using the Voronoi gridding to simulate the reservoir model with hydraulically fractured wells. They stressed that the preciseness and effectiveness of reservoir simulators essentially depend on a suitable grid distribution.

Ding and Jeannin (2004) introduced a new logarithmic approach to develop the accurateness of linear approach especially for near-well region simulation by utilizing flexible perpendicular-bisectional grids. They stressed that the preciseness of computational results for well properties are vastly dependent upon the appropriate simulation of near-well region.

Garcia et al. (2006) have proved that for adequate estimation of permeability and initial reservoir pressure, the radial transient flow regime must be reached, otherwise the results for these parameters will not be representative of an actual reservoir data.

Sinha and Al-Qattan (2005) carried out numerical simulation applications on well test design by using perpendicular-bisectional Voronoi grids which in turn yielded good results. Al-Thawad et al. (2007) implemented real full field simulations on a gas condensate reservoir by making a reference to well test interpretations. For near-wellbore zones flexible Voronoi perpendicular-bisectional grids were utilized to simulate multiphase flow in this zone as well as to represent hydraulic vertical fracture.

## CHAPTER 5

### PRESSURE ANALYSIS METHODS IN HETEROGENEOUS OIL RESERVOIRS

#### 5.1 Introduction

This chapter deals with the reasons and causes of pressure-dependent rock and fluid properties, and how analytically the pressure behaviour can be estimated. It also discusses the interpretation techniques of pressure profile in reservoirs with faults or other barriers. After all, for extreme heterogeneous reservoirs numerical solutions should be utilized for the realistic reservoir description (Streltsova, T., 1984).

#### 5.2 Effect of pressure on rock properties

It's ubiquitously known fact from lab observations along with the encountered pressure profile from some wells that there is a linear proportionality between porosity, permeability with the reservoir pressure, i.e., porosity and permeability factors decrease with the reservoir pressure reduction. For the reservoirs with the normal pressure profile under normal compaction procedures these effects are not so tangible in comparison with the reservoirs with abnormal high pore pressure – geopressured reservoirs. Carbonate rocks are known more for its heterogeneous nature, whereas sandstone rocks are by and large less complicated in terms of pressure behaviour. Moreover, it's only possible by virtue of laboratory calculations to estimate the porosity value driven by the various factors acting simultaneously. Sandstone along with the other clastic rocks appear to be more elastic – gaining back its previous condition compared with carbonate rocks. Limestone rocks however, is a kind of plastic in terms of its reaction.

By and large, it can be predicted to observe 10% odd reduction in permeability from pressure transient tests conducted through the whole range of reservoir life, but due to the other factors involved such as three-phase flow influences, etc. a realistic estimation of permeability becomes technically challenging for the engineers. That's why laboratory-based plots of porosity and permeability against pressure needs to be utilized for the forecasting of pressure profile.

However, it's a general conclusion from various authors that the estimation of permeability or skin factor from conventional build-up or drawdown tests should not be conducted in reservoirs with the pressure-dependent permeability profile. Figure 5-1 depicts some of the factors concerned with that.

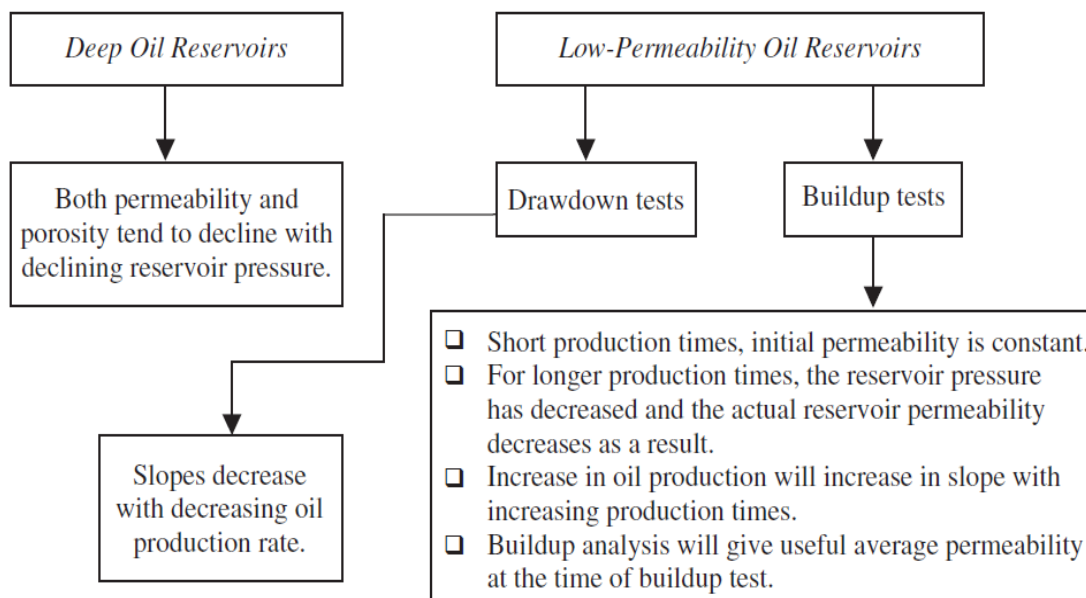


**Figure 5-1.** Effect of pressure-dependent permeability on drawdown and build-up tests (Chaundry, 2004).

### 5.3 Pressure Responses Near to No-Flow Boundary

Reservoirs with the complexities, i.e. with faults, pinch-outs and so on have always been an attractive topic in well-test literature (Forstyh P., 1986). In order to understand the effect of faults on pressure transient tests, the analytical equations are

used. For instance, the following formula is utilized to depict the pressure response at a well locating near to sealing boundary, i.e., fault:

$$[\Psi(p_{WD}(t_D))] = -0.5 [E_i\left(-\frac{1}{4t_D}\right) + E_i(-r_{dD}^2) + s] \quad (5-1)$$

In this equation  $r_{dD} = 2L/r_w$ , in which L is the length between fault and well. If time is so small so that the second term can be neglected, then the following equation is used:

$$[p_D(r_D, t_D)] = 0.5 E_i\left(-\frac{r_D^2}{4t_D}\right) \quad (5-2)$$

However, equation (5-2) can be further modified by the use of logarithmic expression to exponential integral:

$$[p_D(r_D, t_D)] = 0.5[\ln\frac{4t_D}{r_D^2} - 0.5772] \quad (5-3)$$

Making one final scenario which is assuming that the flow times are long enough so that both exponential expressions can be written in logarithmic expressions:

$$[p_{WD}(t_D)] = \ln\left(\frac{4t_D}{e^{0.5772}}\right) - \ln(r_{dD}) + s \quad (5-4)$$

These formulas written above show that, one should attain a second straight line whose slope is 2 times greater than the slope of first line. From practical sense, the slope with the two times greater of the preceding line is an indicative of the fault in the reservoir. If this is the case, then the first line should last for the given range of time:

$$6 < t_D < 0.08r_{dD}^2 \quad (5-5)$$

The following straight line however should begin at  $3r_{dD}^2$ . During the obvious time interval of  $0.08r_{dD}^2 < t_D < 3r_{dD}^2$  pressure estimations or forecasting of pressure behaviours can be conducted.



## **CHAPTER 6**

### **STATEMENT OF THE PROBLEM**

One of the main aims of this study is to understand the applicability of the analytical equations for well test design purposes taking into consideration of different scenarios. Essentially, the preciseness of analytical calculations results for well test design under different reservoir conditions is investigated.

Another aim of the study is to assess the effects of using unstructured Voronoi gridding in simulation of reservoir models with different scenarios, i.e. faults with horizontal and inclined channel, reservoir models with and without gas phase. Reservoir simulations with unstructured and structured gridding techniques and analytical equations applicability and reliability are investigated

The determination of optimum values for several well test design parameters such as production time, production rate, and shut-in times are also explored under various scenarios to check how these variations affect well test design procedure.



## CHAPTER 7

### METHODOLOGY

#### 7.1 Introduction

In this study for the purpose of highlighting the advantages of using the simulators over the analytical methods on well test design simple reservoir model has been built by using CMG IMEX simulator considering the following different scenarios:

- 1) One producing well on the centre of the reservoir;
- 2) 2 wells producing close to each other;
- 3) Reservoir models with different reservoir shapes (square and rectangular);
- 4) Reservoir Models with and without gas phase;
- 5) Faults with different orientation – straight and deviated with respect to the orientation of structured grids.

These different scenarios have been considered to see the effects of various scenarios on well test design and decide how long radial flow regime would last, how long the entire test should be run to see the boundary effects and so on.

One important assumption that was made in this study is that the reservoir model has been built based on the data from different reservoirs with similar rock and fluid characteristics. Since as an assumption of this study, the reservoir is brought into production for the first time, no previous production has been initiated before, and simple reservoir model has been built based on exploration and appraisal DST/WFT well test data and based on data from different reservoir model with similar rock and fluid characteristics.

Another assumption that was made in analytical equations is that Formation Volume Factor, viscosity and other dynamic reservoir parameters do not change throughout the whole production. Because, analytically it's not possible for instance to introduce

the gas saturation change in a saturated reservoir in every time step when the reservoir pressure goes below the saturation pressure. That's why this assumption was made so that it can be possible to compare the analytical results against numerical output values.

So, for the purpose of analytical-numerical results comparison a simple reservoir model has been constructed in CMG IMEX and simulation runs have been performed. Based on the pressure values derived from CMG IMEX simulators, build-up and drawdown tests are conducted by using ECRIN well testing tool to see the end of infinite-acting – transient flow regime or to see the start of second straight line in reservoirs with fault, to observe the boundary effects so that well design can be adequately implemented. The values for the end of radial flow regime and for the start of second straight line on ECRIN are compared with the values derived from analytical equations taking into account of different aforementioned scenarios.

Second part of work is the assessment of the applicability of Voronoi gridding simulation by use of Ecrin Rubis on well test design. Based on the pressure values from Voronoi gridding simulation, well tests are conducted on Ecrin Saphir results based on Ecrin Rubis and CMG IMEX pressure output values to judge the applicability and reliability of using unstructured gridding for well test design procedures.

## **7.2 Part – 1. Use of CMG IMEX and ECRIN Saphir**

A simple reservoir model has been built by use of BUILDER and 2 scenarios are considered: with and without gas phase. For the model of without gas phase, OILWATER water model is used, whereas with the gas phase only BLACKOIL model is used. BLACKOIL model is capable of simulating 3 phases flowing simultaneously in the reservoir. SI unit system is used for the modelling of reservoir.

### *7.2.1 OILWATER MODEL*

For the first part of the work which is to highlight the advantages of using simulators on well test design over the analytical methods a simple reservoir model is built in CMG IMEX BUILDER. The specifications of our reservoir is shown in Figure 7-1.

**Table 7-1.** Reservoir Model specifications from CMG IMEX Builder.

The screenshot shows the 'Create Cartesian Grid' dialog box with the following settings:

- Grid Type:** Cartesian (selected), Corner point (orthogonal)
- K Direction:** Up, Down (selected)
- Number of Grid Blocks:** I direction: 120, J direction: 120, K direction: 5
- Block widths:** I direction: 120\*10, J direction: 120\*10
- Controlling Grid spacing:** Snap spacing (unchecked)
- Snap grid lines as multiples of:** I direction: 1, J direction: 1

**Table 7-2.** Reservoir Model specifications from CMG IMEX Builder.

<b>Properties</b>	
Viscosity, <i>cp</i>	0.2
Formation Volume Factor, <i>rb/stb</i>	1.2
Oil compressibility, 1/psi	3.00E-05
Water Compressibility, 1/psi	5.76E-05
Formation compressibility	4.00E-06
Total Compressibility, 1/psi	2.75764E-05
Porosity	0.2
Reservoir Thickness, ft	16.4042
Well Radius, ft	0.25
Oil Saturation	0.9
Permeability, <i>md</i>	50
Production Rate, <i>m<sup>3</sup>/day</i>	200

Table 7-2 shows rock, fluid, and well properties for this case. The question may arise how the porosity and permeability values are known when building a reservoir model in which no production has been initiated before. Several sources may be available on this point. Data from similar rock and fluid characteristics, logs and cores from appraisal wells can yield us reservoir properties with some degree of confidence.

In this model, there's only one well producing at the centre of the reservoir with the rate of  $200\text{ m}^3/\text{day}$ . The production continues for 190 days, after 116 days the well is closed so that build-up test can be performed on ECRIN software. So, the following figure depicts how bottom-hole pressure changes over the production. As it can be seen after 116 days, the bottom-hole pressure abruptly goes up due to the closure of the well located on the centre.

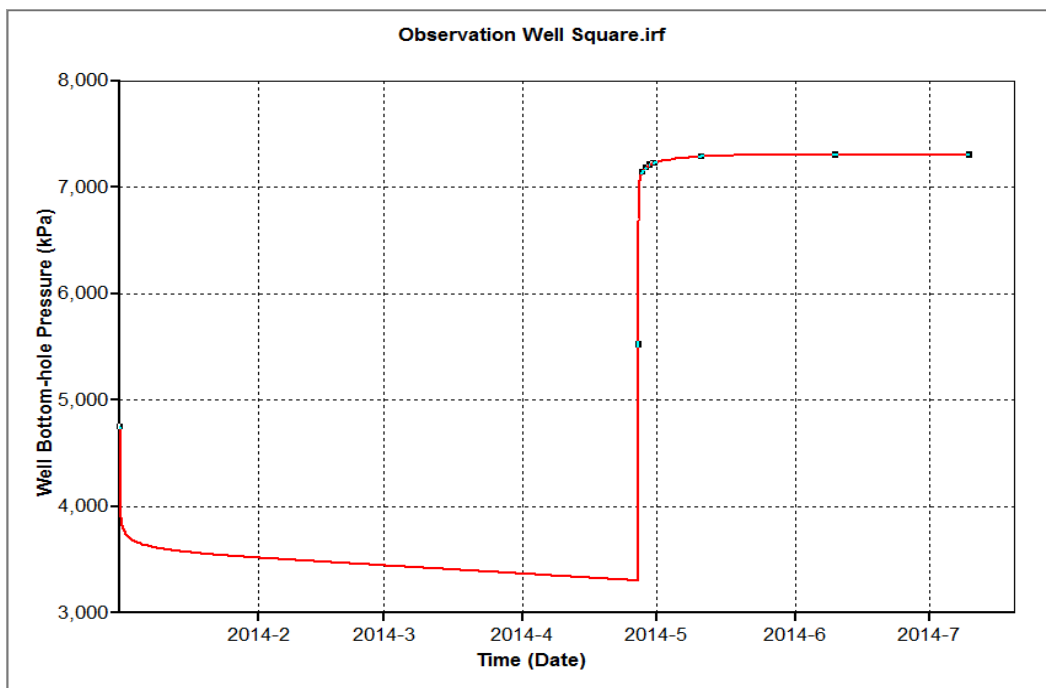


**Figure 7-1.** Well bottom-hole pressure change over the production and build-up period.

Having obtained the pressure values from CMG IMEX, the next step is to perform build-up testing on ECRIN and finding out the end of radial flow regime, boundary effects and so on. The following figure and table shows the log-log diagnostic plot and the reservoir parameters obtained from ECRIN software respectively.

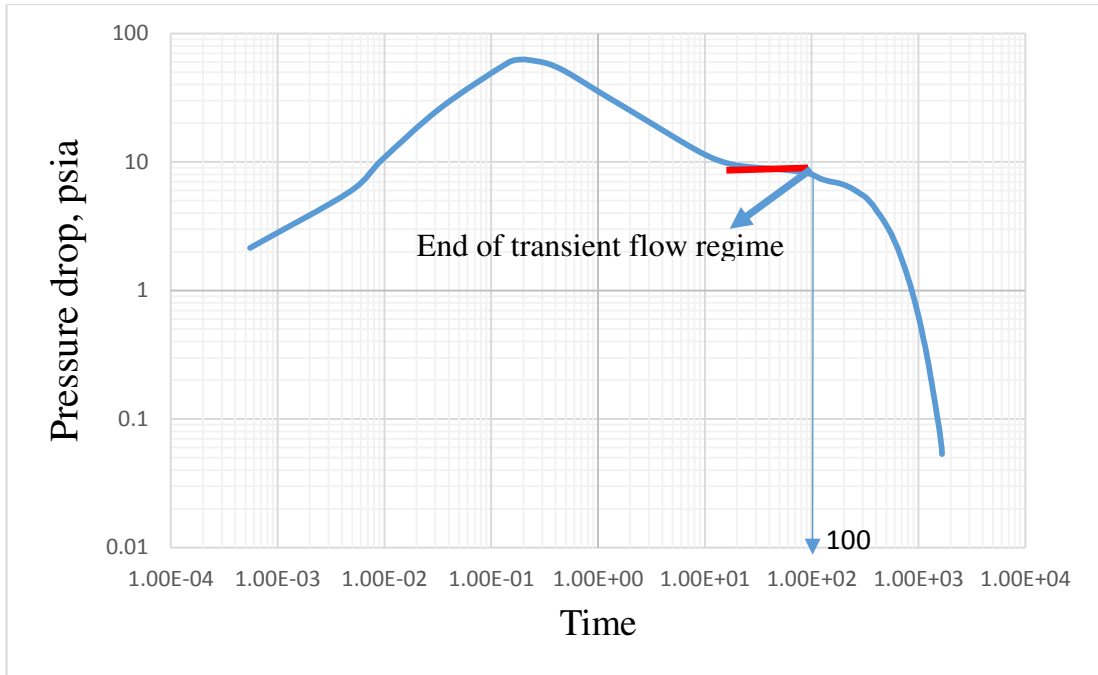


**Figure 7-2.** Diagnostic log-log plot of the OILWATER Reservoir Model.

As it can be seen from Figure 7-3, end of flow regime is 100 hr. In other words, one needs to wait 100 hours to get information about the reservoir boundary, i.e. Late Time Region. The line in LTR going down is an indicative of pressure maintenance effect through the aquifer expansion because of pressure drop.

From the Table 7-2 it can be seen that the effective permeability to be derived as 51.2 md from ECRIN. This is quite pretty good match with the CMG IMEX input data in which permeability value of 50 md is set in I and J direction based on logs, cores, and other fields from database with similar rock and fluid characteristics.

➤ Analytical Calculation

For the analytical calculation of the transient flow regime, the following equation was used:

$$t > \frac{\phi * \mu * c_t * A * t_{DA}}{2.637 * 10^{-4} * k} \quad (7.1)$$

Giving the following values:

$$c_0 = 0.00000435113 \text{ 1/kPa} = 0.00003 \text{ 1/Psi}$$

$$c_w = 0.000000835922 \text{ 1/kPa} = 0.000057635 \text{ 1/Psi}$$

$$c_f = 0.000004 \text{ 1/Psi}$$

$$S_o = 0.9$$

$$S_w = 0.1$$

$$c_t = c_o * S_o + c_w * S_w + c_f = 0.00003 * 0.9 + 0.0000057635 * 0.1 = 0.0000275764 \text{ 1/Psi}$$

$$Area = 1200 \text{ m} \times 1200 \text{ m} = 1440000 \text{ sq m.} = 15\,500\,031.99 \text{ sq. ft}$$

$$\Phi = 0.2;$$

$$\mu = 0.2 \text{ cp};$$

$$k_{avg} = \sqrt[3]{50 * 50 * 15} = 33.471 \text{ md}$$

$$t_{DA} = 0.05 \text{ (Shape factor for square reservoir)}$$

The following result from the equation is obtained (7.1):

$$t > 96.8 \text{ hr} \tag{7.2}$$

So, equation (7.2) states that one needs to wait at least 96.8 hours to see the pseudo-steady state in the reservoir.

**Table 7-3.** Results of Build-up testing with reservoir parameters taken from Ecrin Saphir.

Name	Value	Unit
<b>Selected Model</b>		
Model Option	Standard Model	
Well	Vertical	
Reservoir	Homogeneous	
Boundary	Infinite	
<b>Main Model Parameters</b>		
TMatch	1.73E+6	[hr]-1
PMatch	0.0197	[psia]-1
C	7.16E-7	bbl/psi
Total Skin	2.79	--
k.h, total	841	md.ft
k, average	51.2	md
Pi	1150.91	psia
<b>Model Parameters</b>		
Well & Wellbore parameters (Tested well)		
C	7.16E-7	bbl/psi
Skin	2.79	--

### 7.2.2 BLACKOIL MODEL

Giving the fact that, in most of the reservoirs around the world, there's also gas phase flowing simultaneously with oil, there's an actual necessity to simulate the two-phase reservoirs in our study. For this purpose, BLACKOIL simulator is utilized. It's capable of simulating three phases (oil, gas and water) altogether. In order to be able to compare the simulator output data against the analytical method output for the reservoir model with the gas phase, a simple reservoir model was built by use of BUILDER through BLACKOIL simulator.

So, in this model there is again a well on the centre of the reservoir with the rate of  $80 \text{ m}^3/\text{day}$ , and after 116 days the well is closed until 130 days allowing the pressure to build-up. After the simulation, the following graph is obtained:

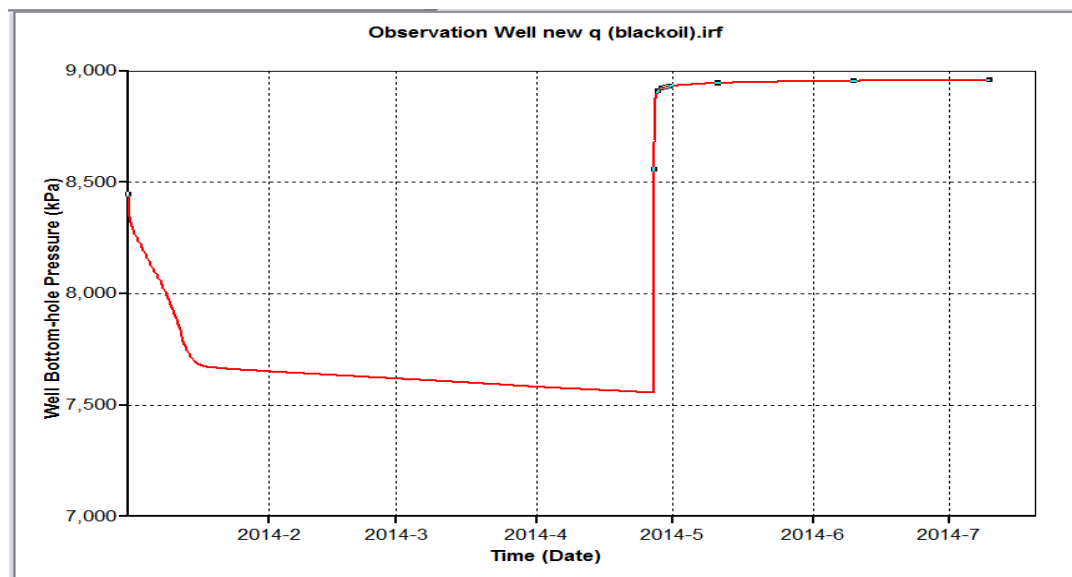


**Figure 7-3.** Bottom-hole Pressure of the well located on the centre of reservoir taken from CMG IMEX .irf file.

So, having obtained the pressure values in CMG IMEX, the next stage is conducting build-up testing in ECRIN. For this purpose, the reservoir parameters that were introduced to CMG IMEX – BUILDER were also introduced exactly as it is to ECRIN for the sake of consistency. Giving the fact that unlike the OILWATER model, there is now the gas phase as well flowing simultaneously through the reservoir, the effective permeability value in ECRIN simulator output is supposed to decrease. Before giving the difference in ECRIN graph, the results of build-up testing performed in ECRIN software can be shown as:

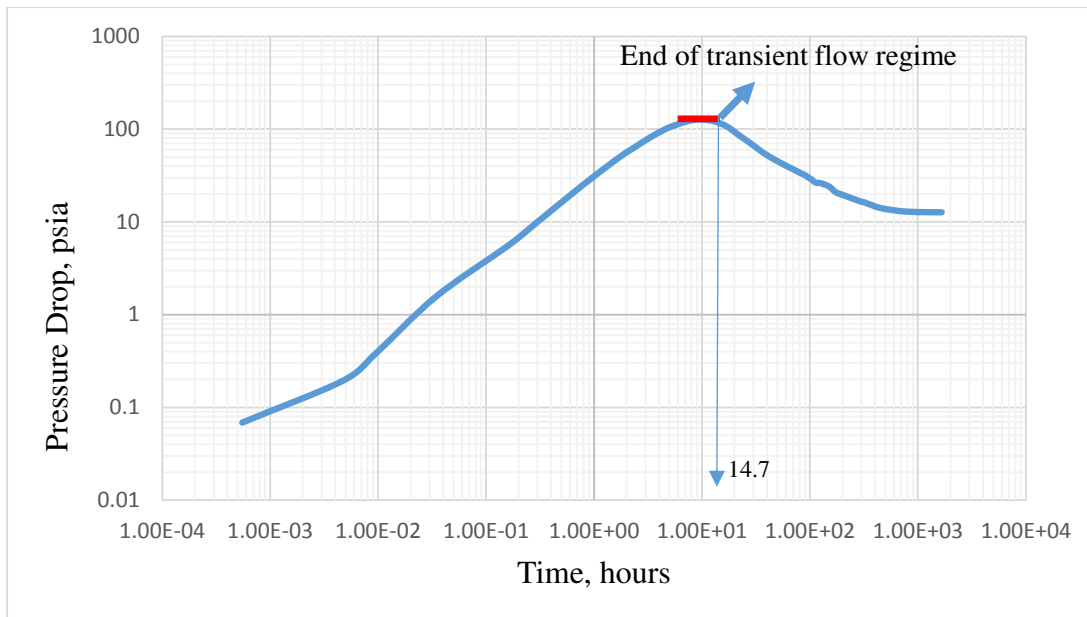


**Figure 7-4.** Diagnostic log-log plot of the BLACKOIL Reservoir Model.

As it can be seen the end of radial flow regime is now 15 hours. This result will later be compared with the end of radial flow regime value obtained from analytical methods. The following table illustrates the reservoir parameters results obtained from this simulation:

**Table 7-4.** Results of Build-up testing of BLACKOIL reservoir model.

Name	Value	Unit
<b>Selected Model</b>		
Model Option	Standard Model	
Well	Vertical	
Reservoir	Homogeneous	
Boundary	Infinite	
<b>Main Model Parameters</b>		
TMatch	5.11E+6	[hr]-1
PMatch	0.0121	[psia]-1
C	1.49E-7	bb/psi
Total Skin	8.05	--
k.h, total	516	md.ft
k, average	31.5	md
Pi	1311.62	psia
<b>Model Parameters</b>		
Well & Wellbore parameters (Tested well)		
C	1.49E-7	bb/psi
Skin	8.05	--

Now it can be seen that the effective permeability decreased to 31.5 md value because of presence of oil and gas competing for the same pore spaces. For instance, this value in OILWATER model equalled to 51.2 md.

➤ Analytical Calculations

The analytical calculation result that was performed for the previous case won't change for this case as well, because any fluid properties, reservoir shape and other parameters were not changed.

### 7.2.3 RESERVOIR MODELS WITH DIFFERENT SHAPES

In this section 2 different reservoir shapes - rectangular and squared shapes are considered, and then these results are compared with analytical methods in the upcoming chapter. Please note that all the other parameters remained the same with previous reservoir models with only reservoir shape distinction. The following figures depict the different shapes of reservoir models.

➤ Rectangular Shape

In this case rectangular shaped reservoir model which was built in CMG IMEX BUILDER. Once the runs have been performed and the pressure values have been acquired, the next stage is using these values in ECRIN software for the build-up testing. The following graph illustrates how the results look like in log-log diagnostic plot:

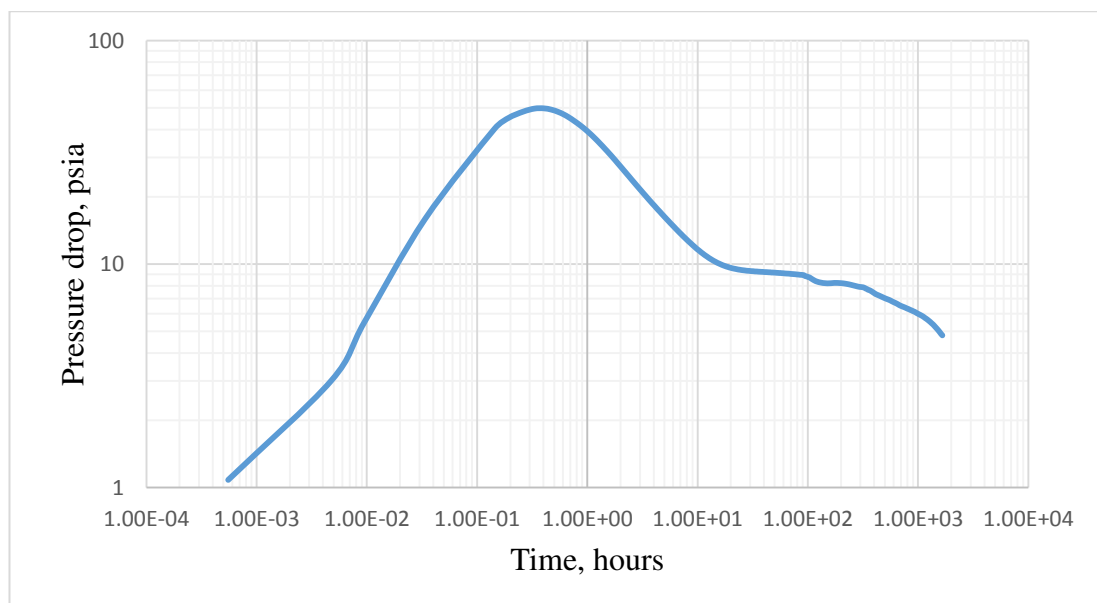


**Figure 7-5.** Rectangular shaped reservoir model log-log plot result.

From Ecrin Saphir build-up results it was found that the end of radial flow regime is 370 hours. In other words, it is needed to wait approximately 15 days for the pressure propagation to reach the boundary.

➤ Analytical Calculation for Rectangular shape

Please note that the fluid and rock properties remained the same for this case also with one distinction that now our shape factor is not 0.05, but 0.15 because of its rectangular shape. So, by using equation (7.1), the following result was obtained for this case:

$$t > 581 \text{ hours} \tag{7.3}$$

So, as it can be seen from result (7.3), analytical equations offer to wait more to see the boundary effect on log-log plot than numerical simulators for the rectangular reservoir shape.

➤ Square Reservoir Model

The next shape that is considered is square reservoir model. The following figure illustrates the shape of it:

Now the following figure depicts ECRIN build-up results:

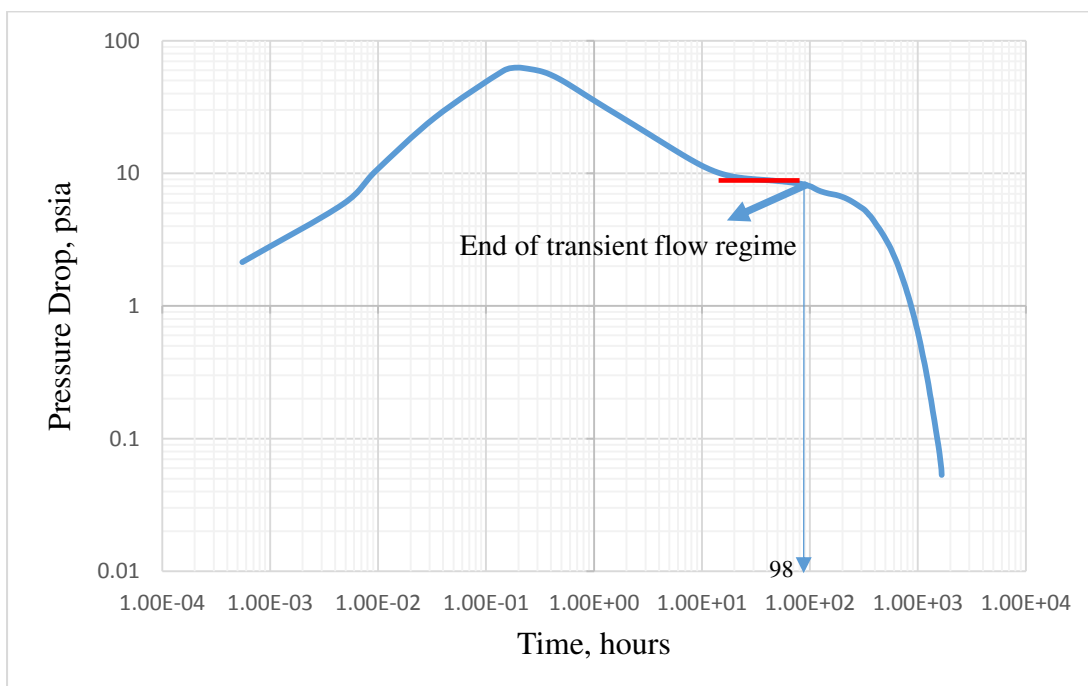


**Figure 7-6.** ECRIN build-up testing results for the squared reservoir model.

So, it is apparent that the end of radial flow regime is 98 hours. Now analytical calculations are considered for comparison.

➤ Analytical Calculation for Squared Reservoir.

Please be informed that the equation used in (7.1) was calculated for squared reservoir shape model with the same fluid and rock properties, and from (7.2) the end of radial flow regime was found as 96.8 hours.

#### 7.2.4 RESERVOIR MODELS WITH 2 WELLS

In this chapter 2 wells are considered which are producing close to each other to see how they affect the well test design through superposition principle.

So, for the first model where two wells are producing close to each other, a simple reservoir model was built. Observation well is producing in the middle of the reservoir and Well-2 is also producing adjacent to it. The following picture is taken from CMG IMEX illustrating how pressures are propagating from these wells:



**Figure 7-7.** 2 wells producing close to each other in a reservoir model.

This figure is taken from CMG IMEX output file with 3D view option. As it can be seen from the figure the boundary of the reservoir will be affected by pressure propagation from both Well-2 and Observation well. Obviously, because of superposition principle the pressure drop in Observation Well will be affected by the pressure drop in Well-2 and the difference in these two models will be shown after (with and without Well-2). So, the next plot illustrates the bottom-hole pressure drop in Observation well with another well operation adjacent to it:

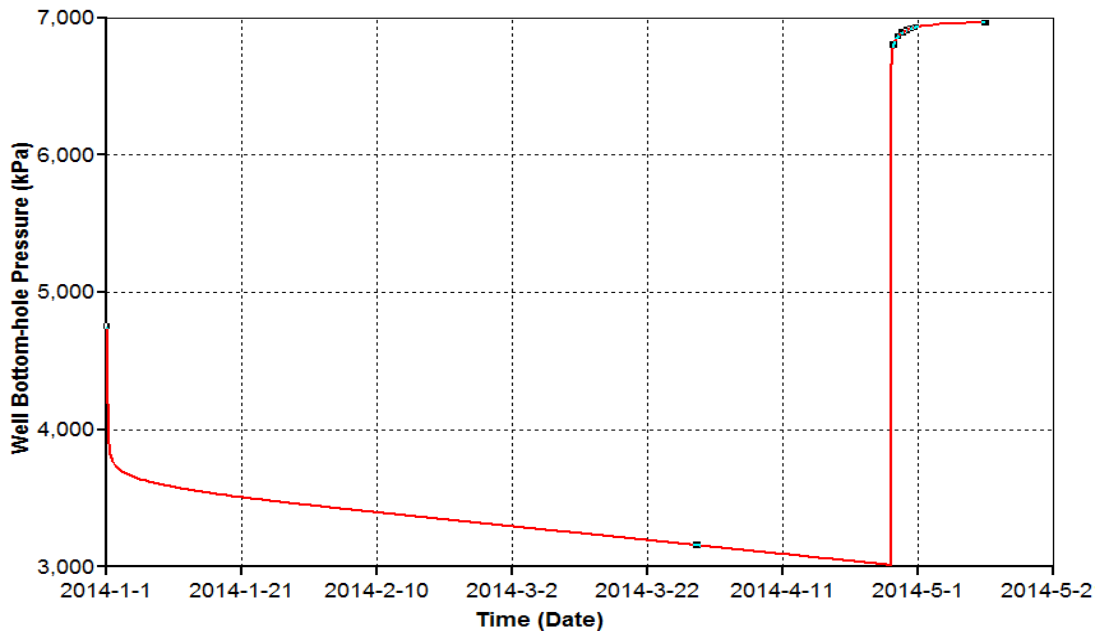


**Figure 7-8.** Bottom-hole pressure value for the Observation Well with another well operating adjacent to it.

Now the following plot describes the change of the bottom-hole pressure for the Observation well without any another well producing close to it:

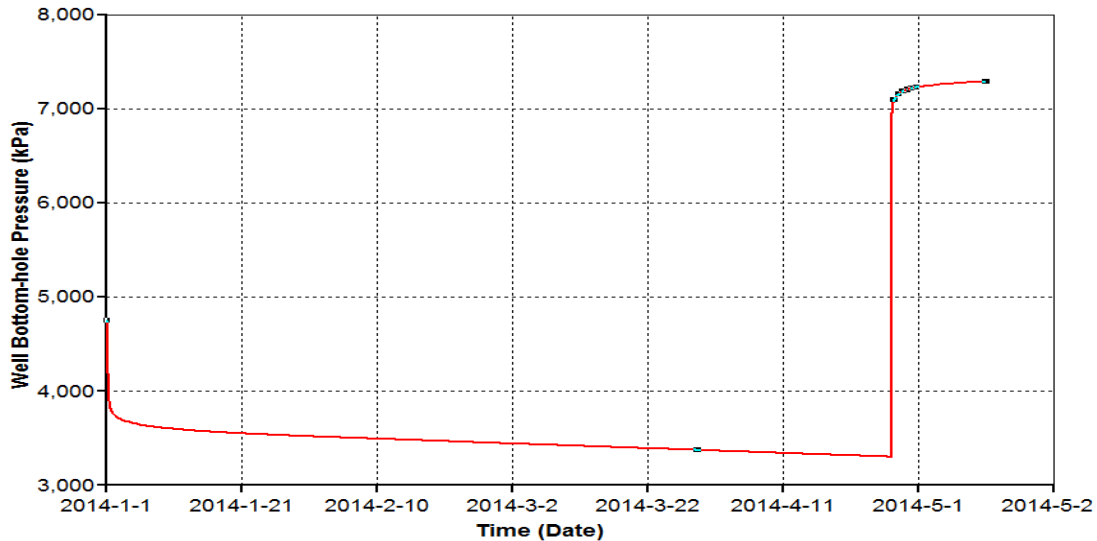


**Figure 7-9.** Bottom hole pressure value for the Observation well without another well producing close to it.

As it can be seen, the pressure range in this model never hits 3000 kPa pressure line, being always higher than that, whereas in previous model it is apparent that the pressure range line hits 3000 kPa line after some days of production, meaning the bottom-hole pressure decreased through superposition principle.

Back to the topic which is to investigate how it will affect our test design process, build-up testing in ECRIN Saphir was performed for the reservoir model where there are 2 operating wells. The following ECRIN output file describes the results:

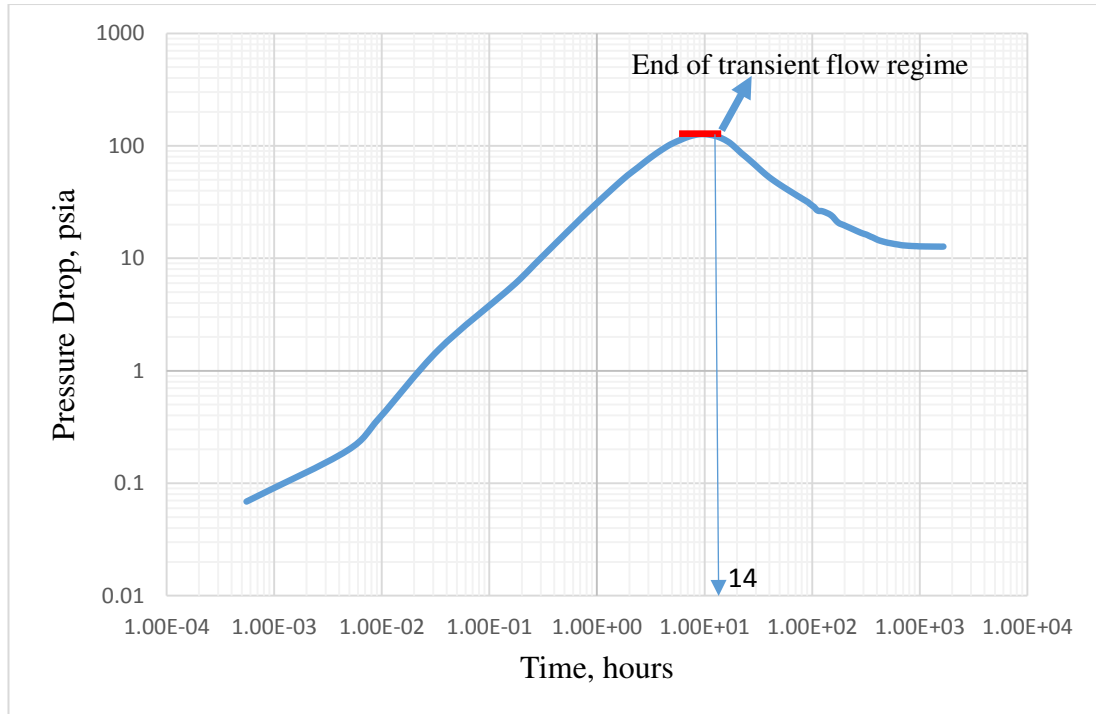


**Figure 7-10.** Build-up log-log testing plot in a reservoir model with 2 wells.

As the Figure 7-13 illustrates, it takes approximately 14 hours for the pressure propagation in Observation Well to reach the boundary because of the fact that Well-2 operating close to it is another boundary in a reference with Observation Well.

➤ Analytical Method for calculating pressure drop

The aim to perform analytical calculations here is to check how analytical results can be compared against the numerical simulators. For this purpose, analytically pressure drop value (pressure drawdown) can be calculated by using the following equation:

$$(P_i - P_{wf})_{total A} = -70.6 * \frac{q_A * B * \mu}{k * h} \left[ \ln \left( \frac{1688 * \phi * \mu * c_t * r_{wA}^2}{k * t} \right) - 2S_A \right] - 70.6 * \frac{q_B * B * \mu}{k * h} \left[ Ei \left( \frac{-948 * \phi * \mu * c_t * r_{AB}^2}{k * t} \right) \right] \quad (7.4)$$

Equation 7.4 is used for this purpose taking into account of superposition principle since during the calculations pressure values only up to shut-in time are referred, because until that time the reservoir acts as if it's infinite in size (L.P.Dake, 1998).

So, after the calculation the pressure drop equalled to 449.336 psia. Please note that the 2.1 days were taken as a reference time for calculating this expression. Whereas from CMG it was found that this value – the pressure drawdown equals to 542.584 psia. So, if to continue to calculate pressure drop for some series of time, the following plot is obtained showing how analytical pressures are different from numerical simulators:

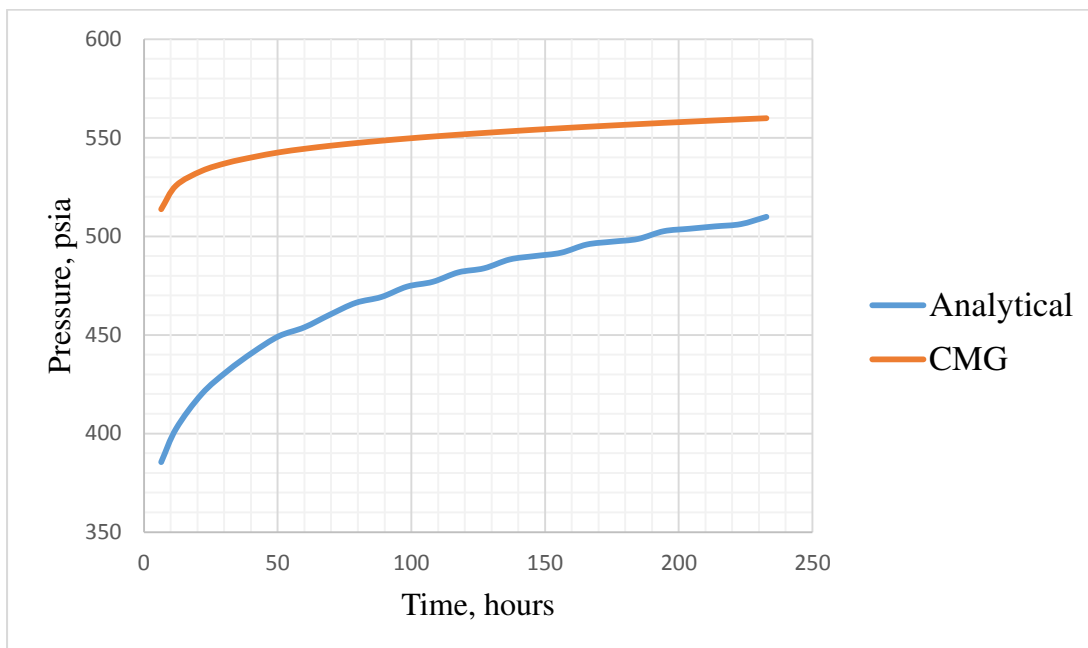


**Figure 7-11.** Pressure drop value differences between analytical and numerical results.

### 7.2.5 RESERVOIR MODEL WITH VERTICAL FAULT

In this part of work the reservoirs models with and without fault will be considered, because most of reservoirs around the world contain faults to some extent, and there is an actual necessity to implement our study for the reservoirs with faults.

For this purpose a simple reservoir model in CMG IMEX was built, and after the run following figure was obtained:

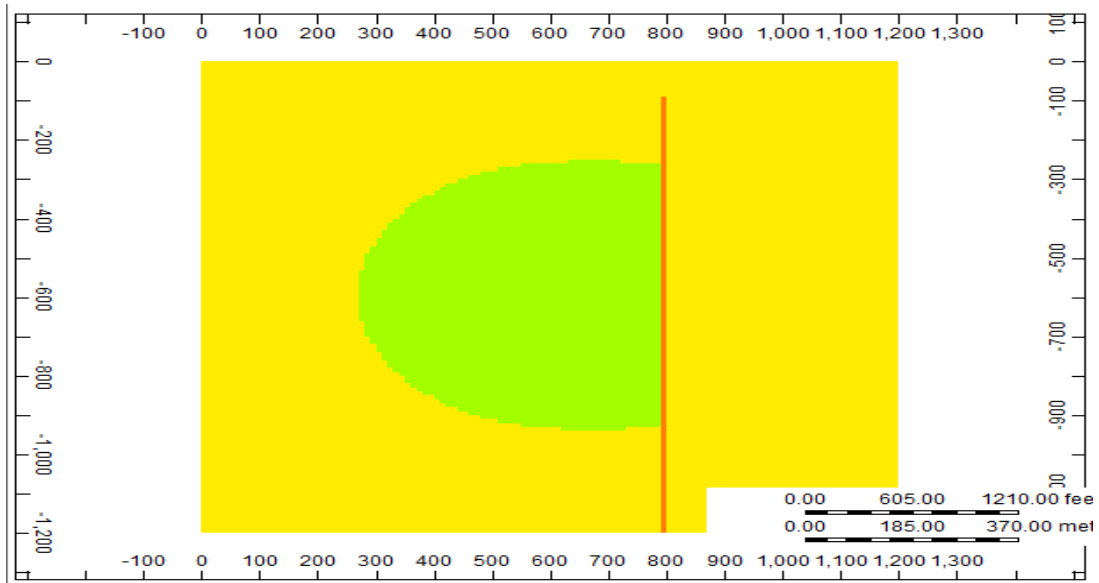


**Figure 7-12.** Reservoir Model with a well producing close to vertical fault.

After the simulation, by using the pressure values in CMG IMEX, a build-up testing was performed in ECRIN Saphir and end of radial flow regime was checked as well as the time when the second straight line begins to be conspicuous because of the fault was also investigated. So, having acquired the pressure values, the following ECRIN result was acquired:

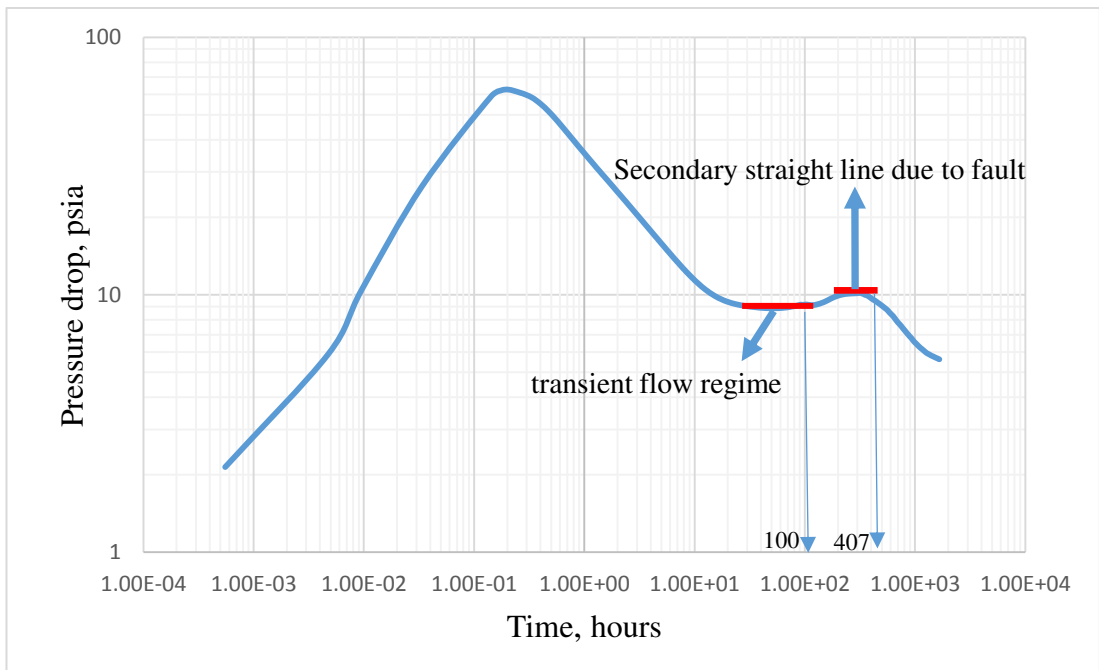


**Figure 7-13.** ECRIN build-up log-log plot for the reservoir with the vertical fault.

It can be seen that after 100 hours, the second line goes up and stabilizes because of the fault. Late Time Regions starts to be noticed after 407 hours. The following

ECRIN Saphir log-log plot for the reservoir model without any fault is illustrated for the comparison between these two models:

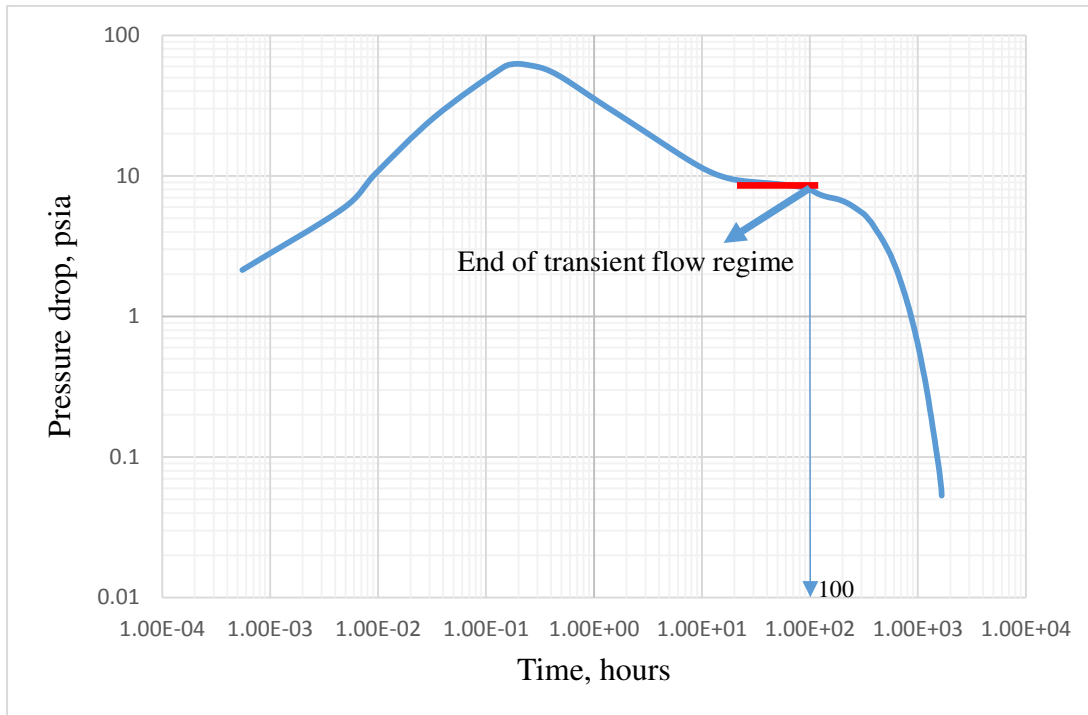


**Figure 7-14.** ECRIN build-up testing results for the reservoir model without any fault.

In this model, in Late Time Region the line goes down after 100 hour indicating the pressure support from the aquifer without any fault, whereas in the previous model the line goes up after exactly 100 hour because of fault presence.

➤ Analytical Calculation for vertical fault model

Analytically, it can be estimated the time when the second straight line goes up and stabilizes by using the following equation:

$$t = \frac{\phi * \mu * c_t * r_w^2 * t_D}{2.64 * 10^{-4} * k} \quad (7.5)$$

So, using the information below, it's estimated that:

$$t_D = 0.08 r_{dD}^2;$$

$$r_{dD} = 2L/r_w;$$

$$r_{dD} = 2 * 656.168/0.25 = 5249.344$$

$$t_D = 0.08 * 5249.344^2 = 2.204449 * 10^6;$$

$$t = \frac{\phi * \mu * c_t * r_w^2 * t_D}{2.64 * 10^{-4} * k} = 335 \text{ hours} \quad (7.6)$$

Analytical calculations show one needs to wait at least 335 hours to see the starting time for the second stabilizing line as opposed to 100 hour from Ecrin Saphir results based on CMG IMEX pressure data.

### 7.2.6 RESERVOIR MODEL WITH INCLINED FAULT

Unlike the previous case, in this model a model with inclined fault will be considered, not vertical. It is not secret that reservoirs around the world are comprised of not only vertical but also inclined faults. So, from that sense there is an actual necessity to implement this study for this kind of reservoirs also. Structured gridding simulates the inclined fault geometry in zig-zag method when the fault geometry is not parallel to the orientation of the structured grids. The following figure depicts how inclined fault looks like in CMG IMEX simulator:

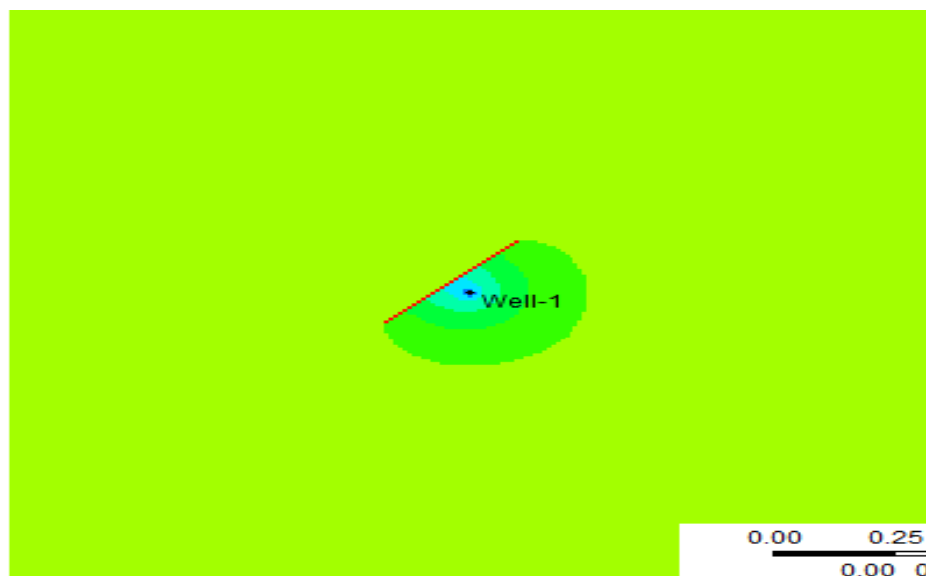


**Figure 7-15.** Reservoir model with inclined fault built in CMG IMEX simulator.

So, after acquiring pressure values for the reservoir model with the inclined fault the next stage is proceeding with the ECRIN to implement the build-up testing in this reservoir model. The following figure illustrates the build-up result:

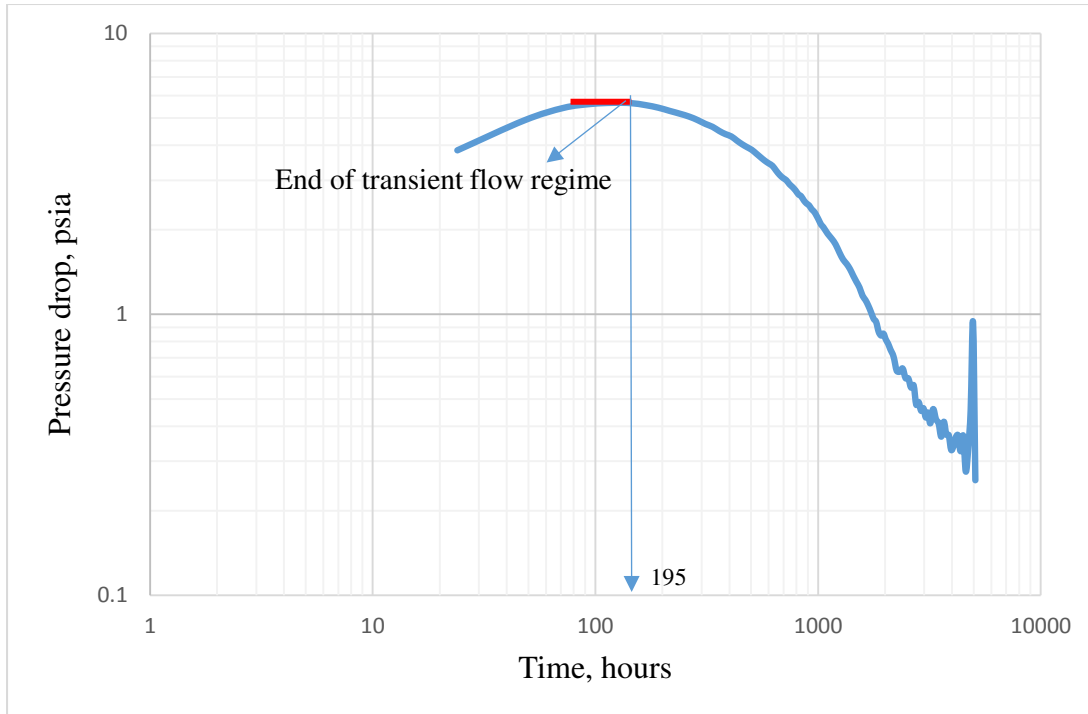


**Figure 7-16.** Build-up result on a reservoir model with inclined fault model by use of ECRIN software.

In this model the Late Time Region starts to be noticed after 195 hours as against to 335 hours with analytical model calculations.

➤ Analytical Calculation

Analytical calculations results for this case won't change, because no fluid and rock properties were changed. So, analytically one needs to wait at least 335 hours to see the second straight line in log-log plot according to equation (7.6).

**7.3 Part – 2.** Use of ECRIN Rubis and CMG IMEX

As it was mentioned before, the aim for this part is to check the applicability of Voronoi gridding by use of ECRIN Rubis module. Now there are 2 cases: undersaturated and saturated reservoirs.

### 7.3.1. UNDERSATURATED

As the name implies, in this case there is only oil without gas phase. In order to assess the Voronoi gridding simulation for well test design, a reservoir model was built for different scenarios by use of Ecrin Rubis. For the comparison, the same reservoir model with the same fluid and rock properties was built by using CMG IMEX. Then numerical simulations were performed for both models and the results were compared. It's ubiquitously known fact that for the correct well test design one needs to select optimum value of production rate, build-up time and production time. In order to come up with the reasonable selection of these values, it was considered to build models by taking into account the following scenarios:

- **Case 1** – 150 days production, 214 days build-up, 80 stb/day rate.

In this case, production continues for 150 days, shut in time lasts for 214 days, rate is 80 stb/day. For this case, the same reservoir model in CMG IMEX and Ecrin Rubis was built, build-up testing in Ecrin Saphir was conducted and then it was compared how these two pressure values from Ecrin Rubis and CMG IMEX match with each other.

#### ✓ *Ecrin Rubis Model*

The reference time was set for Ecrin Rubis as 01.01.2015. The well has been producing for 150 days, then shut-in the well for build-up for 214 days, and simulation runs last until 31.12.2015. After the initialization of the model prior to simulation, the following figure appears:

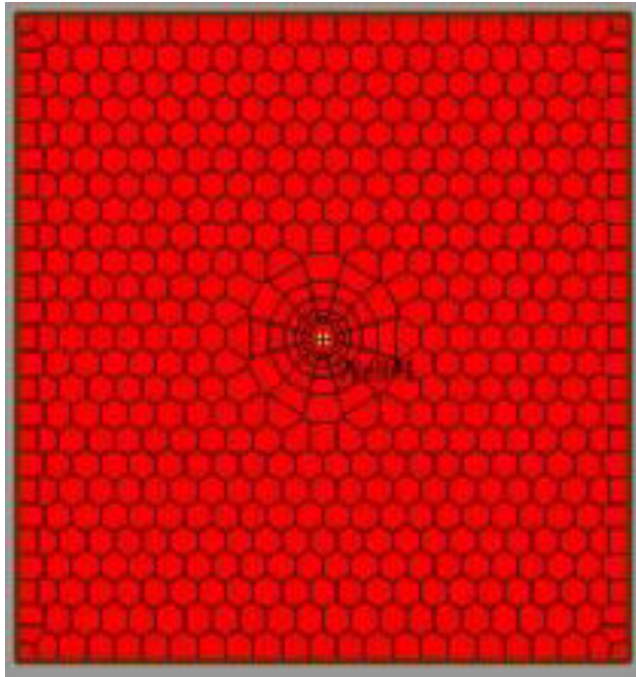


**Figure 7-17.** Voronoi Gridded reservoir model built in Ecrin Rubis.

When it comes the properties of oil in Rubis, it was specified exact correlations for both CMG IMEX and Ecrin Rubis so that these properties can be equalized. Oil Formation Volume Factor from Standing, oil compressibility from Vasquez-Beggs, and oil viscosity from Beggs-Robinson correlation were referred. After the simulation the following figure is obtained:

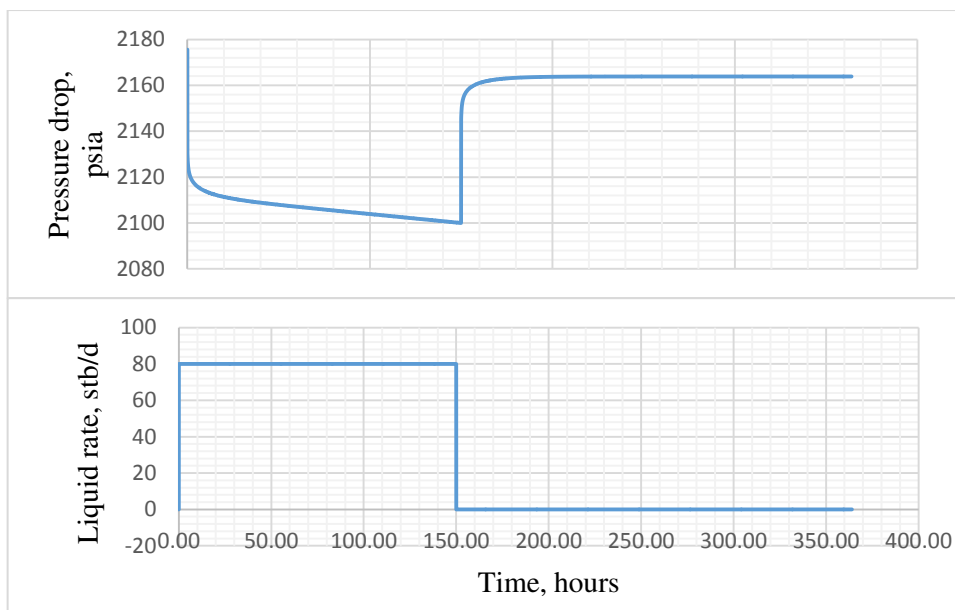


**Figure 7-18.** Pressure-Rate plot for Undersaturated case taken from Ecrin Rubis.

✓ *CMG IMEX Model*

Once pressure values have been acquired from the Ecrin Rubis, then the same reservoir model with the same fluid properties was built in CMG IMEX Builder. The same fluid properties were introduced to CMG for the sake of consistency with Rubis module. Having built the model, the following structured gridding the program yields:

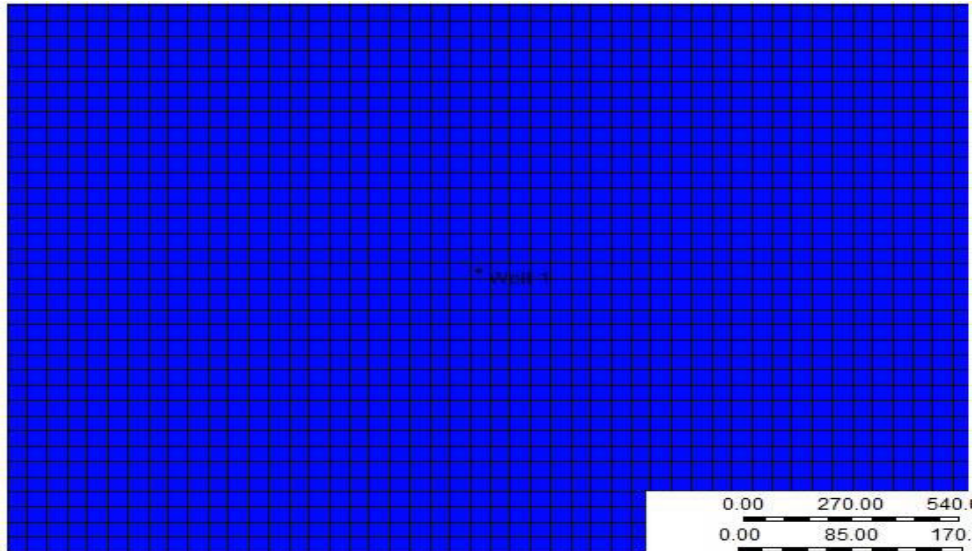


**Figure 7-19.** Reservoir gridding built and taken from CMG IMEX.

After that a simulation runs were performed and for the Well-1 located in the centre of the reservoir the following figure was acquired illustrating the bottom-hole pressure values change:

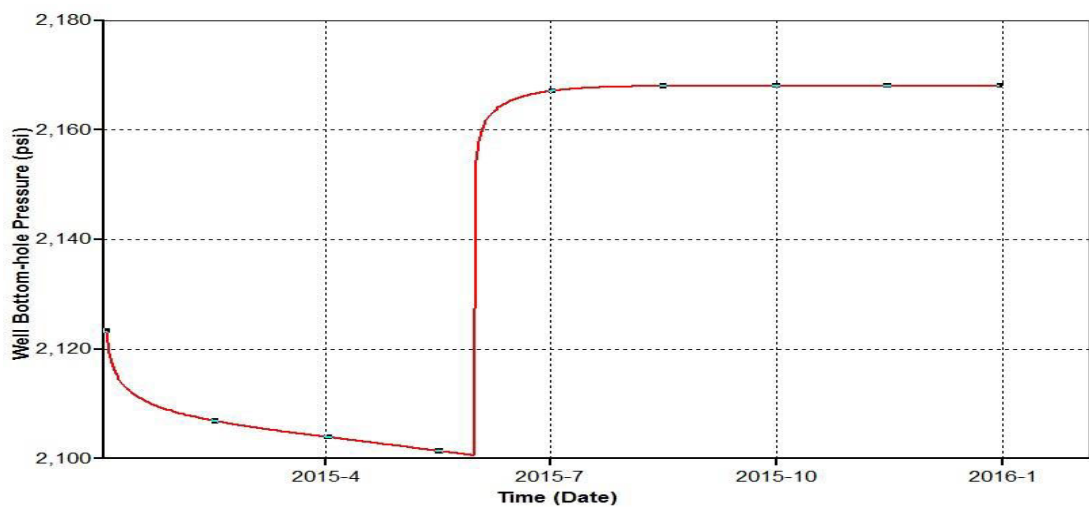


**Figure 7-20.** Well bottom-hole pressure for Well-1 taken from CMG IMEX.

✓ *Ecrin Saphir results for Case-1*

The next stage is performing build-up test by using Ecrin Saphir based on Rubis pressure values. Initial conditions and the same fluid with reservoir properties were introduced to Saphir, then the following build-up log-log plot was appeared:

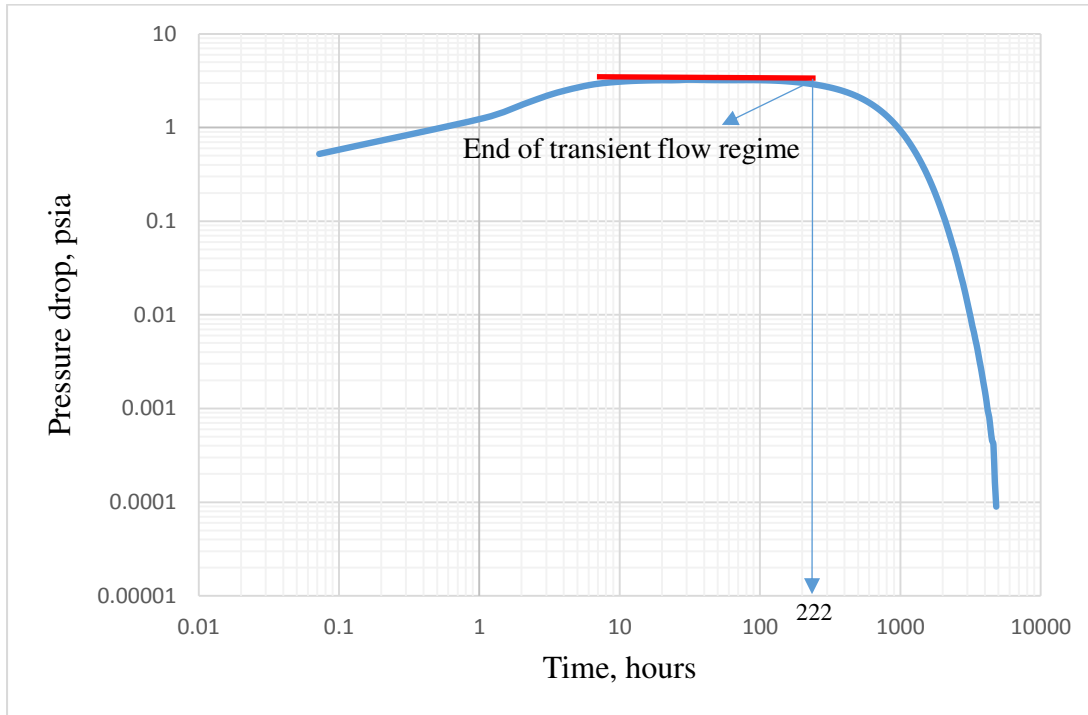


**Figure 7-21.** Ecrin Saphir log-log build-up plot for case 1.

Here it can be seen that the end of radial flow regime happens after 222 hours.

✓ *Analytical Method*

For the analytical calculations, the following equation was used:

$$t > \frac{\phi * \mu * c_t * A * t_{DA}}{2.637 * 10^{-4} * k} \quad (7-1)$$

Giving the values of porosity 0.2 md, viscosity 0.4957 cp, total compressibility 3.218E-6 1/psi, area is  $10^8 \text{ ft}^2$ , shape factor is 0.05, then t needs to be higher than 209 hours. It's the time when one needs to wait more than 209 hours to pass to pseudo-steady state from transient flow regime.

- **Case 2.** 150 days production, 214 days build-up, 500 stb/day higher rate.

In this case production and build-up time doesn't change, but the well is producing with higher production rate – 500 stb/day. In this case the purpose is to see the effect of high production rate on the well test design. For that purpose the same model was built in Ecrin Rubis with only production rate input data distinction. After that, Rubis yields the following pressure-rate data plot:

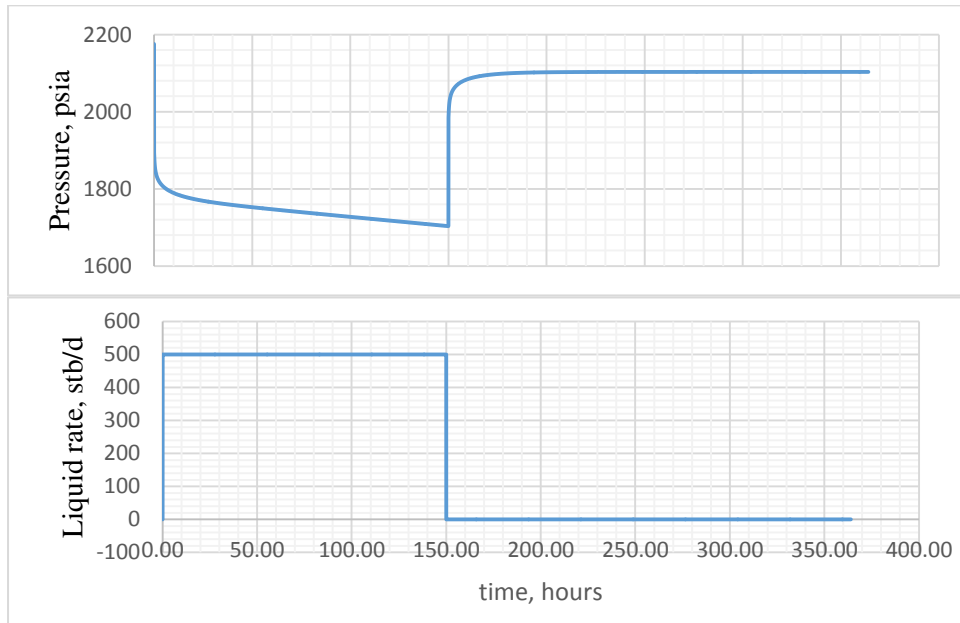


**Figure 7-22.** Pressure-Rate plot for the case 2 taken from Ecrin Rubis.

Then based on these pressure values derived from Rubis, it was conducted build-up pressure testing on Ecrin Saphir, and obtained the following log-log plot:

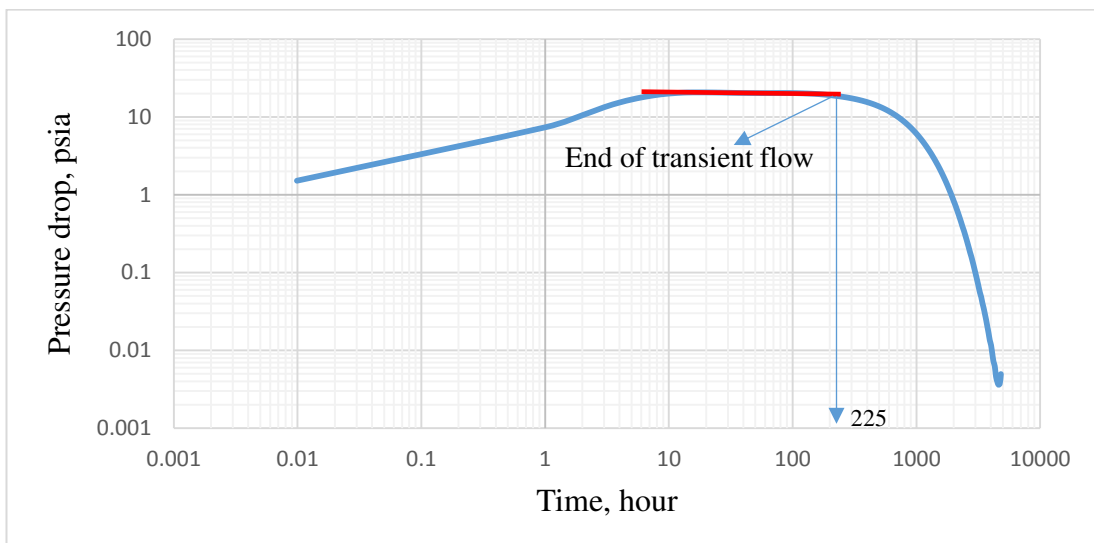


**Figure 7-23.** Ecrin Saphir build-up results for case 2.

From Figure 7-24 it can be seen that the end of radial flow regime is 225 hours. Analytical calculations for this case won't change, because no fluid and rock properties were changed, shape factor won't change also, because the reservoir is in the same shape.

- **Case 3.** 3 days production, 214 days build-up, 80 stb/day rate.

In this case the production time for the well is 3 days, build-up time is the same of 214 days, and the rate is 80 stb/day. The aim for this case is to see the shorter production time effect on well test design parameters, and to figure out the optimum production time. Again the same reservoir model was built in Rubis and after the simulation it gave the following plot:

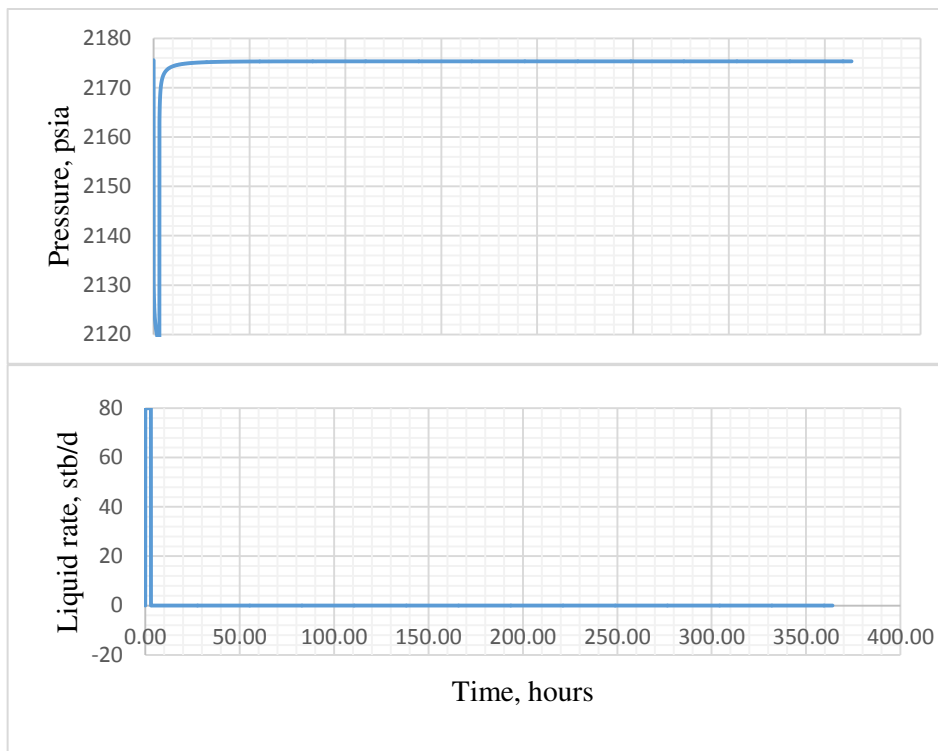


**Figure 7-24.** Pressure-Rate plot for case 3.

And based on the Rubis pressure values, build-up testing on Ecrin Saphir is performed to see the end of the transient flow regime:

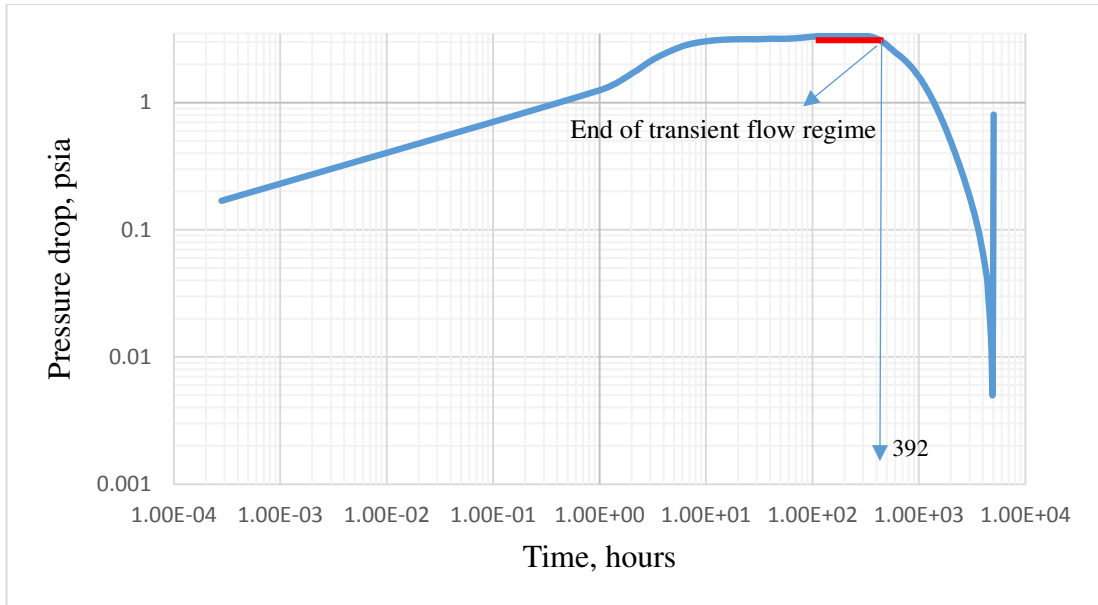


**Figure 7-25.** Build-up log-log plot testing on Ecrin Saphir.

Now it's obvious from the figure that end of radial flow regime changed to 392 hours, because the pressure disturbance is weak due to very short production time, it takes much longer to reach the boundary.

Again analytical calculations are not performed, because no properties were changed.

- **Case 4.** 10 days production, 214 days build-up, 80 stb/day rate.

In this case by stating normal production, it is meant production lasts for 10 days, long build-up again lasts for 214 days, and normal rate is 80 stb/day. For this case again Rubis simulations were conducted and the following pressure-rate plot were achieved:

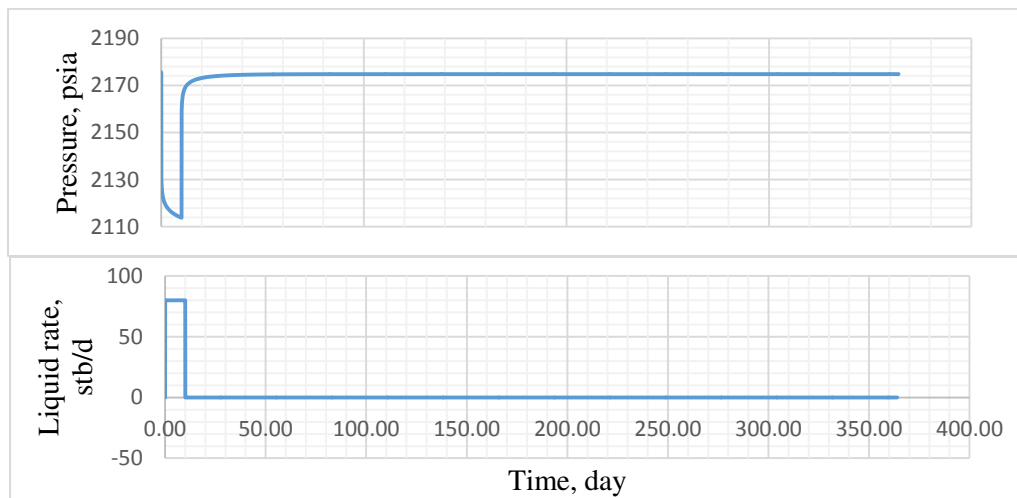


**Figure 7-26.** Rubis pressure-rate plot for the case 4.

After that, based on these pressure values build-up testing on Ecrin Saphir can be conducted and following figure illustrates that:

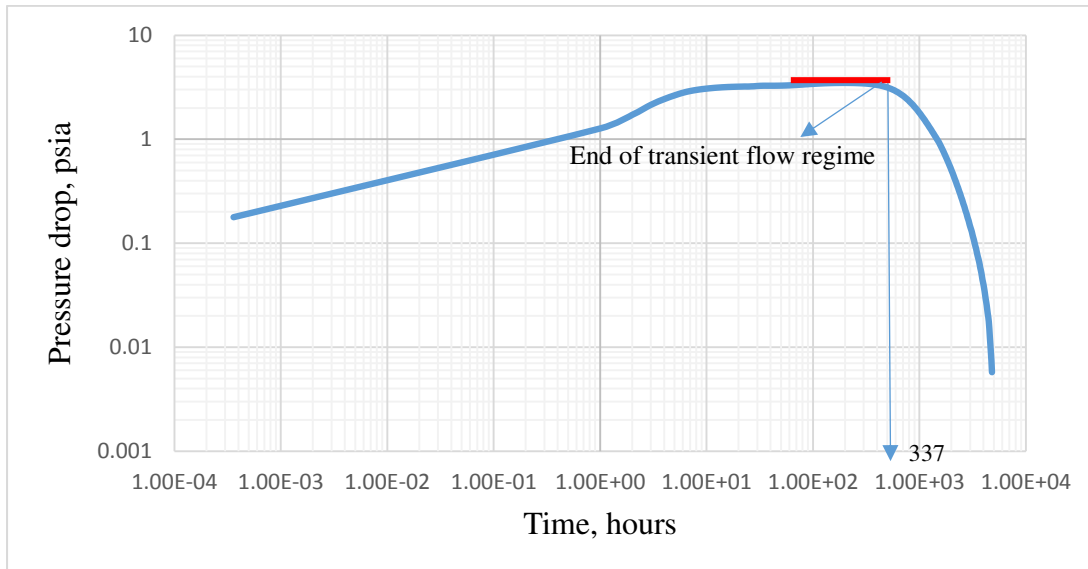


**Figure 7-27.** Ecrin Saphir build-up log-log plot for the case 4.

From Figure 7-28, it's seen that the end of flow regime is 337 hours.

- **Case 5.** 10 days Production, 2 days short build-up, 80 stb/day rate.

In this case normal production lasts for 10 days, very short build-up is 2 days, and normal rate is 80 stb/day. The aim here is to check if the well is closed for very short time how it will affect well test design parameters. The same reservoir model with the same rock and fluid characteristics was built in Ecrin Rubis model, and after the simulation the following figure was obtained:

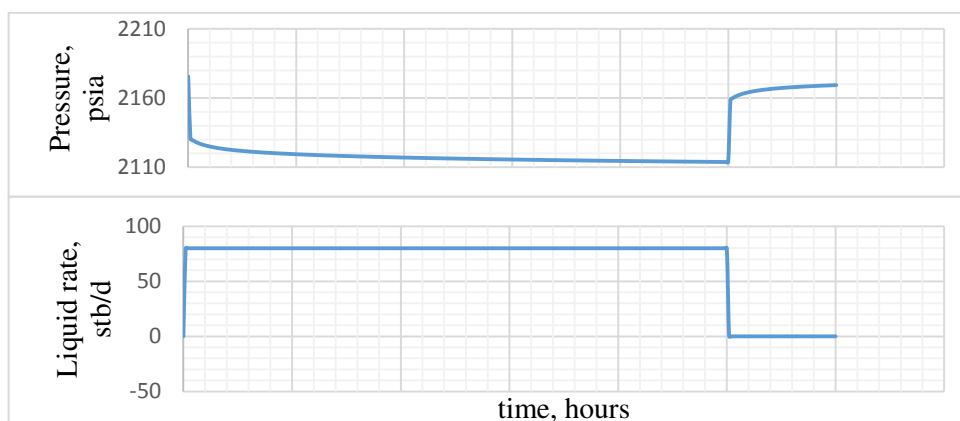


**Figure 7-28.** Ecrin Rubis pressure-rate plot for the case 5.

Now it can be performed build-up testing on Ecrin Saphir based on these pressure values to see end of the transient flow regime:

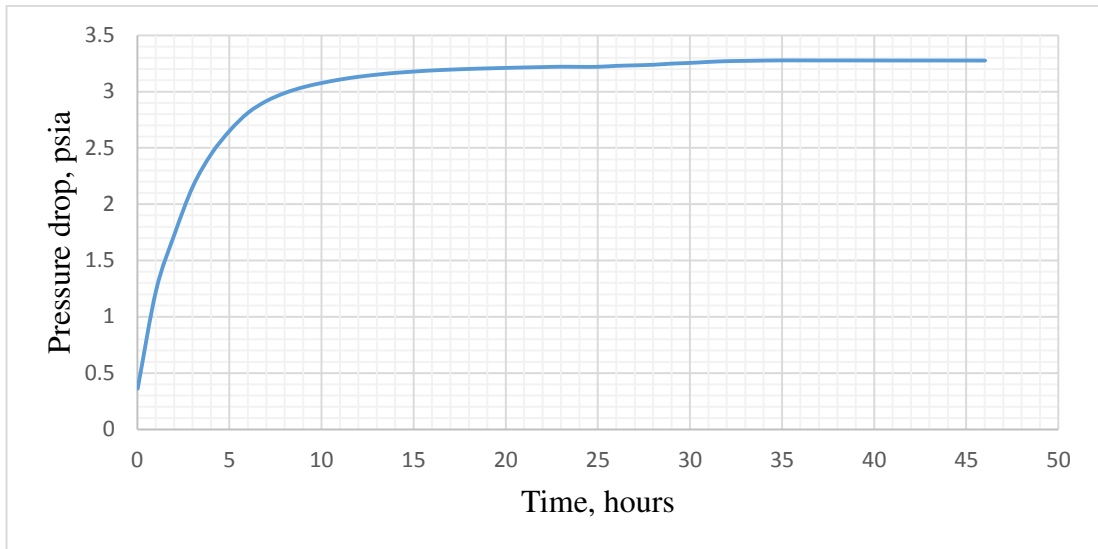


**Figure 7-29.** Ecrin Saphire log-log build-up testing for the case 5.

Because of limited amount of shut-in time Late Time Region is not detected in log-log plot. It shows the reservoir is producing only in transient regime.

- **Case 6.** 52 days Production, 78 days build-up, 80 stb/day rate.

In this case, production time was set as 52 days, build-up time as 78 days, and production rate is 80 stb/day. Again for this case the same reservoir model was built in Ecrin Rubis and numerical simulations were performed. After that, the following figure was obtained:

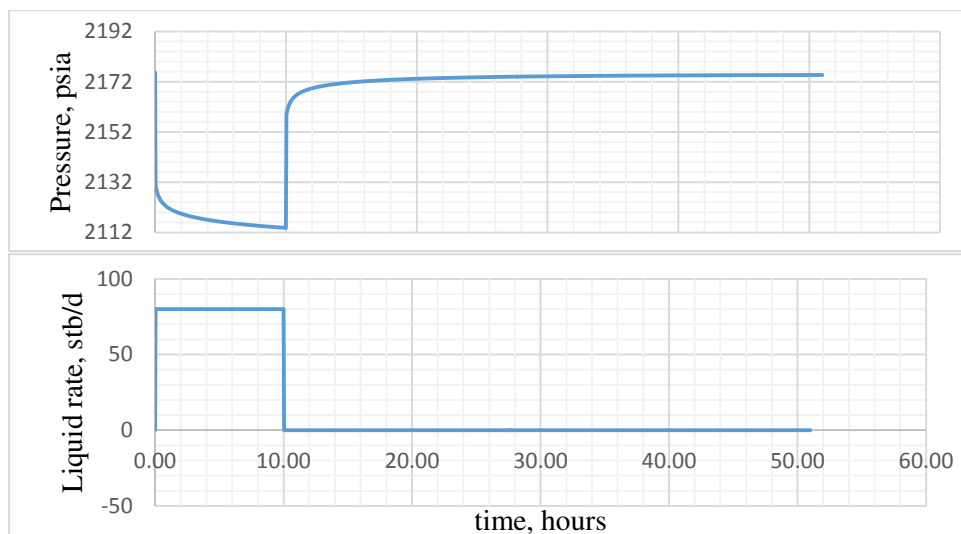


**Figure 7-30.** Ecrin Rubis pressure-rate plot for the case 6.

Now build-up testing can be carried out on Ecrin Saphir based on these pressure values. So, Saphir yielded the following log-log plot:

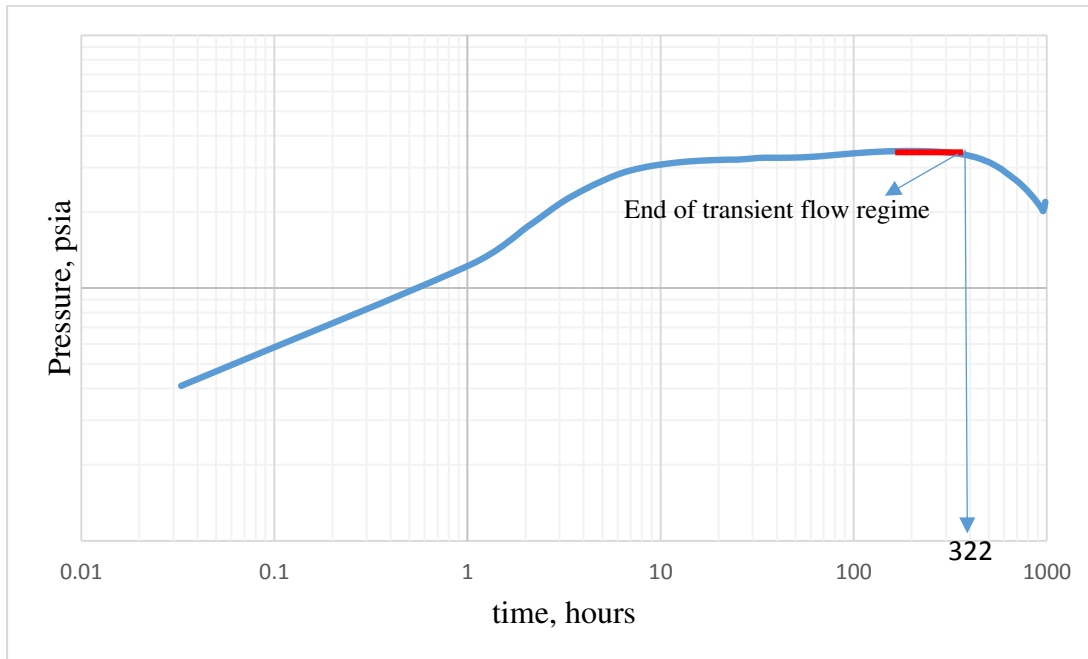


**Figure 7-31.** Ecrin Saphir build-up log-log plot for the case 6.

In this case, the Late Time Region can be detected as well because of optimum production rate, duration and build-up time. Time to pass to pseudo-steady state is 322 hours.

- **Case 7.** Under-saturated Reservoir Model with horizontal Fault.

In this case horizontal fault was added to our model to see how the presence of fault alter the well test design parameters. For this case the same reservoir model was used both in Ecrin Rubis and CMG IMEX with the same rock and fluid properties with the presence of fault. Then build-up testing was performed on Ecrin Saphir by using both simulators pressure values. The fault length is 4000 ft, the distance between the fault and well is 500 ft. These fault parameters were kept fixed in both simulators for the consistency.

✓ *Ecrin Rubis Module*

In order to be able to assess how Voronoi gridding technique is applicable when there's a fault in the reservoir, it was performed simulations runs on Ecrin Rubis module. The following image illustrates the location of well and fault:

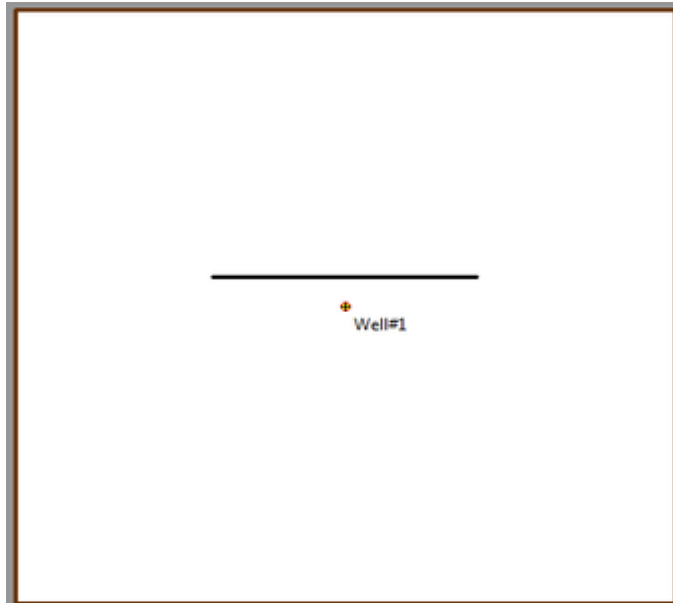


**Figure 7-32.** Ecrin Rubis module for the under-saturated horizontal fault.

The following figure illustrates how unstructured gridding simulates horizontal fault:

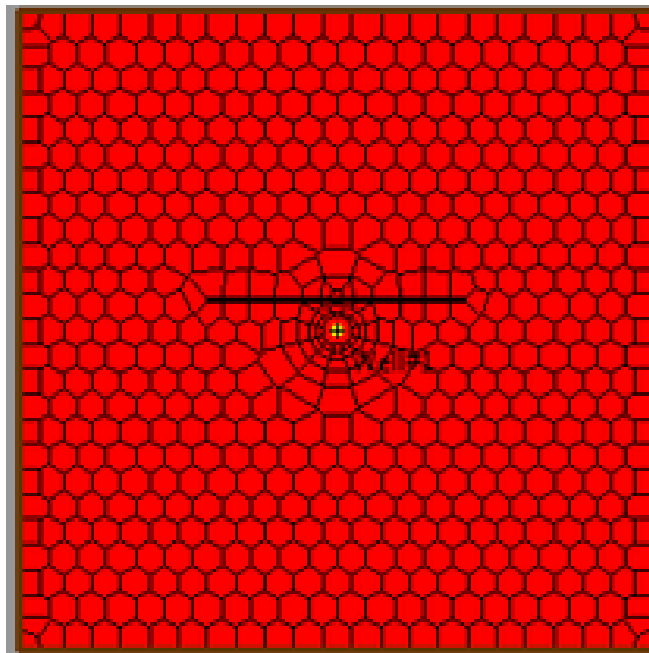


**Figure 7-33.** Ecrin Rubis under-saturated reservoir model with horizontal fault.

Having built the model, simulation runs were performed on Rubis and the following pressure-rate plot was obtained as a result:

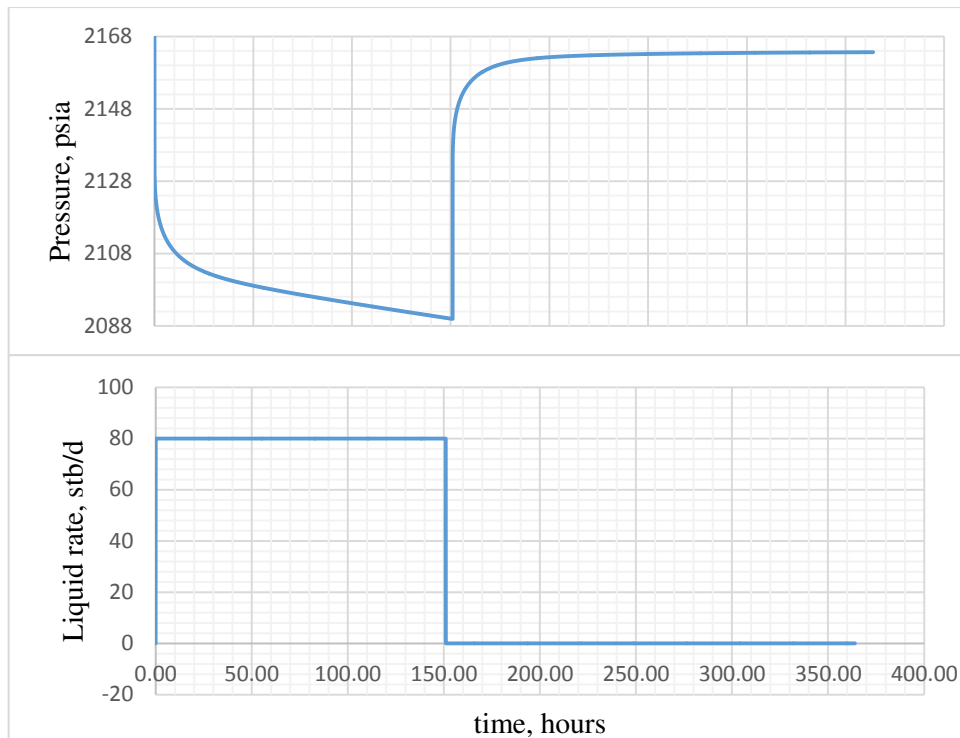


**Figure 7-34.** Rubis Pressure-rate plot for the undersaturated reservoir model with horizontal fault.

✓ *CMG IMEX Module*

In this model the same reservoir model with the same fluid, rock and fault parameters was built to compare the structured gridding applicability versus unstructured gridding accuracy. The following figure illustrates how the model looks like in structured gridding:

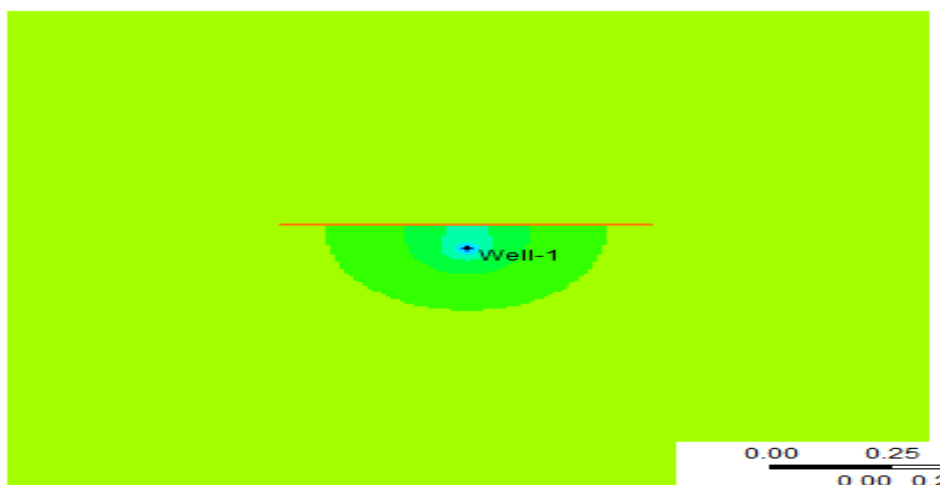


**Figure 7-35.** CMG IMEX Model with horizontal fault for the under-saturated reservoir case.

Having obtained that, simulation runs can be performed on this model from which the following figure was obtained illustrating the pressure values change for the Well-1 located in the middle of the reservoir:

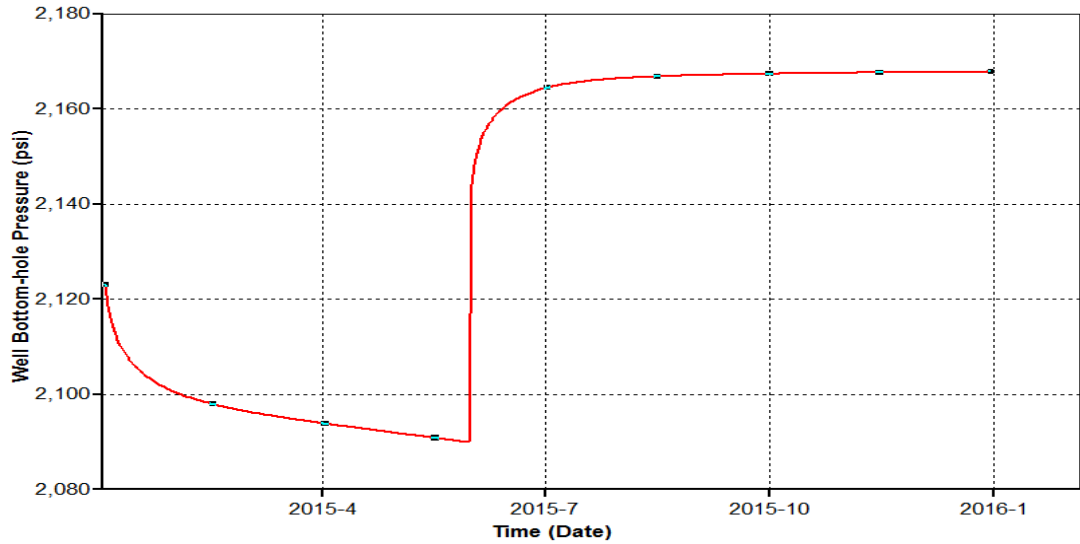


**Figure 7-36.** Bottom-hole pressure change for well-1 taken from CMG IMEX.

✓ *Ecrin Saphir*

Now after acquiring pressure values from both simulators for the same reservoir model with the same fault properties, build-up testing was performed by using Ecrin Saphir. The following figure illustrates build-up plot based on Rubis pressure values:

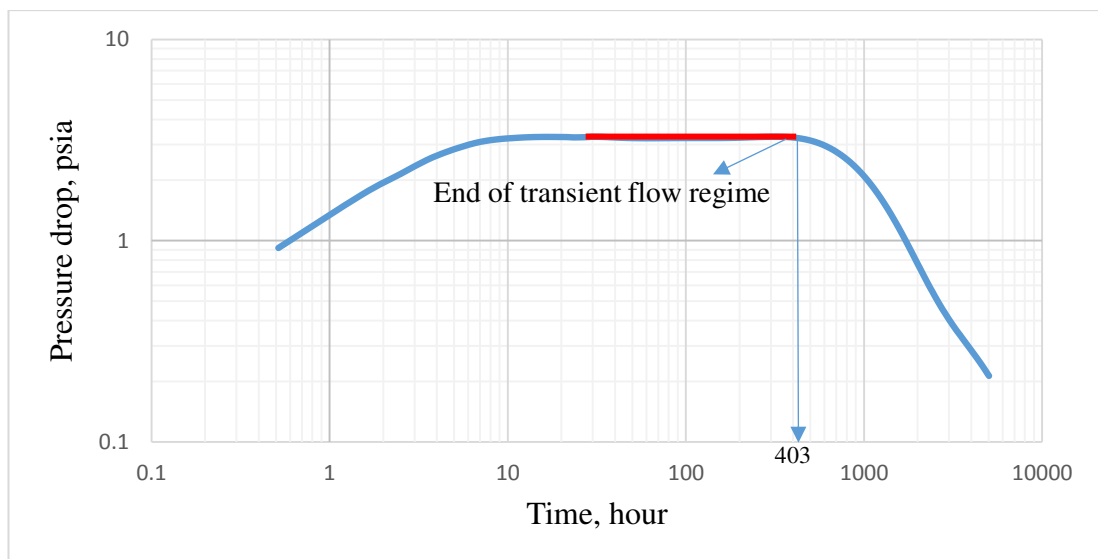


**Figure 7-37.** Ecrin Saphir build-up log-log plot based on Rubis pressure values for under-saturated reservoir model.

After that, build-up testing was implemented on Ecrin Saphir based on CMG IMEX pressure values. The following log-log plot illustrates that:

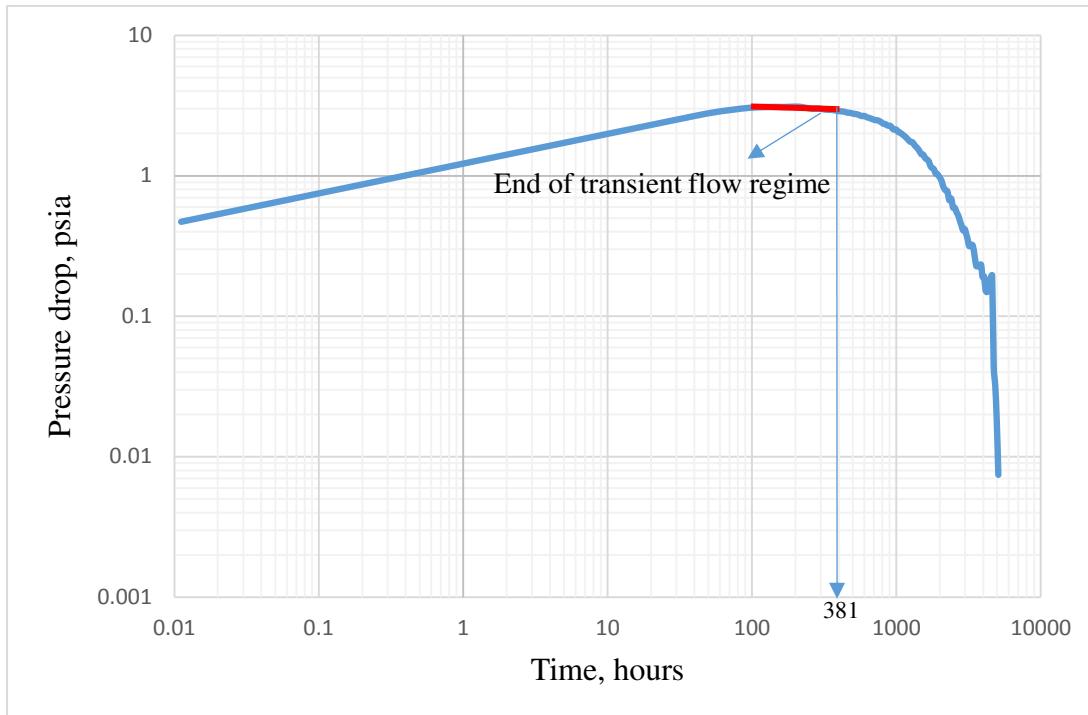


**Figure 7-38.** Ecrin Saphir build-up log-log plot for the undersaturated reservoir model with fault by using CMG IMEX pressure values.

In Rubis model, it can be seen that the transition time required to reach the pseudo-steady state is 403 hour, whereas in CMG IMEX model it is 381 hours. So, there's a fair agreement between these models.

- **Case 8.** Under-saturated Reservoir model with inclined fault

In this case deviated fault model was introduced and compared how unstructured gridding technique can match with structured gridding technique. In theory, unstructured Voronoi gridding offers more flexibility especially when this kind of deviated faults are involved. For the support of this theory the previous procedure for the horizontal fault model were repeated step-by-step.

✓ *Ecrin Rubis Module*

In this part the fault orientation from horizontal to inclined model was changed to see how unstructured Voronoi gridding cope with this challenge. The following 2D image shows the fault orientation and the well in the centre of the reservoir:

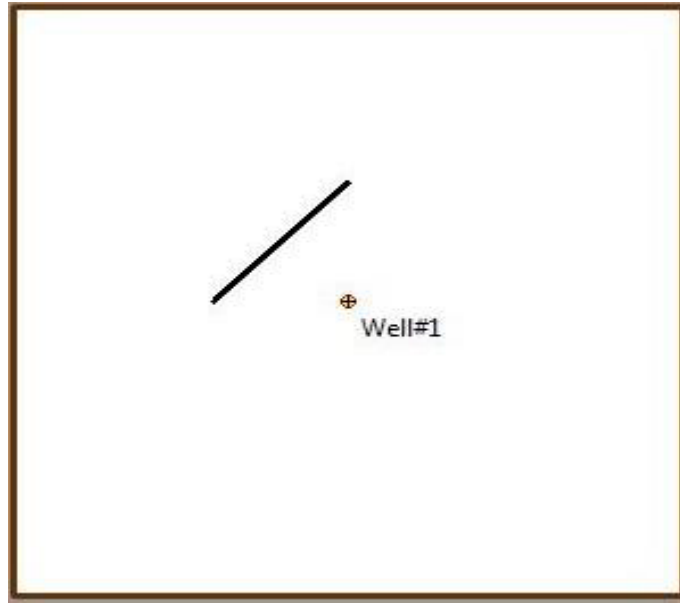


**Figure 7-39.** Undersaturated reservoir model with inclined fault built on Ecrin Rubis.

The following plot illustrates how unstructured Voronoi gidding represents inclined fault model in Ecrin Rubis:

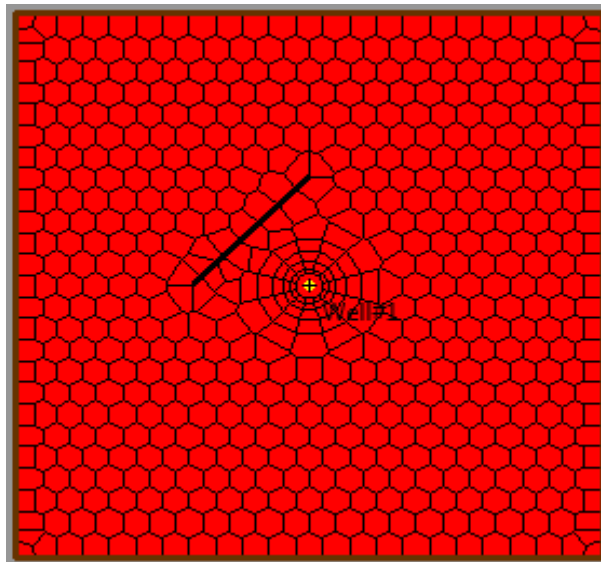


**Figure 7-40.** Ecrin Rubis Module representing inclined fault model for undersaturated reservoir case.

Now after building the model and specifying inclined fault to the model, simulation runs for this model were performed. The following figure illustrates the pressure-rate plot for this run:

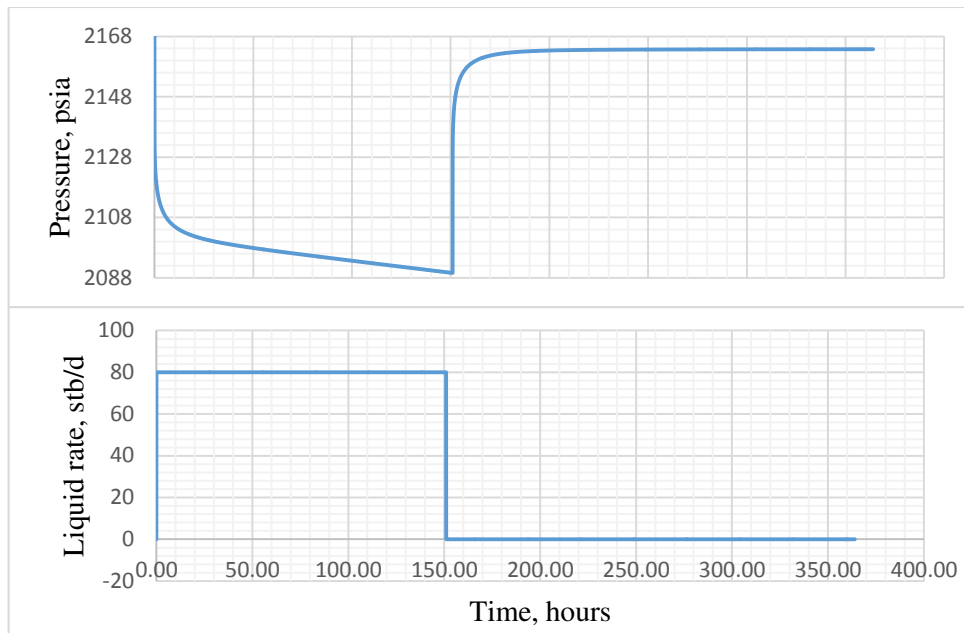


**Figure 7-41.** Ecrin Rubis pressure-rate plot for the undersaturated reservoir model with inclined fault.

✓ *CMG IMEX Module*

In order to be able to assess the applicability of structured gridding technique for the deviated fault models, the inclined fault was introduced to our model in CMG IMEX. But now the difference is that, their shape will not be the same, in CMG IMEX deviated fault channel can be best represented as follows:

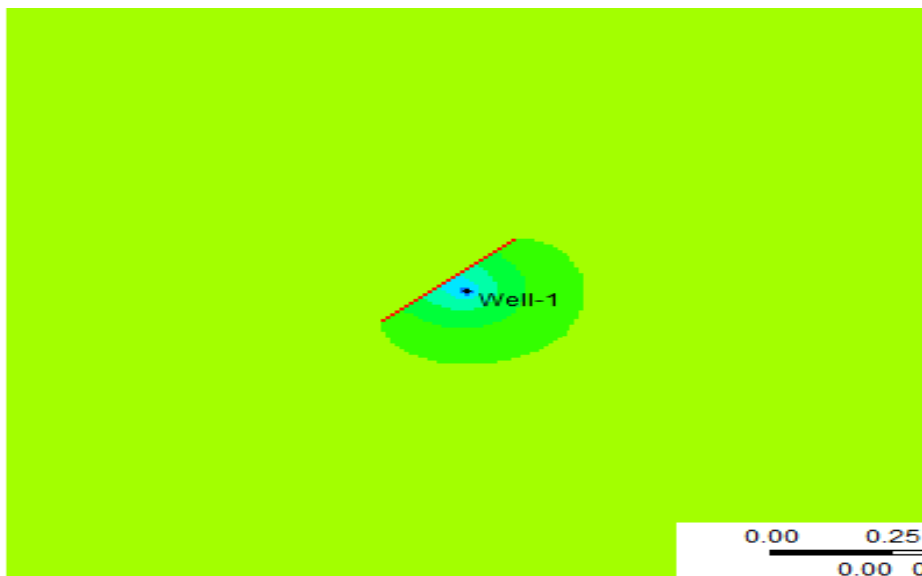


**Figure 7-42.** CMG IMEX undersaturated reservoir model with inclined fault channel.

After the simulation of this model, the following figure was obtained depicting the bottom-hole pressure change for the well located in the centre of the reservoir:

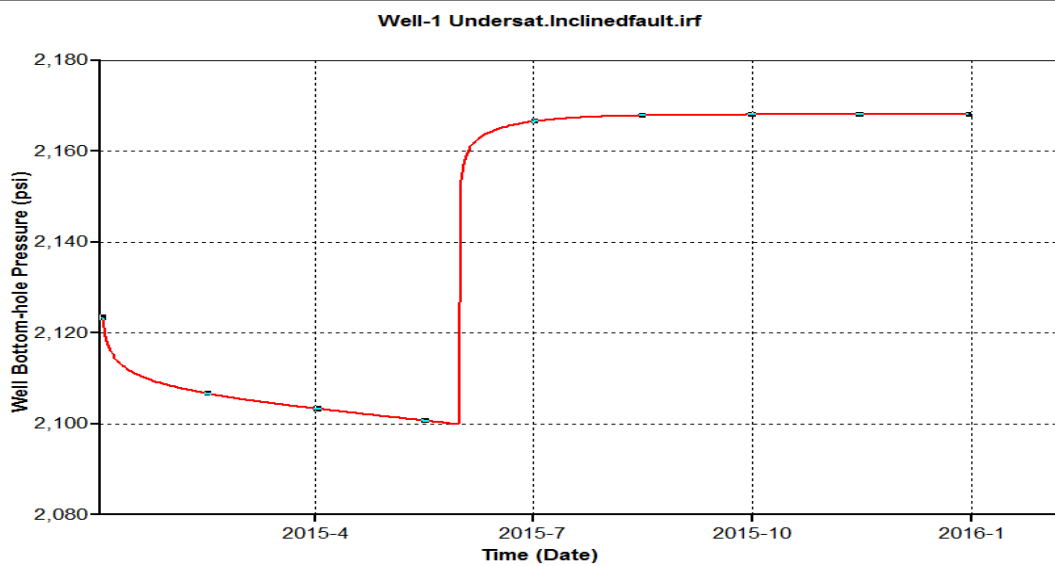


**Figure 7-43.** CMG IMEX under-saturated reservoir model with inclined fault depicting bottom-hole pressure value change.

✓ *Ecrin Saphir*

Next step after obtaining the pressure values from both simulators is to perform build-up testing by using Ecrin Saphir. So, the next figure illustrates build-up log-log plot by using Rubis output pressure values:

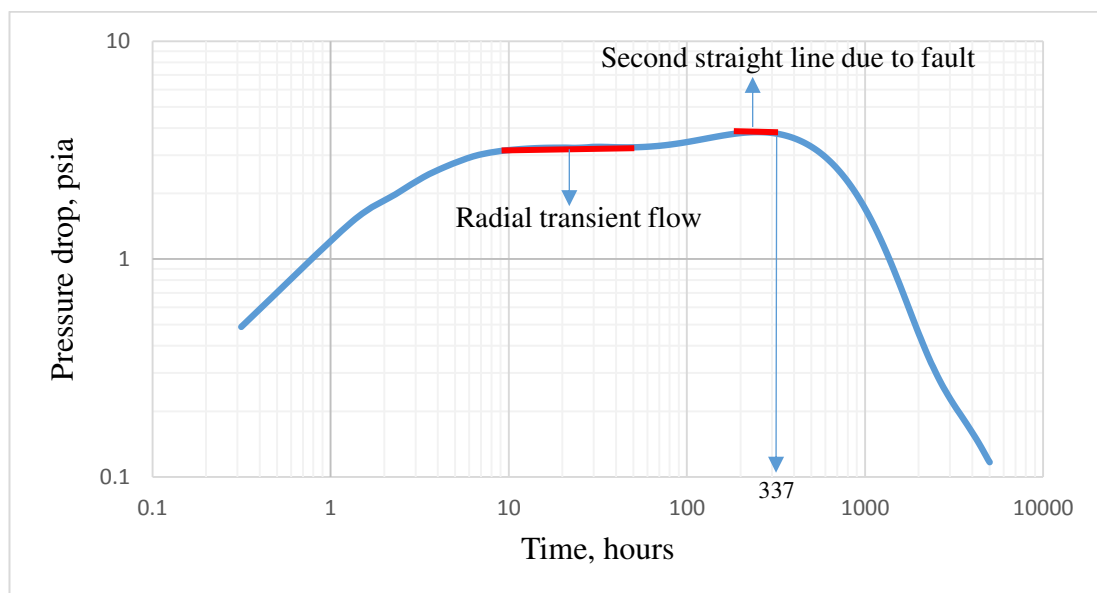


**Figure 7-44.** Ecrin Saphir build-up log-log plot for under-saturated reservoir model with inclined fault by using Rubis data.

Accordingly, the next plot illustrates build-up log-log plot for the under-saturated reservoir model case with inclined fault by using CMG IMEX pressure values.

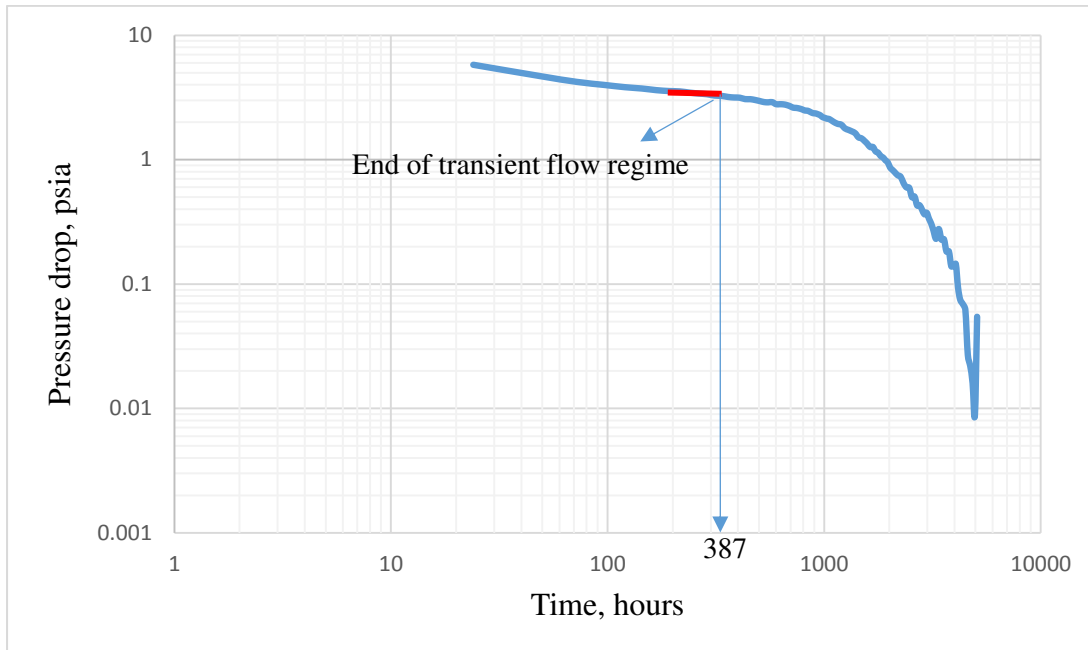


**Figure 7-45.** Ecrin Saphir build-up log-log plot for under-saturated reservoir model with inclined fault by using CMG data.

In this comparison, it can be seen that the fault effect is more clear in the above figure where Rubis module data were used, because in log-log plot where CMG IMEX data were used any second straight line can't be identified, whereas in the former plot the second line rising and stabilising because of fault effect can be detected.

If to compare their timing value for the pressure disturbances to reach the boundary it can be observed that, in Ecrin Rubis module it is 337 hours, whereas in CMG IMEX it is 387 hours. Difference is because of the way how unstructured gridding simulates the inclined fault is not the same how structured gridding simulates.

### 7.3.2. SATURATED

In this case as the name implies gas phase was added to reservoir models. Now there are oil and gas flowing through the porous media. For this case it was also checked how unstructured gridding technique can cope with reservoir modelling issues and how it compares against the structured model. Oil-Gas contact is at 500 ft, reservoir

is initially saturated, and GOR value is 500 scf/stb. These parameters were kept constant throughout the whole following scenarios.

- **Case 1. Saturated Reservoir Model without fault.**

In this part it was compared how Voronoi gridding technique is accurate on simulating 2 phases by comparing it with structured gridding. For this purpose the same reservoir models were built with the same oil and gas properties in Ecrin Rubis and CMG IMEX. Z factor is calculated by using Dranchuk correlation, gas viscosity is used by using Lee Et. Al. correlation and the same correlations were introduced to CMG IMEX for the sake of consistency between these two models.

✓ *Use of Ecrin Rubis*

In this part reservoir model with gas phase was constructed by specifying aforementioned oil and gas properties. Having built the model, simulation runs were implemented for the saturated reservoir model and the following figure was obtained:

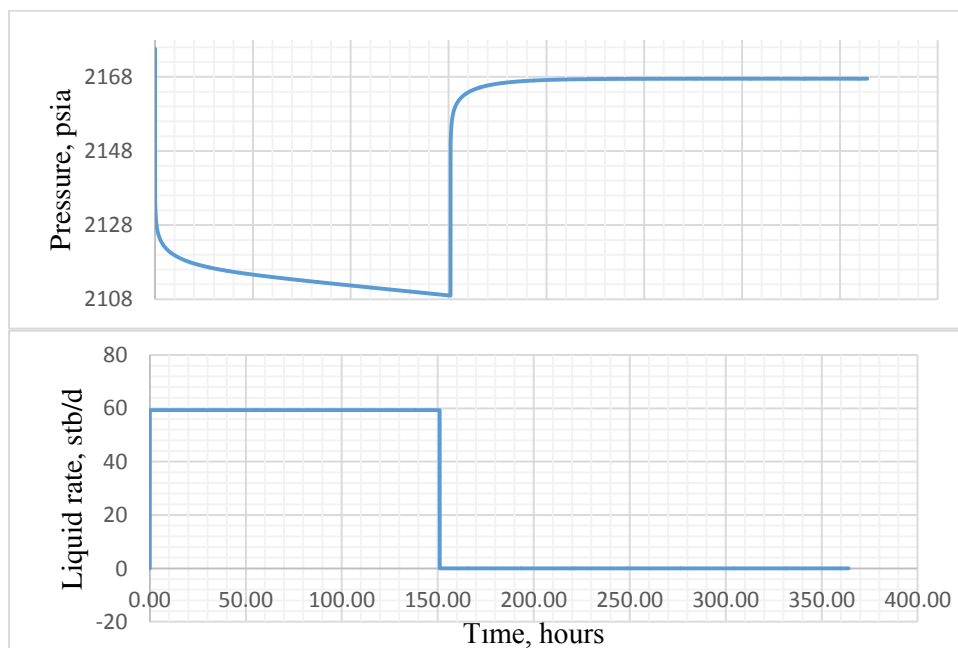


**Figure 7-46.** Ecrin Rubis pressure-rate plot for the saturated reservoir model.

✓ *Use of CMG IMEX*

For this part again the same reservoir model was used with the same properties without fault in CMG IMEX and the following figure describes how the bottom-hole pressure changes for the well located in the middle of the reservoir:

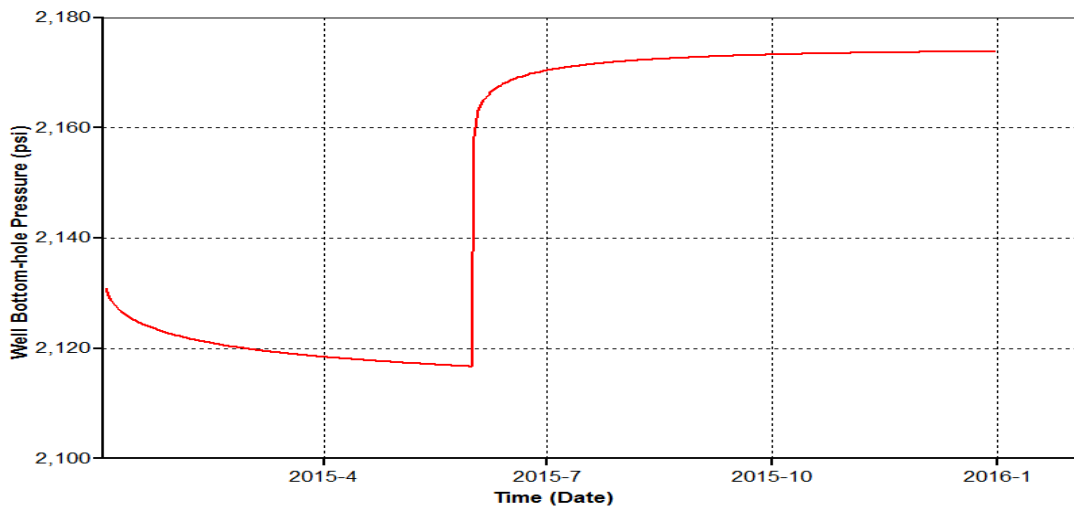


**Figure 7-47.** CMG IMEX Bottom-hole pressure change for the well.

✓ *Use of Ecrin Saphir*

In this case build-up testing was performed by using both simulators pressure output values. The first one illustrates how build-up log-log plot changes by using Ecrin Rubis module:

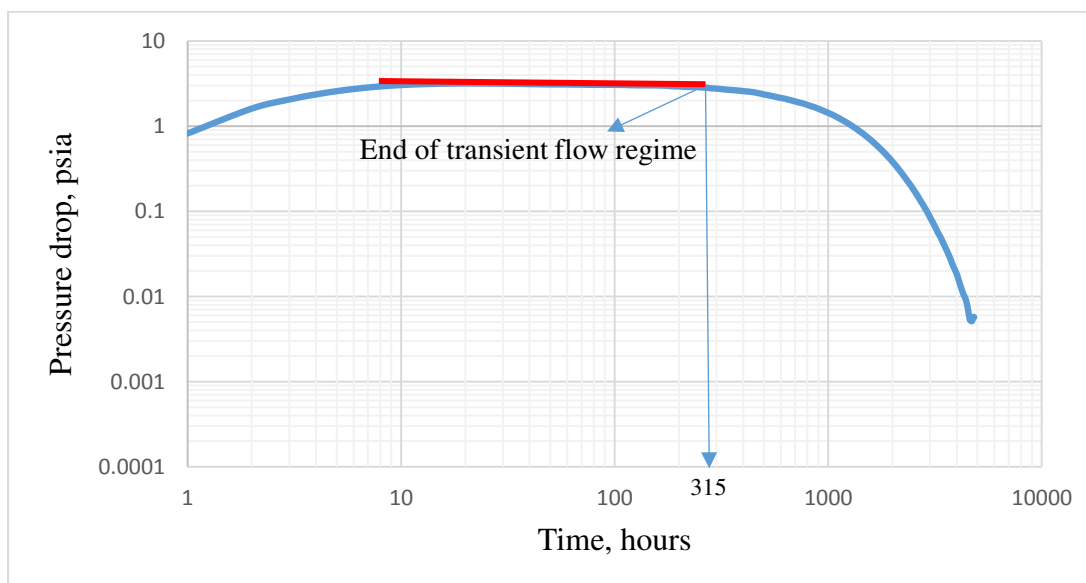


**Figure 7-48.** Ecrin Saphir log-log build-up plot by using Rubis pressure data.

Accordingly, the next figure illustrates the build-up well testing results on Ecrin Saphir by using CMG IMEX pressure values:

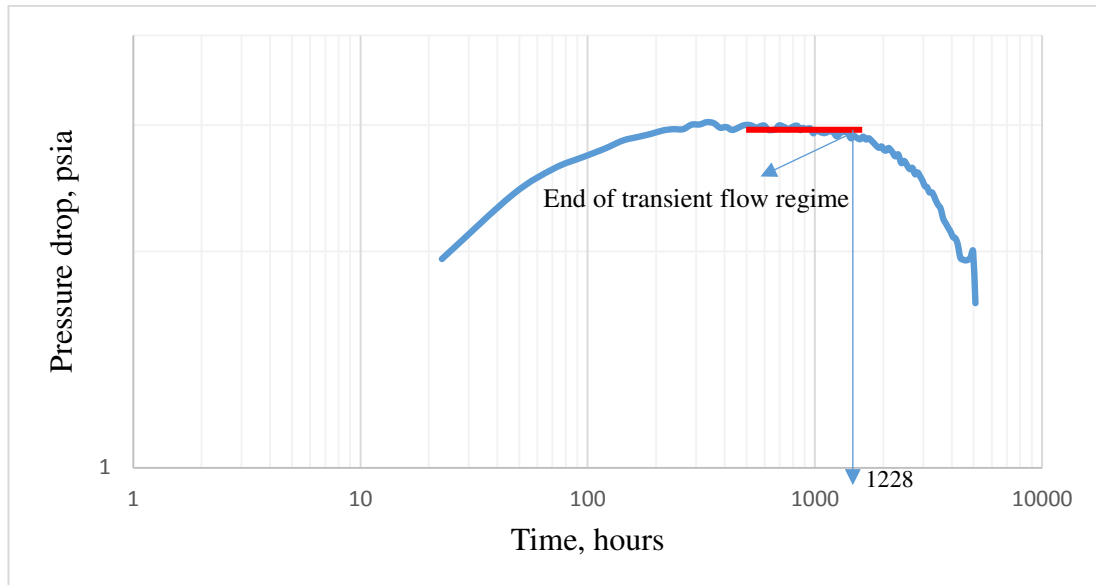


**Figure 7-49.** Ecrin Saphir build-up results by using CMG IMEX pressure data.

It can be seen that end of transient flow regime is not the same for these simulators. With CMG IMEX data transient flow regime tends to last more compared with what Ecrin Rubis data offers. In Ecrin Rubis module, the transition time to pseudo-steady state is 315 hours, whereas in CMG IMEX it tends to last more than 1000 hours. For this difference the fluid permeability data was checked, and in both models it was equalled. The following plot illustrates this:

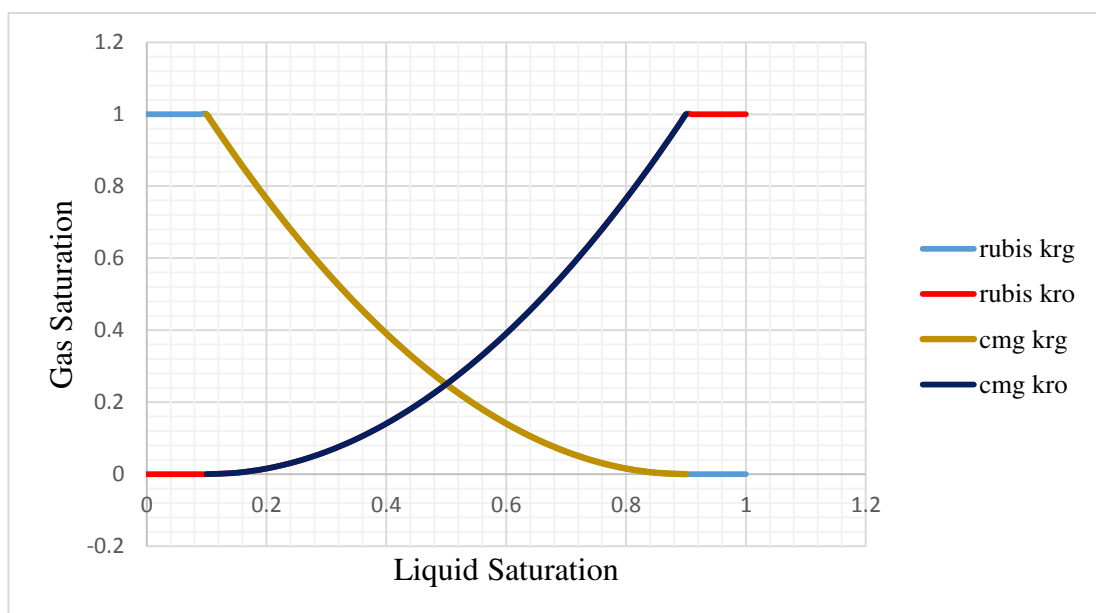


**Figure 7-50.** Relative Permeability data for both models.

So, analytical correlations are the same, relative permeability data is also the same, the difference is because of the way how structured and unstructured gridding simulates the saturated reservoir.

- **Case 2.** Saturated model with horizontal fault model.

In this case it's compared how the unstructured gridding can be accurate with horizontal fault taking into account of gas phase. For this case the same reservoir model was constructed by using Rubis Ecrin, CMG IMEX with the same aforementioned fault properties in our previous cases. It was then performed build-up well testing analysis by using Ecrin Saphir.

✓ *Use of Ecrin Rubis*

In this case the reservoir model by using Ecrin Rubis was constructed and simulation runs were implemented in the model. After that the following pressure-rate plot is obtained:

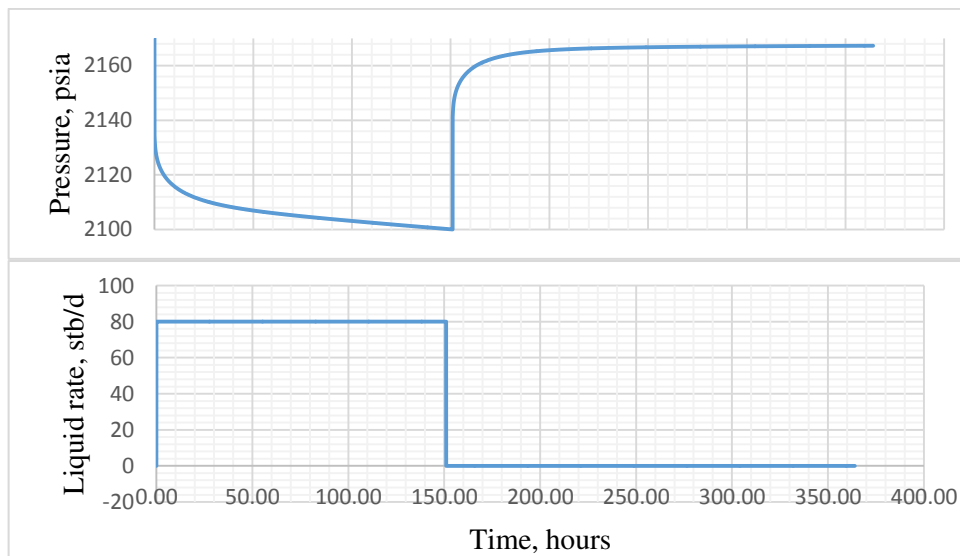


**Figure 7-51.** Ecrin Rubis pressure-rate plot for the saturated reservoir model with horizontal fault.

✓ *Use of CMG IMEX*

In this case, the same reservoir model was constructed by using CMG IMEX with the same parameters that were mentioned before. Having built the model, the simulator yielded following figure showing the bottom-hole pressure value change for the well:

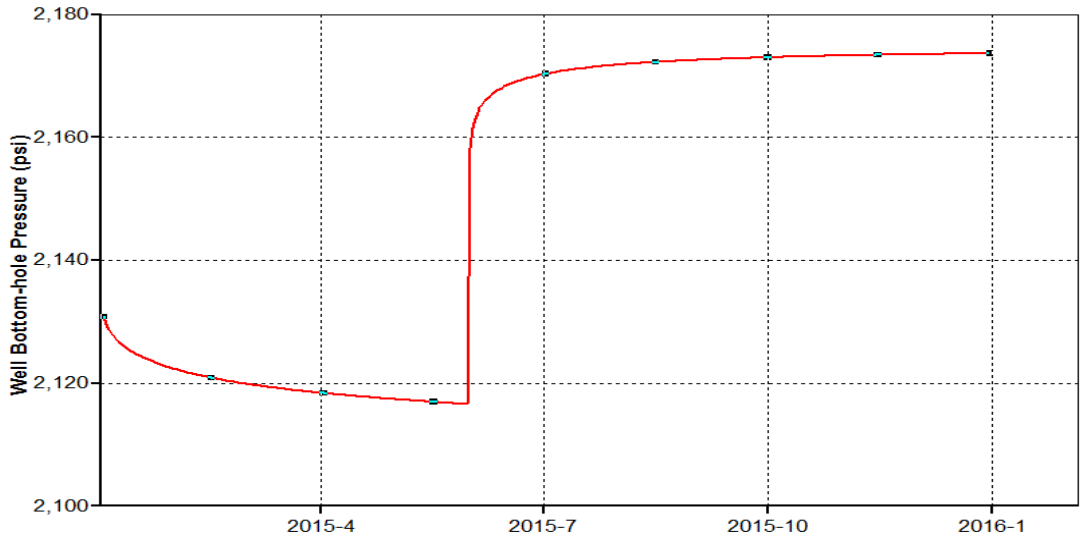


**Figure 7-52.** CMG IMEX plot describing bottom-hole pressure change for the well located in saturated reservoir model with horizontal fault.

✓ *Use of Ecrin Saphir*

Having acquired the pressure values from the both simulators the next step is performing pressure build-up testing by using both software output results. So, the next figure shows build-up log-log plot by using Rubis pressure data:

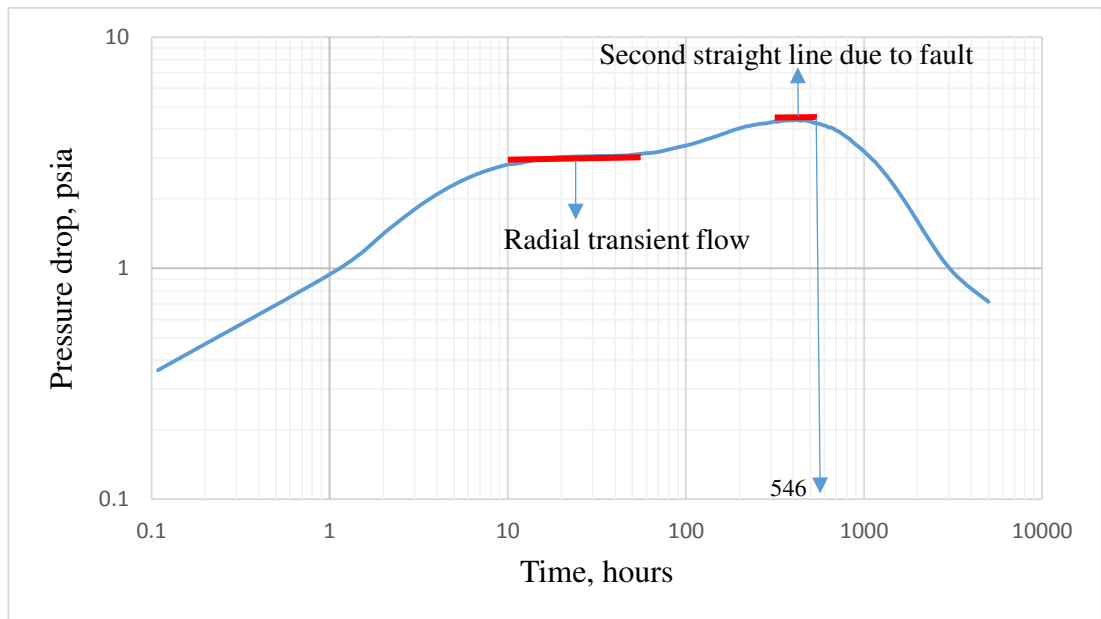


**Figure 7-53.** Ecrin Saphir build-up testing on saturated reservoir model with horizontal fault by using Rubis pressure data.

Accordingly, the next figure shows build-up pressure testing log-log plot by using Ecrin Saphir based on CMG IMEX pressure data:

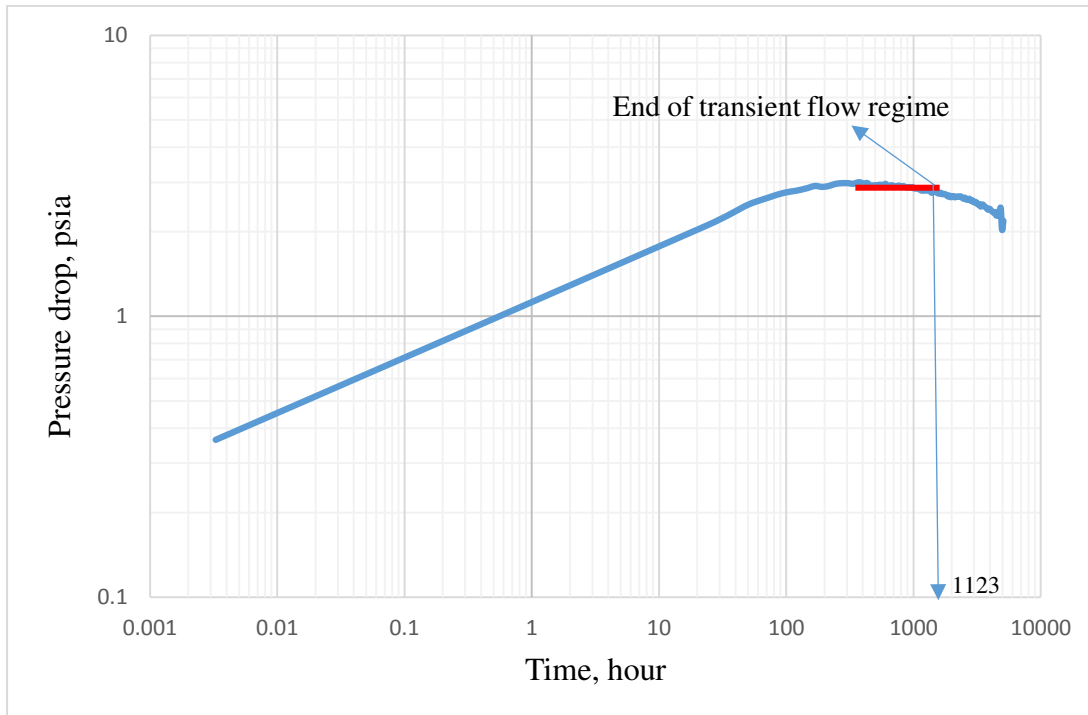


**Figure 7-54.** Ecrin Saphir pressure build-up testing log-log plot for the saturated reservoir model with horizontal fault by using CMG IMEX data.

Again, by taking into account of fault presence one should see second straight line in log-log plot. In former plot there is some degree of confidence that the second line going up and stabilizing is an indicative of fault, whereas for the latter plot there is no such confidence.

Comparing the time for the time to reach the pseudo-steady state it can be seen that in Ecrin Rubis module this time is 547 hours, whereas in CMG IMEX module it equals to 1123 hours. So, with the gas phase the match between structured and unstructured gridding results gets decreased.

- **Case 3.** Saturated Reservoir Model with inclined Fault channel.

In this case deviated fault channel was introduced to the model considering both oil and gas phase. The aim here is to check how unstructured gridding can represent and simulate deviated fault channels in multi-phase reservoirs by comparing against

structured gridding technique. For that purpose the same reservoir model was constructed in Ecrin Rubis module and CMG IMEX with aforementioned rock and fluid characteristics with one distinction that fault here is not straight, but inclined. Based on pressure values derived from both simulators, it was performed build-up testing by using Ecrin Saphir and compared the results.

✓ *Use of Ecrin Rubis*

As it was mentioned, the aim here is to check the applicability of Voronoi gridding technique by using Ecrin Rubis module in multi-phase reservoirs. Having built the same reservoir model with the deviated fault channel, it was performed simulation runs on this model, and the following figure was obtained:

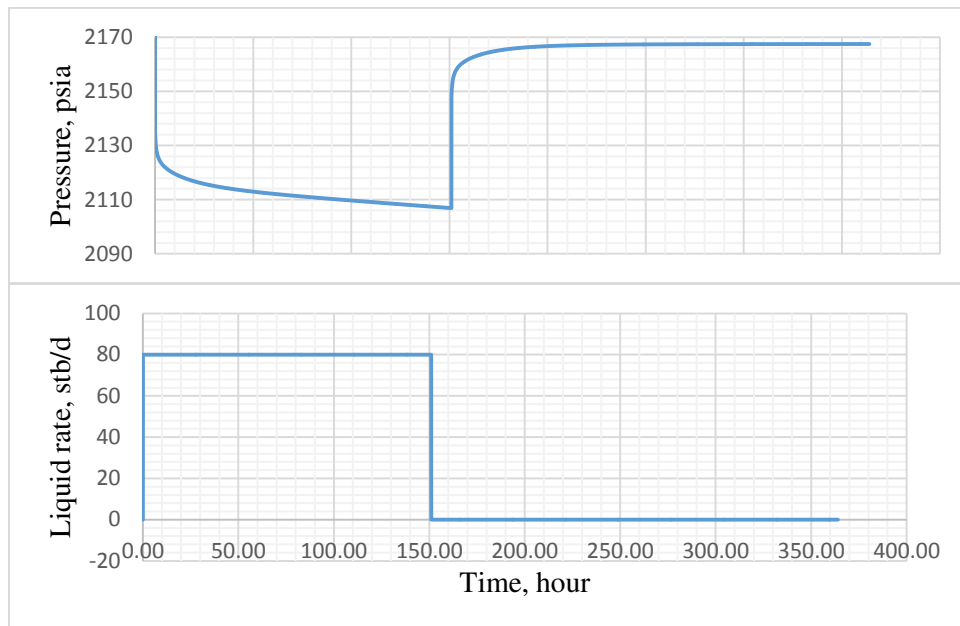


**Figure 7-55.** Ecrin Rubis pressure-rate plot for the saturated reservoir model with inclined fault.

✓ *Use of CMG IMEX*

For assessing the applicability of structured gridding simulation in multi-phase reservoirs with inclined fault model, the same model was also built based on the same reservoir parameters by using CMG IMEX. Having built the model, simulation

runs were performed and following figure illustrates the bottom-hole pressure change for the well:

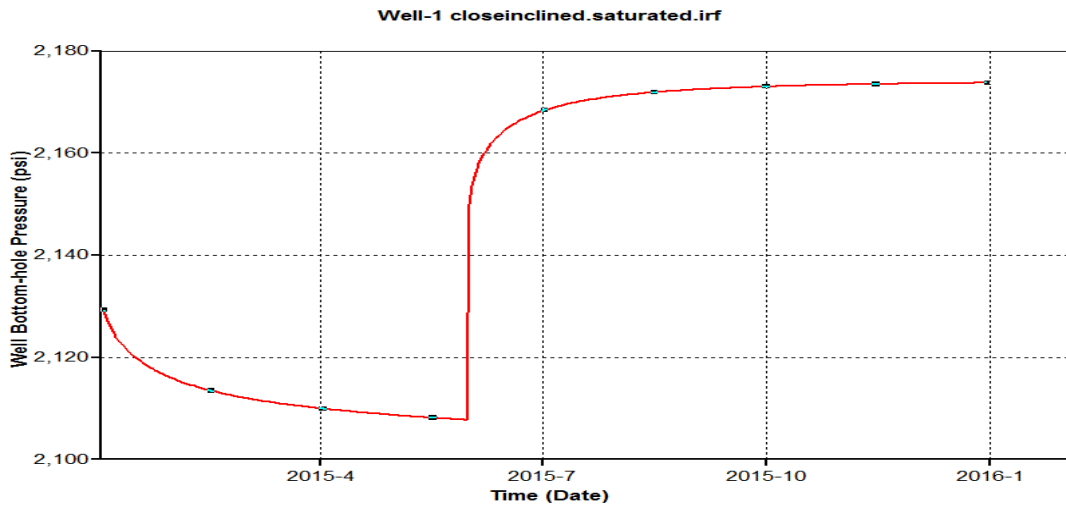


**Figure 7-56.** CMG IMEX plot illustrating bottom-hole pressure change in a well for the saturated reservoir model with deviated fault.

✓ *Use of Ecrin Saphir*

After acquiring the pressure values from the both simulators, it was conducted pressure build-up testing based on both Ecrin Rubis and CMG IMEX pressure output values. So, the next figure illustrates log-log plot for the saturated reservoir model with deviated reservoir channel:

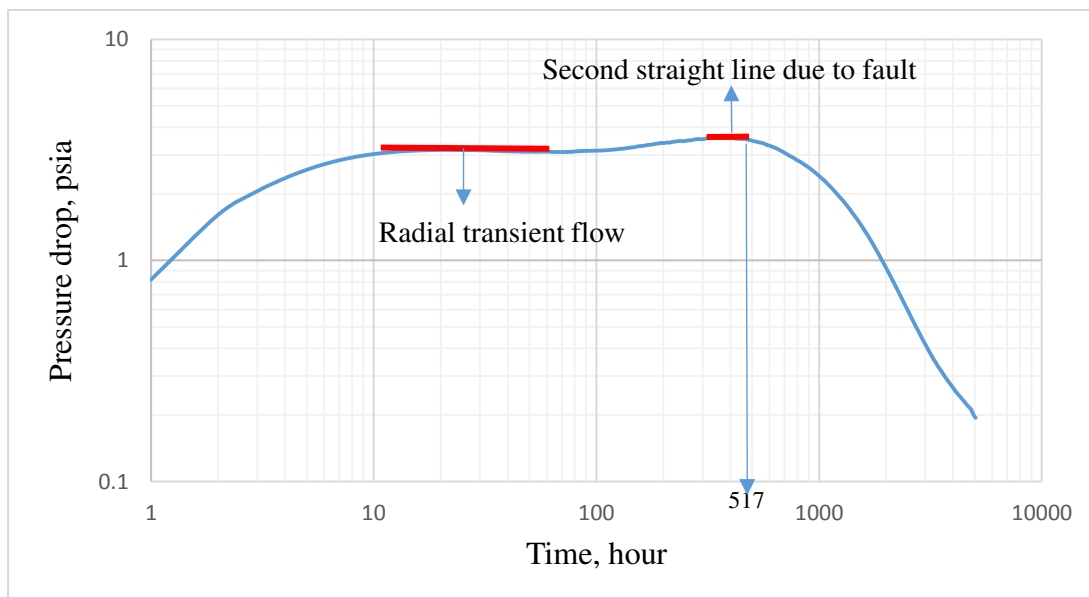


**Figure 7-57.** Ecrin Saphir pressure data for saturated reservoir model with deviated fault channel based on Ecrin Rubis pressure data.

Accordingly, the next figure illustrates the pressure build-up log-log plot by using CMG IMEX pressure data:

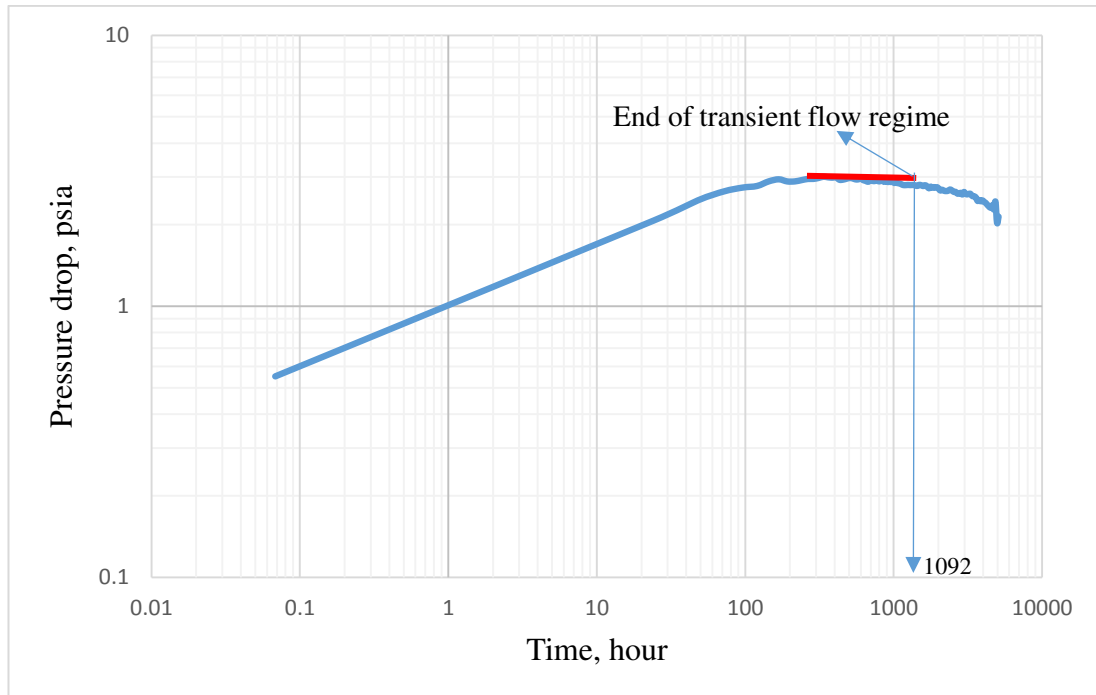


**Figure 7-58.** Ecrin Saphir pressure data for saturated reservoir model with deviated fault channel based on CMG IMEX pressure data.

Again if to make a comparison between these two plots it can be seen that fault is more clear in the former log-log plot rather than in the latter based on visibility of second straight line due to the flexibility and accurateness unstructured gridding can offer for deviated fault channels even in saturated reservoirs. These two techniques and their results preciseness in the example of inclined fault later are presented in the upcoming chapter.

Time to reach the pseudo-steady state is 517 hours when Ecrin Rubis pressure values are used, whereas it is approximately 1100 hours when CMG IMEX results are used.

Please note that wellbore storage effect is ignored due to fluid level rise in the annulus. It was imagined that there are packers, so the wellbore storage effect is negligible for this reason. But there is also fluid level rise in the wellbore after the shut-in. Based on the following equations the following calculations were performed, and found wellbore storage effect negligible for this reason as well:

$$C = V_{wb} * c_{wb} \quad (7-2)$$

$$V_{wb} = \pi * r_w^2 * h \quad (7-3)$$

$$t > \frac{200000 * C}{\left(\frac{kh}{\mu}\right)} \quad (7-4)$$

So, from equations (7-2), (7-3), and (7-4),

$$V_{wb} = 3.14 * 2.5^2 * 25 = 201.2583 \text{ ft}^3 \quad (7-5)$$

$$C = 201.2583 * 1.75 * 10^{-5} = 0.003529 \quad (7-6)$$

$$t > \frac{200000 * 0.003529}{\left(\frac{50 * 25}{0.5737}\right)} \quad (7-7)$$

$$t > 0.323 \text{ hours} \quad (7-8)$$

So, based on these equations, it was found that wellbore storage effect due to fluid rise in the wellbore lasts approximately, 20 min-s, after that it is no longer important. Because this time scale is small, it was neglected wellbore storage effect due to fluid rise in wellbore as well.

## CHAPTER 8

### RESULTS AND DISCUSSIONS

This chapter is dedicated to the results and conclusions for all the cases that were mentioned in previous chapter. The results and its corresponding conclusions are made for each case.

#### **8.1 Results and Discussions for Part-1**

In this part results and corresponding conclusions for the part-1 are discussed where it was showed the advantages of using numerical simulators over analytical methods for well test design purposes by illustrating several scenarios. Results and conclusions are now discussed by going through all of these cases again.

##### *8.1.1 OILWATER MODEL*

In this model the end of infinite-acting flow regime was found by using both numerical simulators and analytical method. Numerical simulators showed this time equals to 100 hr in log-log plot (Figure 7-3), analytical methods yielded 96.8 hours. So, from this comparison it can be concluded that under ideal circumstances, where the reservoir shape is square, only oil phase is flowing, there is no any flow barrier and so on, analytical calculations can generate similar results with numerical simulators, so their usage can be acceptable under these ideal conditions.

##### *8.1.2 BLACKOIL MODEL*

In this case now there is only oil, but also gas phase flowing in the reservoir. Here it was also compared the end of transient flow regime by using Ecrin Saphir, CMG IMEX as numerical simulators and by using analytical method. Numerical

simulators generated 14.7 hours as the end of transient flow regime, whereas analytical methods results remained the same – 96.8 hours due to constant fluid and rock properties. So, here it can be concluded that if there's gas phase also flowing simultaneously with oil through the porous media, analytical methods results can be misleading. Because, it accounts only for the ideal reservoir conditions.

### *8.1.3 RESERVOIR MODELS WITH DIFFERENT SHAPES*

In this part analytical equations applicability was checked by taking into account of reservoir shape variations. 2 shapes are: Rectangular and Square Reservoir. For each part reservoir model was built in CMG IMEX, and build-up testing was performed by using Ecrin Saphir.

#### ➤ Rectangular Shape

Simple reservoir model without any faults was built for rectangular reservoir shape, and according to Ecrin Saphir results, end of transient flow regime happens after 370 hours. Analytical calculations generated this time to be equal to 581 hours. So if to rely on analytical calculations, one then would have to produce 211 hours more in comparison with what numerical methods offers which in turn means a necessary expenditure lost especially in offshore platforms, where rig working time is a key economic question. So, relying upon the analytical equation can be entailed with incorrect well test design procedure.

#### ➤ Square Shape

If the reservoir model is ideally squared, then according to figure (7-9), the boundary effects can be seen after 98 hours, whereas analytical methods offer 96.8 hours. So, it can be concluded that analytical results can be reliable to some extent based on the comparison with numerical simulators result under ideal squared reservoir shape. Giving the fact that, reservoirs around the world are ubiquitously irregular with multiple flow barriers where oil, gas, and water flow simultaneously, the usage of numerical simulators can give more realistic and accurate results.

Even there is some difference for the end of infinite acting regime between these 2 shapes, it's obvious that with more irregularity, more tangible differences will be noticed.

#### *8.1.4 RESERVOIR MODELS WITH 2 WELLS.*

In this case it was checked how 2 wells operating close to each other will affect well test design procedure. So, the same reservoir model was built with previous aforementioned rock and fluid properties, but now 2 wells producing close to each other as Figure 7-10 illustrates. It is obvious from Figure 7-11 that when there are 2 wells because of superposition principle, the pressure drop will be higher compared with only one well model (Figure 7-12). Because, with 2 wells based on superposition principle the pressure drop in observation well will be accompanied by the pressure drop Well-1 producing adjacent to it, so these pressure drops will be added, as a result as Figure 7-11 implies, the pressure drop line hits 3000 kPa axis, whereas in Figure 7-12, this is always higher than 3000 kPa axis, they never intersect.

So, coming to Ecrin Saphir results, Figure 7-13 offers that the end of transient flow regime is 14 hours due to the fact that, the next well operating close to it manifests itself as an another boundary, so it will take less time to hit this boundary.

Analytical methods offered 96.8 hours considering only one well producing in centre of the reservoir. With another well operating close to it, analytical methods lose its reliability.

#### *8.1.5 RESERVOIR MODEL WITH VERTICAL FAULT.*

In this part it was assessed the preciseness of analytical methods results by comparing it against the numerical simulators, i.e. CMG IMEX and Ecrin Saphir. Numerical simulators generated 100 hours for the starting time of second rising and stabilizing straight line in log-log plot due to the presence of fault, and 407 hours for the Late Time Region to be noticed, whereas analytical calculations generated 335 hours for the starting time of the second straight line. So, starting time for the second straight line is different in these two models, 335 hours as opposed to 100 hours.

Time for the Late Time Region to be noticed is also different. Analytical methods offer 96.8 hours for that region to be felt, and ignores any flow barriers, whereas the numerical model implies 407 hours to notice fully Late Time Region. So, it can be concluded that analytical methods results applied for the geological complex

reservoirs with faults should not be considered as a reliable source, instead numerical simulators are capable of generating more accurate and representative information.

It can also be concluded that analytical equation results for the second straight line in log-log plot are not as reliable as numerical simulators, in fact simulation results give more accurate data.

#### *8.1.6 RESERVOIR MODEL WITH INCLINED FAULT*

In this case, inclined fault channel was introduced to our model and how numerical simulators result differs from analytical methods was investigated. So, according to Ecrin Saphir plot (Figure-7-18), the time for the end of transient flow regime is 195 hours in comparison with 335 hours from analytical method. So, there are some differences for that timing considering different fault shapes. It means that, the time scale attached to the identification of reservoir boundaries is also dependent on the fault channel orientation. This is why working with simulators are more preferable and can yield much more realistic results for the well testing design purposes. Analytical methods do not offer such kind of flexibility taking into account of different shapes of the faults.

## **8.2 Results and discussions for Part-2**

As it was mentioned in previous chapter the aim here is to check the voronoi gridding applicability in well test design by using Ecrin Rubis module. Conclusions and discussions are presented for both Under-saturated and Saturated cases.

### *8.2.1 UNDERSATURATED*

For that part as the name states, it was considered only oil phase in order to assess how unstructured gridding affects well test design by taking into account of different production times, production rates, and different build-up times. Because, these are the parameters that need to be optimally selected for the adequate well test design. So, there were 8 cases for this part and conclusions with discussions are provided for each of them.

- **Case 1** – 150 days production, 214 days build-up, 80 stb/day rate.

For this case, just as a remainder, production continued for 150 days, shut-in time lasted for 214 days, and rate was 80 stb/day. So, the same reservoir model was built on Ecrin Rubis and CMG IMEX, made a simulation, and the following chart describes how these pressure values match with each-other:

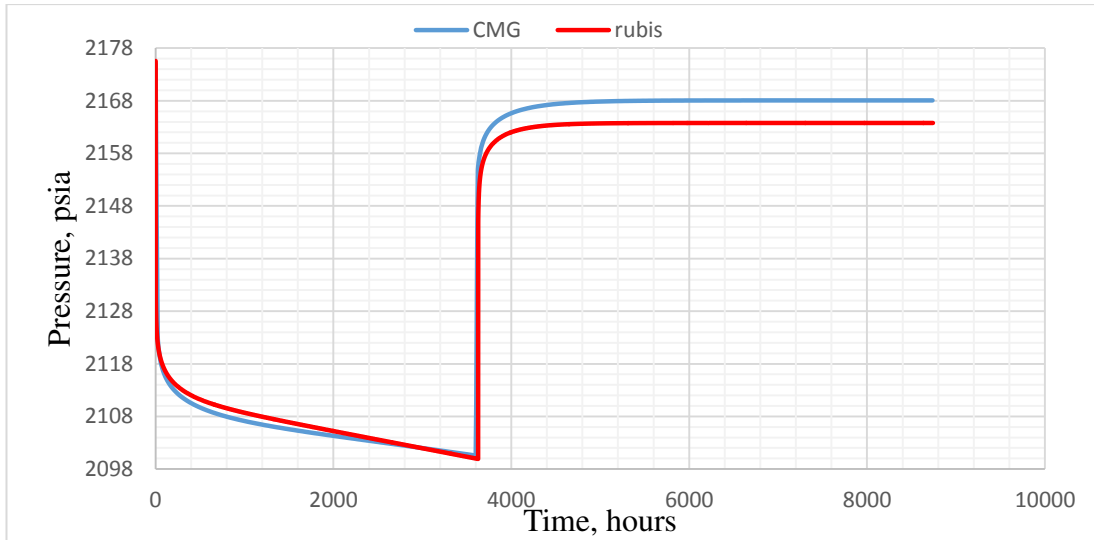


**Figure 8-1.** CMG IMEX-Ecrin Rubis pressure match.

For that case a Horner plot was generated. For this purpose on Ecrin Saphir the data to clipboard was dumped, then pasted in excel. After that, based on the equation of  $((t_p + \Delta t)/\Delta t)$  horner time was calculated. Also note that Horner plot was generated using  $t_x$  against the  $(p-p@dt)$ . Then in semi-log plot the following figure was obtained:

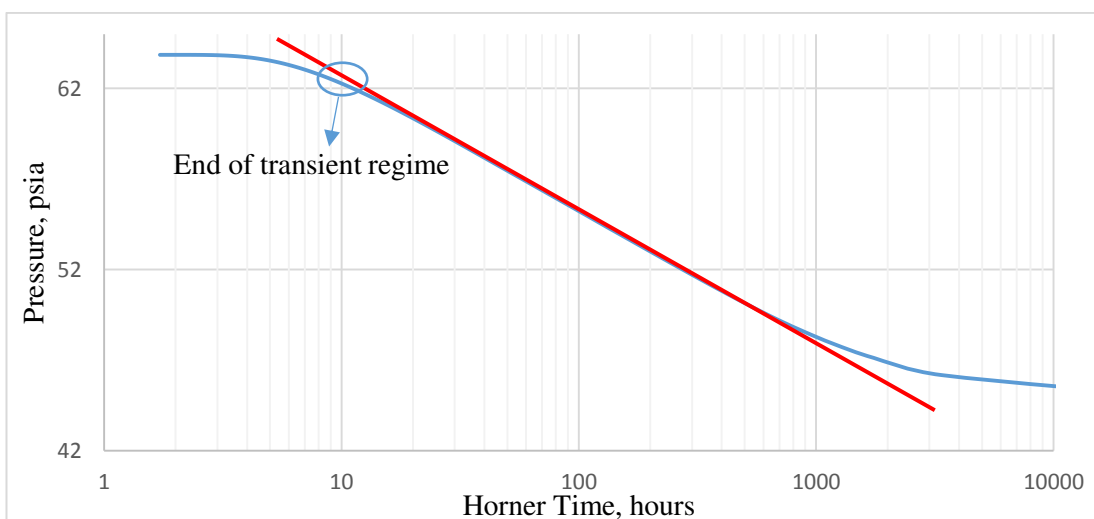


**Figure 8-2.** Horner Plot for the Case-1.

So, in this plot it can be stated that the inclination from the theoretical straight line is due to pseudo-steady state.

For this part it was also performed analytical calculations for the end of transient flow regime and as a result it was obtained 209 hours after which the flow regime is shifted to pseudo-steady state. Based on Ecrin Saphir results by using Voronoi gridding, this timing equals to 222 hours. So there's a match between these two models, and it can be judged that if there's no any fault, no gas, analytical methods can yield similar results with unstructured gridding.

- **Case 2.** 150 days production, 214 days build-up, 500 stb/day rate.

In this case rate value was changed, now production rate is 500 stb/day, and aim here is to see the difference on production rate variation effect on well test design.

Based on Ecrin Saphir results by using Voronoi gridding pressure values, it can be seen that the end of transient flow regime is 225 hours as opposed to 222 hour with 80 stb/day. So, from this comparison, one may conclude that the end of transient flow regime is not dependent upon the production rate. The following plot illustrates how pressure values of CMG IMEX compare with the Ecrin Rubis module:

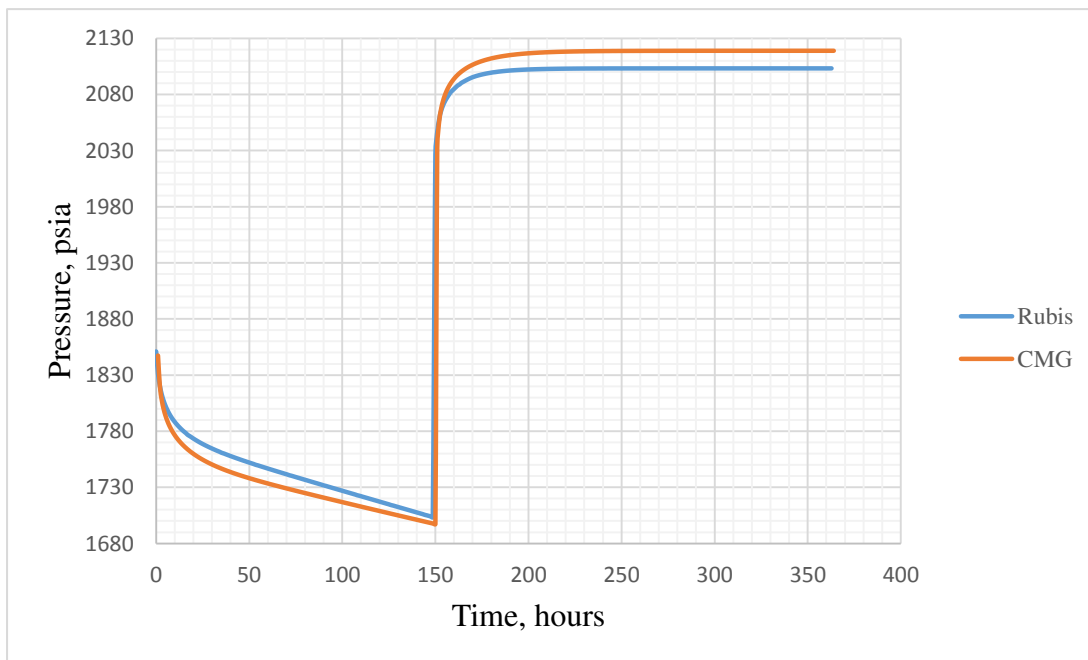


**Figure 8-3.** CMG IMEX pressure values match with Ecrin Rubis

From this plot it is visible that these 2 curves are somewhat identical, so from here one can conclude that pressure responses of unstructured gridded reservoir are somewhat close to pressure responses of structured gridded reservoir for this case.

Horner Plot were also generated for this case. The next figure illustrates that:



**Figure 8-4.** Horner Plot for Case 2.

In this plot it can be identified that the upper inclination part of the line from theoretical straight line is due to the transition from transient regime to the pseudo-steady state.

- **Case 3.** 3 days production, 214 days build-up, 80 stb/day rate.

In this case the production time was changed, it was decreased into three days to see how the change of production time affects to well test design parameters. The following Horner plot illustrates this scenario:

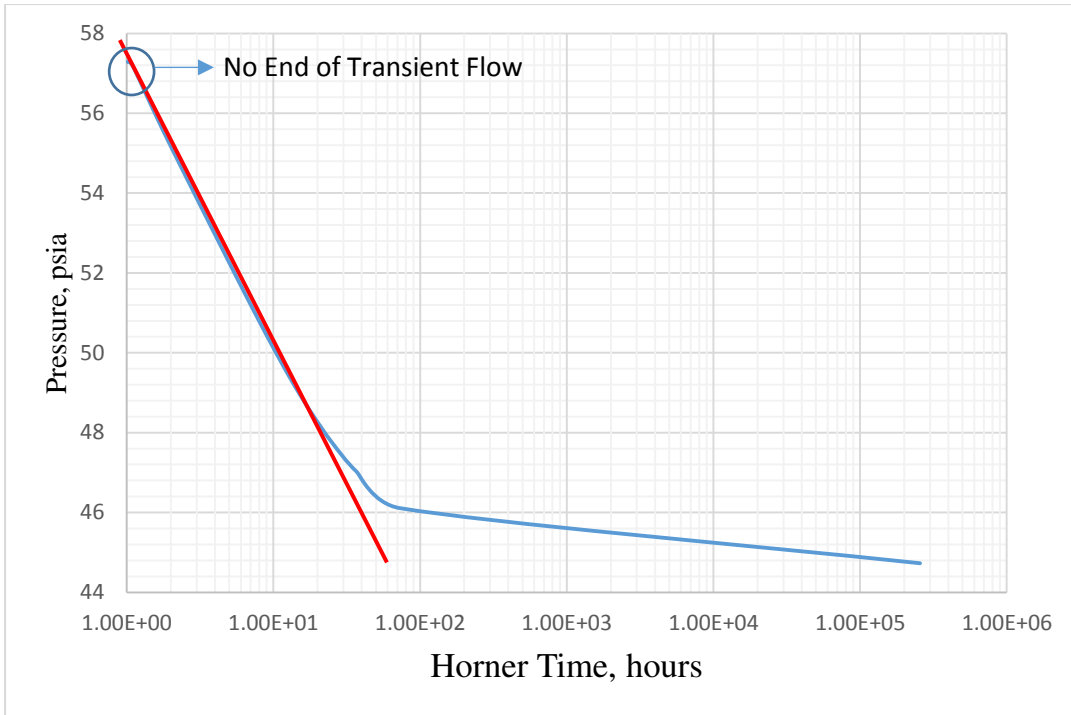


**Figure 8-5.** Horner Plot for the Case 3.

In this plot it is seen that there is no any inclination from the theoretical straight line because of very limited amount of production time. So, as a conclusion for the correct well test design, sufficient pressure disturbance needs to be generated, so that there can be transition from transient flow regime into pseudo-steady state. Alternatively, following figure describes how pressure changes for this scenario:

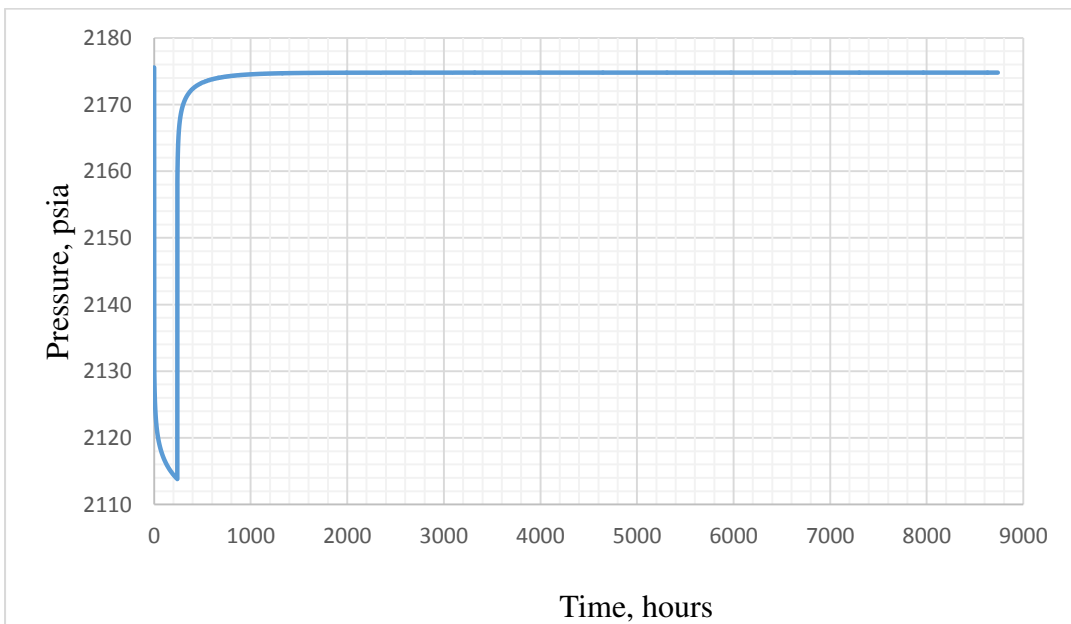


**Figure 8-6.** Pressure change history plot for the case 3.

- **Case 4.** 10 days production, 214 days build-up, 80 stb/day rate.

In this case there was longer build-up time in comparison with shut-in time. The aim here was to see the effect of having longer build-up time on our well test design. The next figure illustrates this scenario:

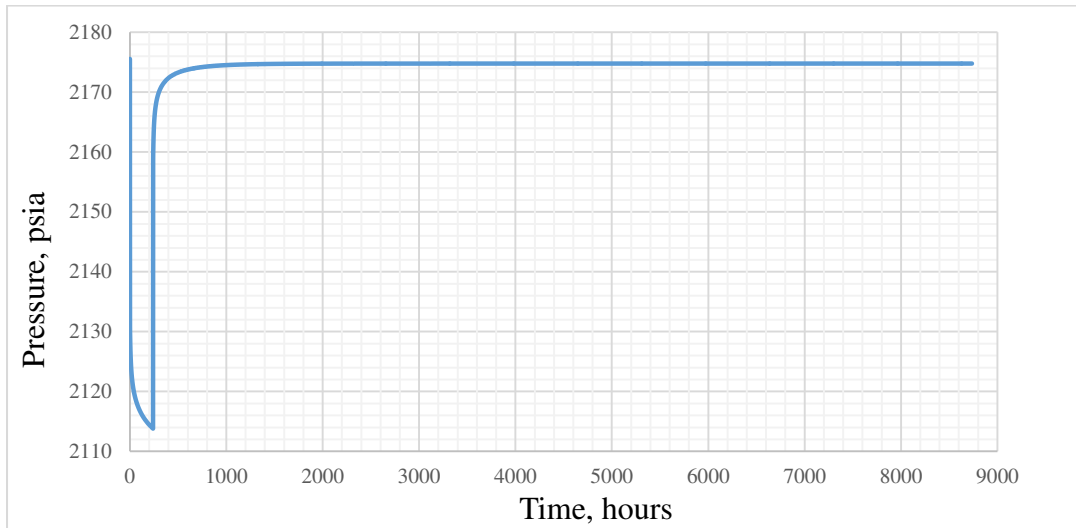


**Figure 8-7.** Pressure change history plot for the case 4.

In this case because of very long build-up time compared with relatively small amount of production time, after the shut-in pressure values roll back to its initial value. Corresponding Horner plot is as following:

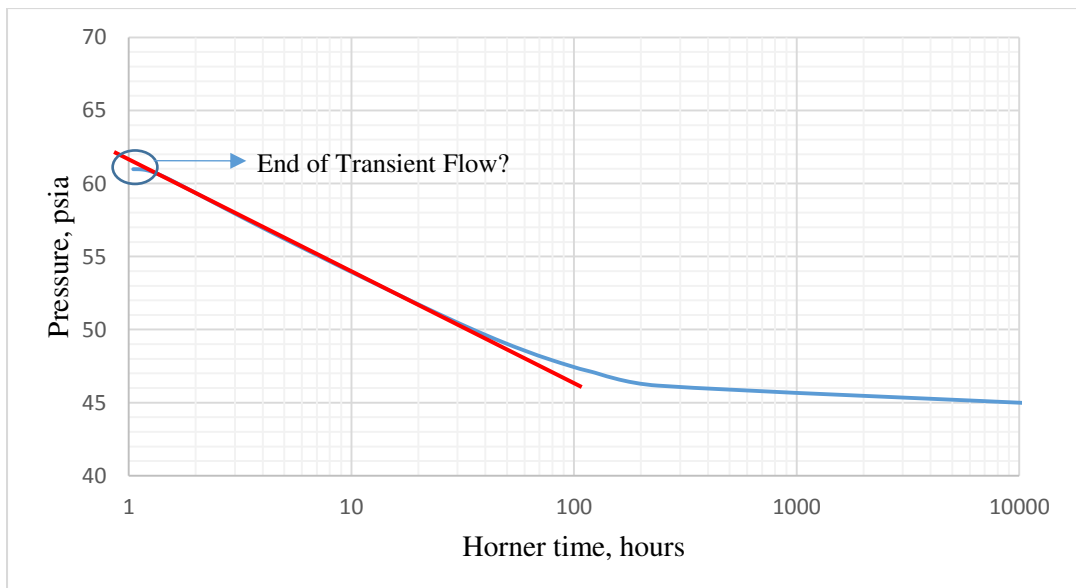


**Figure 8-8.** Horner Plot for the Case 4.

So, very little deviation from the straight line is seen in this plot, that's why it's hard to label this deviation as a transition part from transient to pseudo-steady state, because of the fact that the well had much longer shut-in time compared with the production time.

✓ **Case 5.** Normal Production, very short build-up, normal rate.

In this case production time was not changed, but now there is very short build-up time, which is 2 days. So, in this case the aim here was to see the effect of variation of build-up time on well test design. The next Horner plot was generated for this case as well:

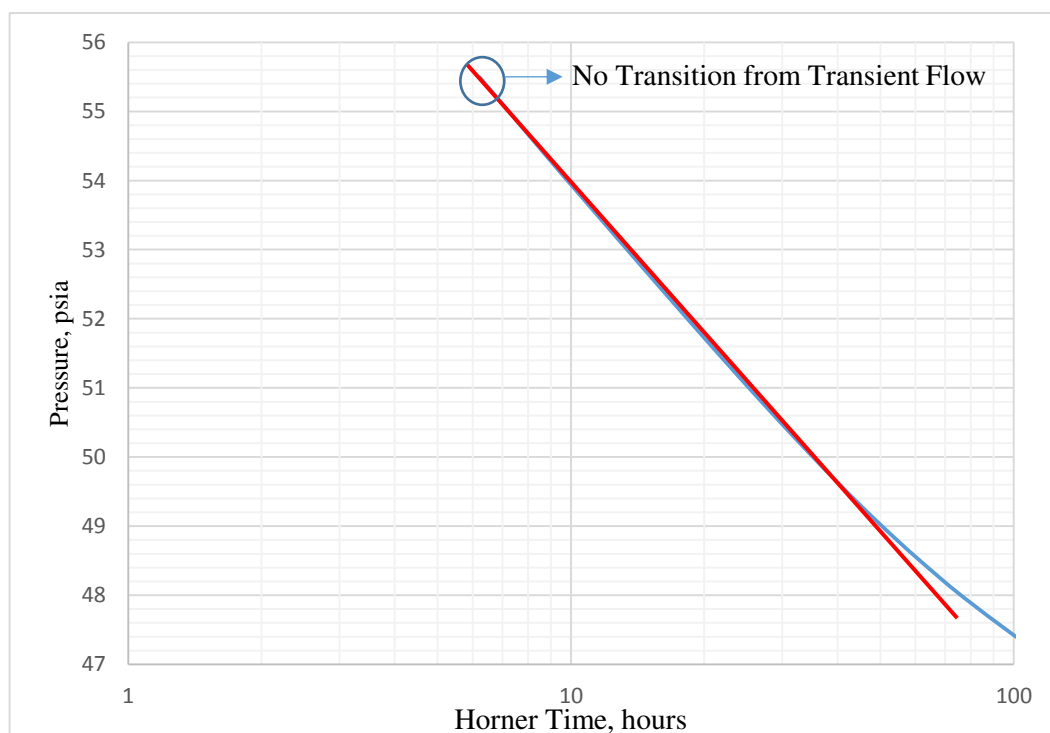


**Figure 8-9.** Horner Plot for the case 5.

So, in this case boundary effects can't be seen, because the reservoir continues to act as if it's infinite in size. This is due to the fact that, the well has not been closed for sufficient time so that the pressure can stabilize in the reservoir. Also the Late Time Region in Ecrin Saphir pressure build-up plot couldn't be identified as well.

✓ **Case 6.** 52 days Production, 78 days build-up, 80 stb/day rate.

In this case it's imagined that reservoir produced for 52 days, and shut-in for 78 days, with 80 stb/day. Using this data, the following Horner plot was obtained:

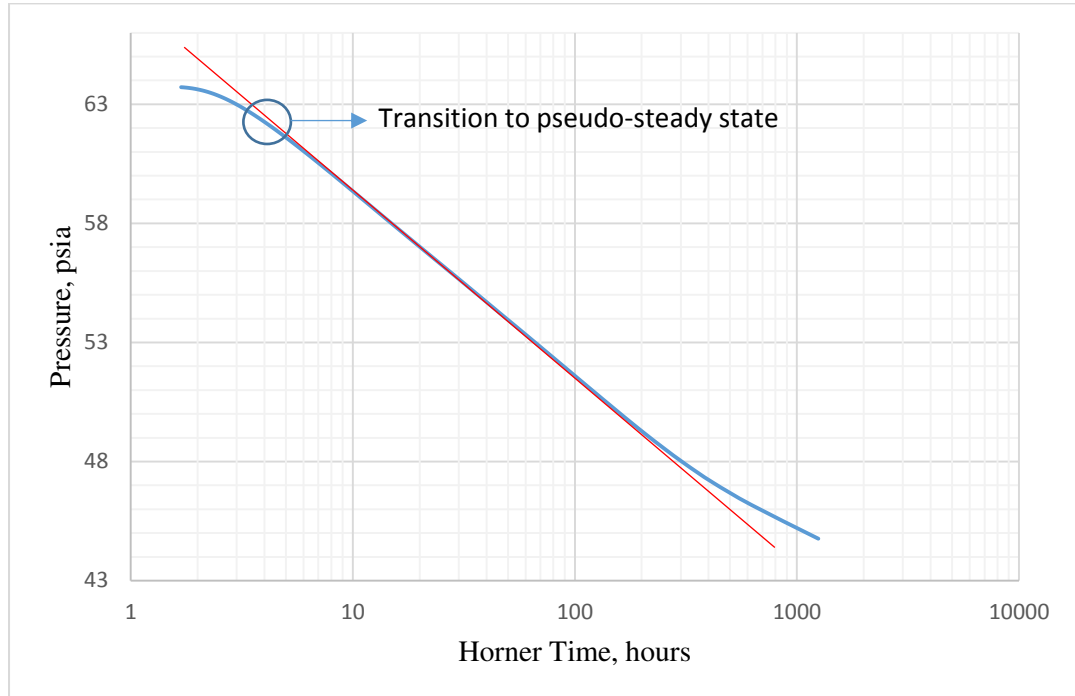


**Figure 8-10.** Horner Plot for Case-6.

From this plot it can be seen the deviation from the straight line meaning that pressure disturbances have reached to the boundary.

So, the conclusion for is that for the adequate well test design procedure, optimum production time, production rate, and shut-in time are required. In general, shut-in time needs to be 1.5 times higher than production time allowing the pressure to stabilize and make it possible for the engineer to identify reservoir boundaries (G.Steward, 2010). Otherwise as it was shown in previous cases, well test design can not be appropriately designed, especially if pressure disturbances have not reached the boundary.

✓ **Case-7.** Under-saturated Reservoir Model with horizontal Fault.

In this case it was checked how the unstructured reservoir gridding can simulate horizontal faults when there is no gas in porous medium. So, the same reservoir model was built by using both CMG IMEX and Ecrin Rubis, and based on their

pressure values, the following excel figure was obtained illustrating how these values match with each other:

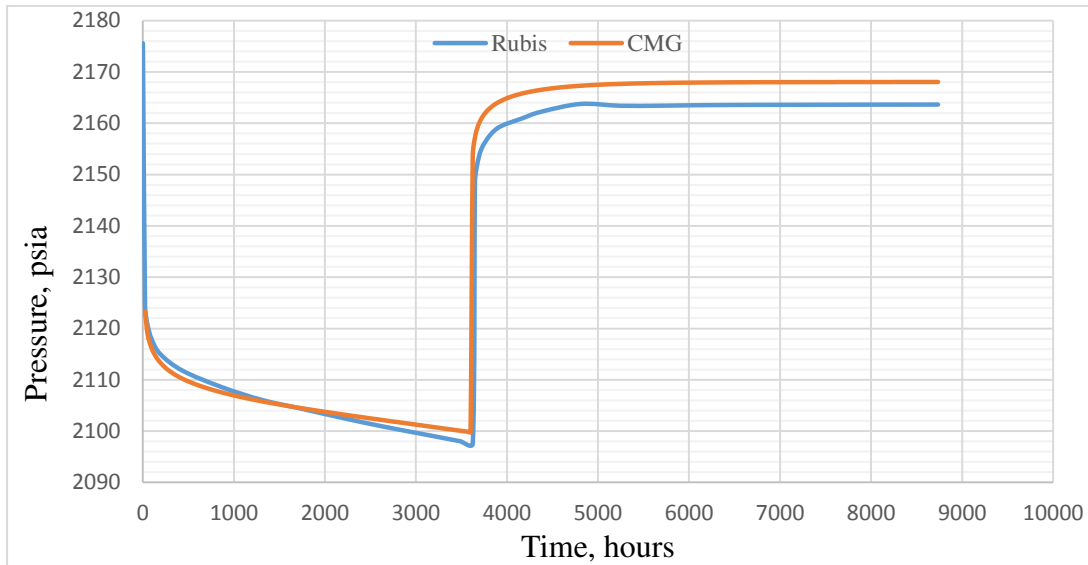


**Figure 8-11.** CMG-IMEX pressure values comparison with Ecrin Rubis module.

Based on Ecrin Saphir comparisons for the both model, it can be stated that Ecrin Rubis represents the fault in our reservoir system more clearly than CMG IMEX, at least in Rubis second straight line rising up and stabilising can be detected.

The preciseness of both simulators results can be checked by calculating the distance between the well and the fault and comparing it with the actual data. So, horizontal fault was introduced to our model and the distance between the fault and the well is set as 500 ft.

Firstly, this distance was calculated based on Horner plot by using CMG IMEX pressure values. The following figure illustrates how Horner plot looks like for this case:

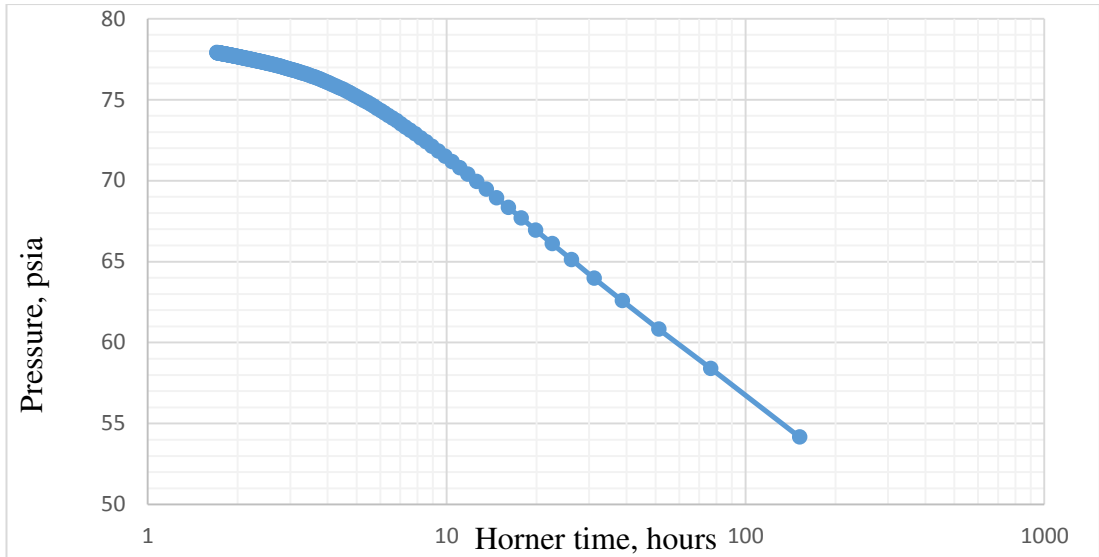


**Figure 8-12.** Horner plot by using CMG IMEX pressure values.

For better comparison the following Horner plot was generated illustrating 2 curves with and without faults:

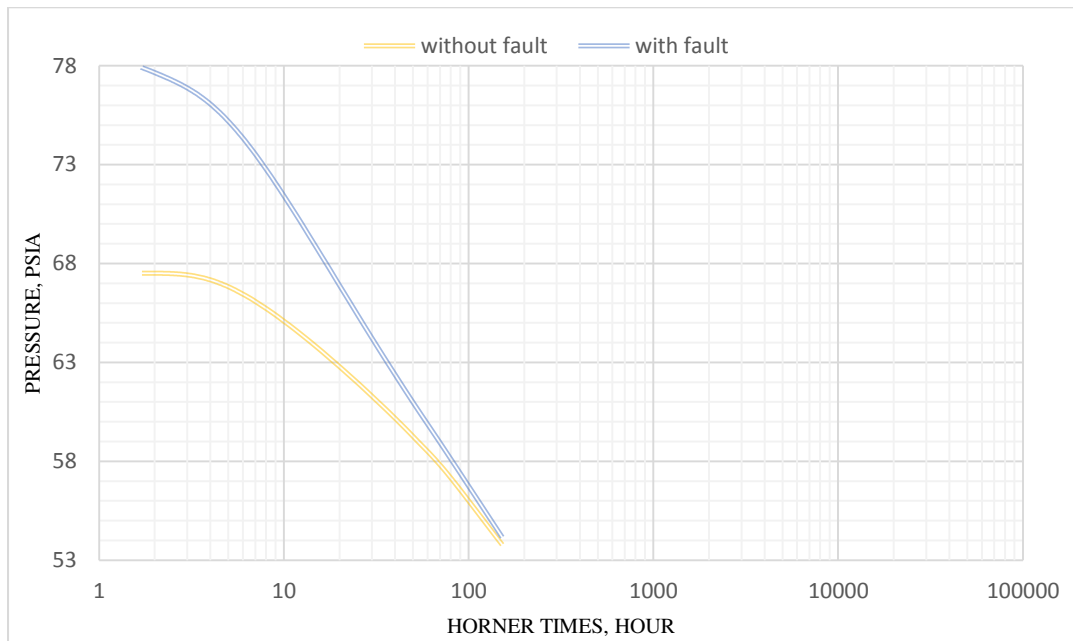


**Figure 8-13.** CMG IMEX Plots describing fault effect.

In this plot, the bottom curve shows pressure values without fault, whereas the top one illustrates pressure values with the fault. So, from this plot it's visible that with fault, reservoir experiences more pressure drop because of no-flow boundary.

The distance from well to fault can be calculated from their intersection point as the next figure illustrates:

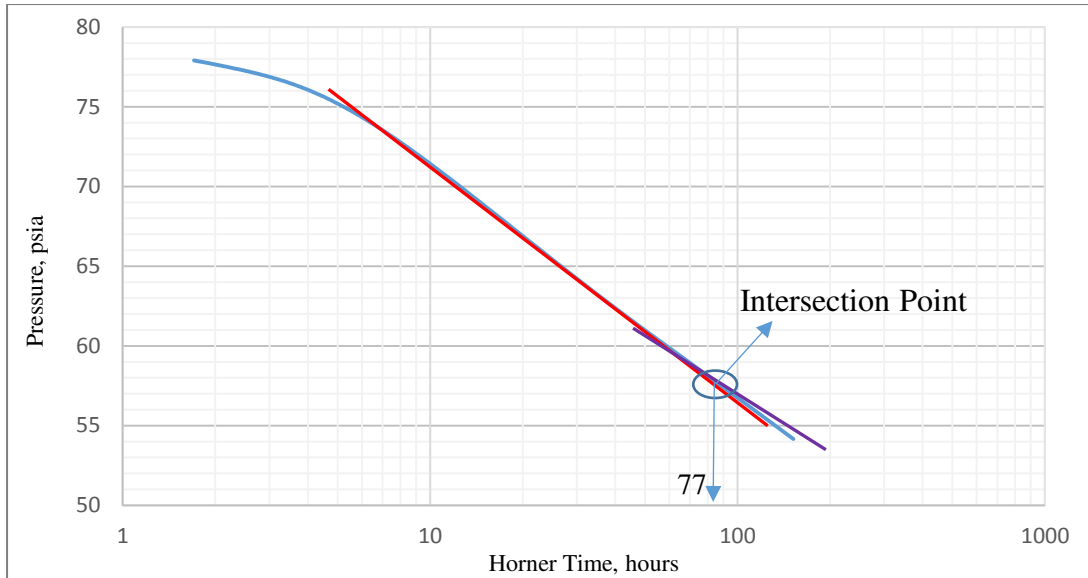


**Figure 8-14.** Horner plot based on CMG IMEX pressure values.

So, from the above, it is seen that the intersection point is 77 hours. Based on the following equation (Gray, 1956) the distance from fault to the well can be calculated as following:

$$L = \sqrt{\frac{0.000148 * k * \Delta t_x}{\phi * \mu * c_t}} \quad (8-1)$$

$$\Delta t_x = \frac{t_p + \Delta t}{\Delta t} \quad (8-2)$$

So, from this equation  $\Delta t_x$  is found based on  $t_p$ -production time value which equalled to 47.68 hours in our case after calculating using equation (8-2). Then using equation (8-1) it can be determined that, L equals to 590 ft as opposed to 500 ft of actual value.

Now, the same distance in the same way can be calculated for Rubis generated pressure value. Horner plot looks like for this case as following:

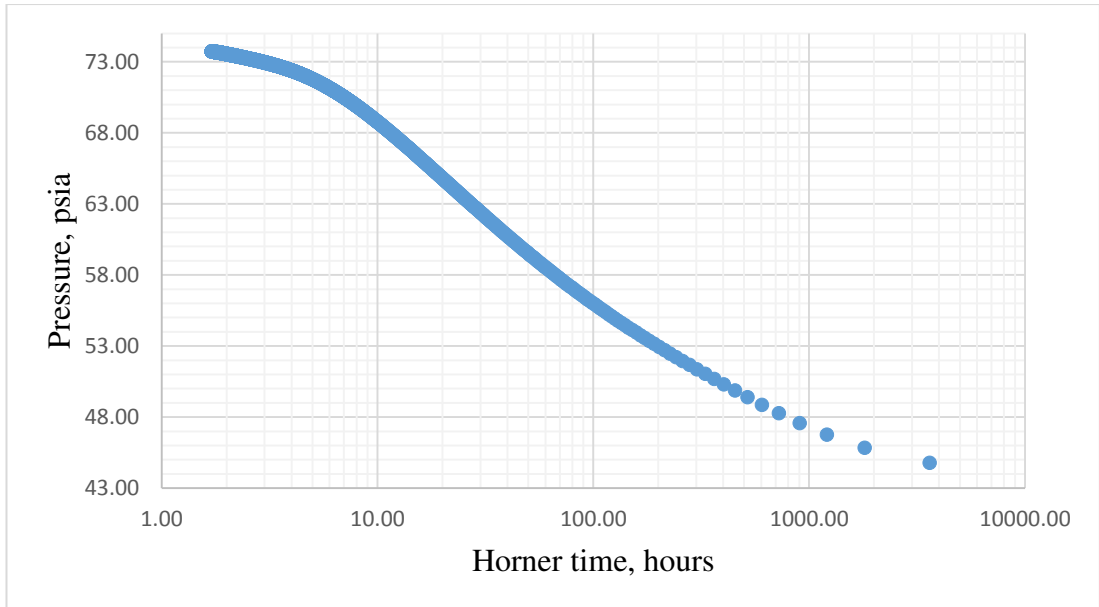


**Figure 8-15.** Horner Plot generated based on Ecrin Rubis pressure values.

For better precision of the intersection points of the 2 straight lines, 2 lines on Excel can be inserted to see where they intersect. So, the following excel figure illustrates it:



**Figure 8-16.** Horner Plot for Rubis Pressure Values.

In this case their intersection point is 107 hours. Based on the equation (8-2), Horner time was found to be equal to 34.1887 and using equation (8-1), the distance was found to be equal to 499.78 ft. Almost exactly the same value as an actual distance from well to fault.

So, conclusion is that unstructured gridding technique offers more accuracy on representing faults.

✓ **Case-8.** Under-saturated Reservoir model with inclined fault

Now in this case, inclined fault channel was introduced to the model and our aim is to check how unstructured gridding technique can represent inclined fault model and which is of them is more accurate. Firstly, Ecrin Rubis and CMG IMEX pressure values were checked, and the following excel plot was obtained depicting how these values match with each-other:

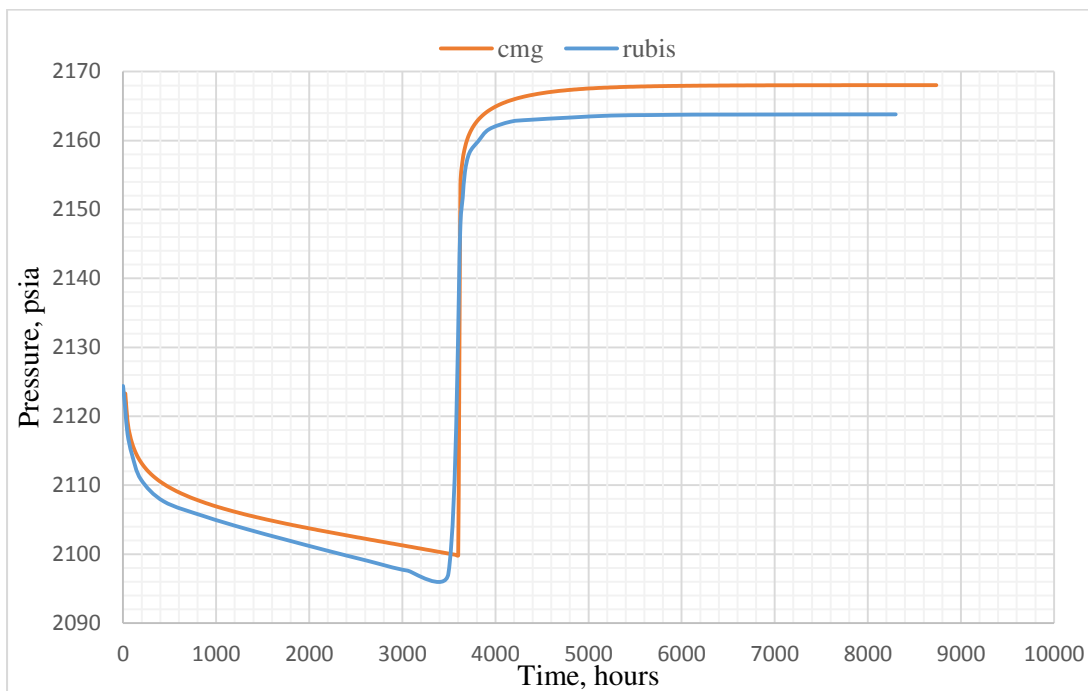


**Figure 8-17.** CMG IMEX pressure values match with Ecrin Rubis module.

In this plot it can be detected some differences on how these two simulators represent inclined fault model. Based on comparison of Ecrin Saphir plots, i.e. Figure (7-48) and Figure (7-49), it can be confidently judged that unstructured gridding technique can represent inclined fault channels more clearly than structured gridding. Because, based on pressure values from Ecrin Rubis the second straight

line can be noticed because of inclined fault presence, whereas from CMG IMEX data, it's barely noticed second straight line as a hallmark of fault.

However, in order to come up with a promising conclusion Horner plot was created that uses both of the simulators pressure values. Based on this Horner plot well to fault distance was calculated and compared against the actual data. In this case the actual distance from well to fault is 283 ft. The following Horner Plot was generated by using Ecrin Rubis pressure values:

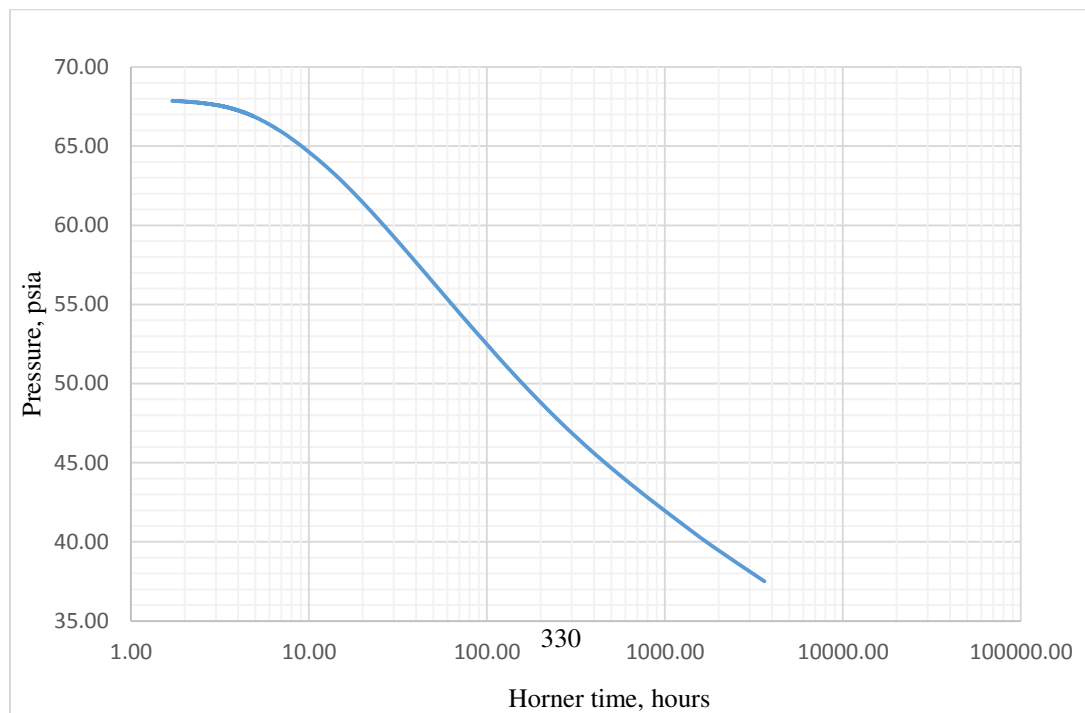


**Figure 8-18.** Horner Plot based on Ecrin Rubis values.

Now if to add two straight lines to the plot to see their intersection point, the following plot is obtained:

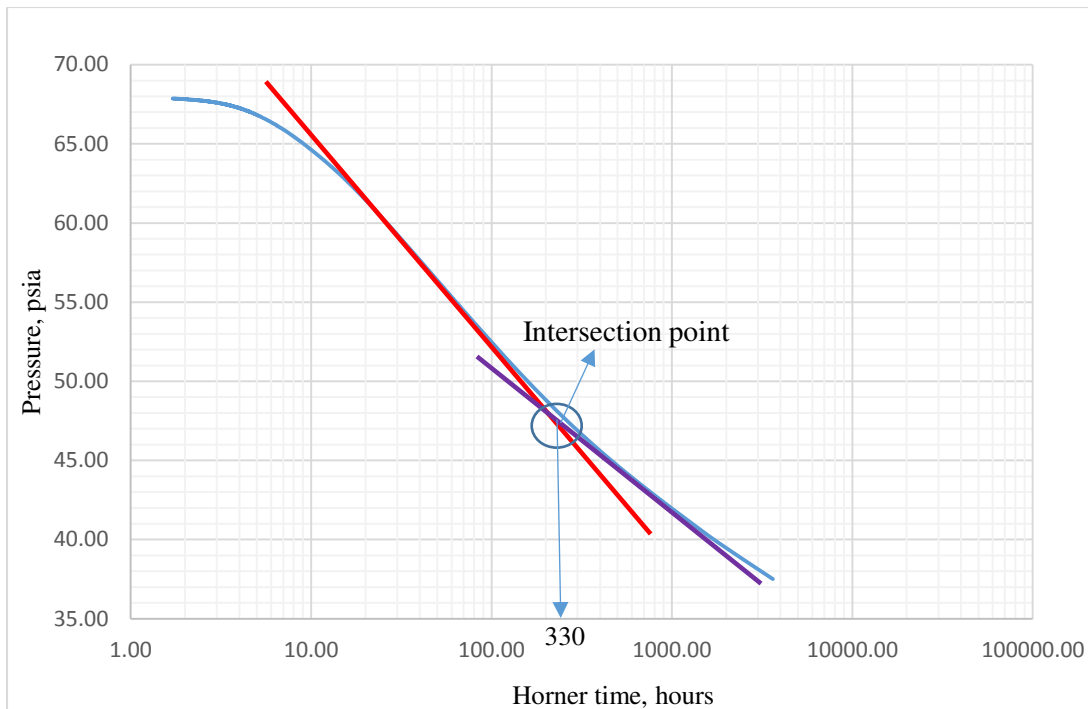


**Figure 8-19.** Horner Plot based on Rubis pressure values with straight lines.

So, it is apparent that in this plot the intersection point between those 2 straight lines due to fault presence is 330 hours. So based on equations (8-1) and (8-2), it was found that, the distance between the well and fault is 284 ft. This is a perfect match with the actual data which is 283 ft. This clearly shows how Voronoi gridding technique is accurate on reservoir simulation.

Now, the distance based on Horner plot can also be determined by using CMG IMEX pressure values output. So, this is how Horner plot looks like when CMG values are used:

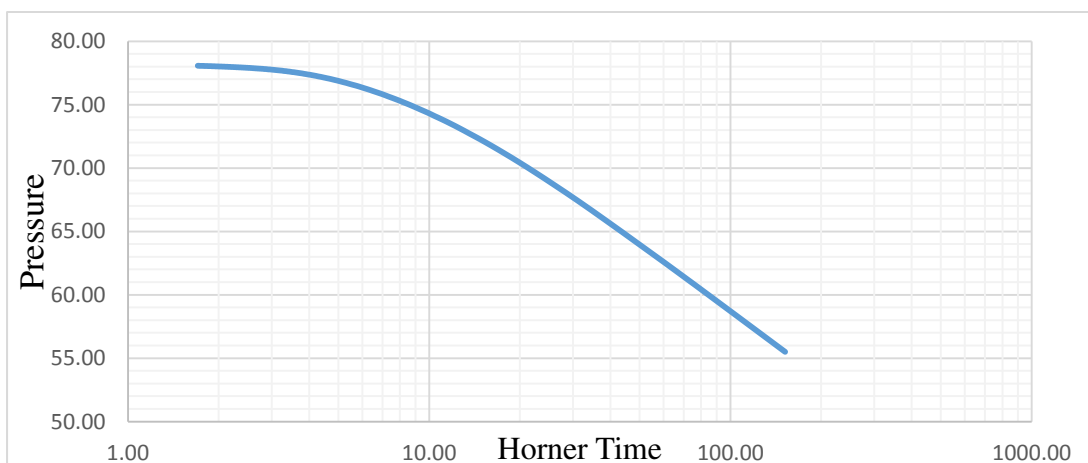


**Figure 8-20.** Horner Plot based on CMG IMEX pressure values.

If to add two straight lines to see intersection point on Horner plot, the following figure is achieved:

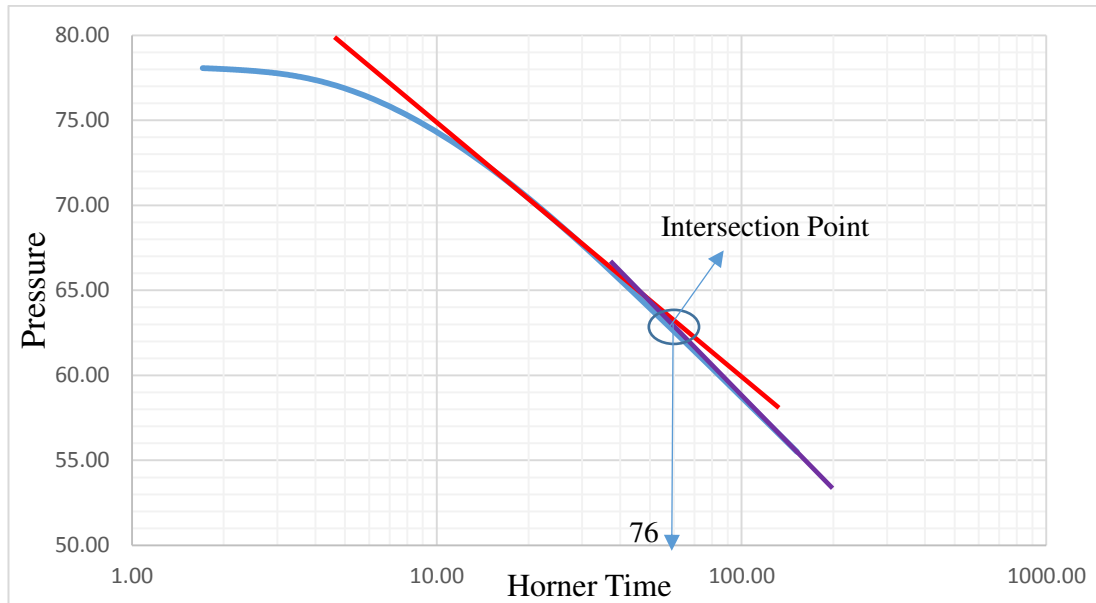


**Figure 8-21.** Horner Plot based on CMG IMEX pressure values with 2 straight lines. From this figure, it is seen that the intersection point of these two straight lines is 76 hours. Using the aforementioned equations, the distance was calculated to equal 594 ft as opposed to 283 ft of actual data. So, from this comparison, as a conclusion it is judged that because of the way how structured gridding simulates inclined fault in the form of zig-zag pattern, the actual distance can be distorted.

That is why using Voronoi gridding simulation on well test design can give more accurate and representative data, because as it was seen in previous example. The actual distance from well to fault was preserved when unstructured gridding was used.

The next plot illustrate how Horner plots are different based on CMG IMEX and Ecrin Rubis values:

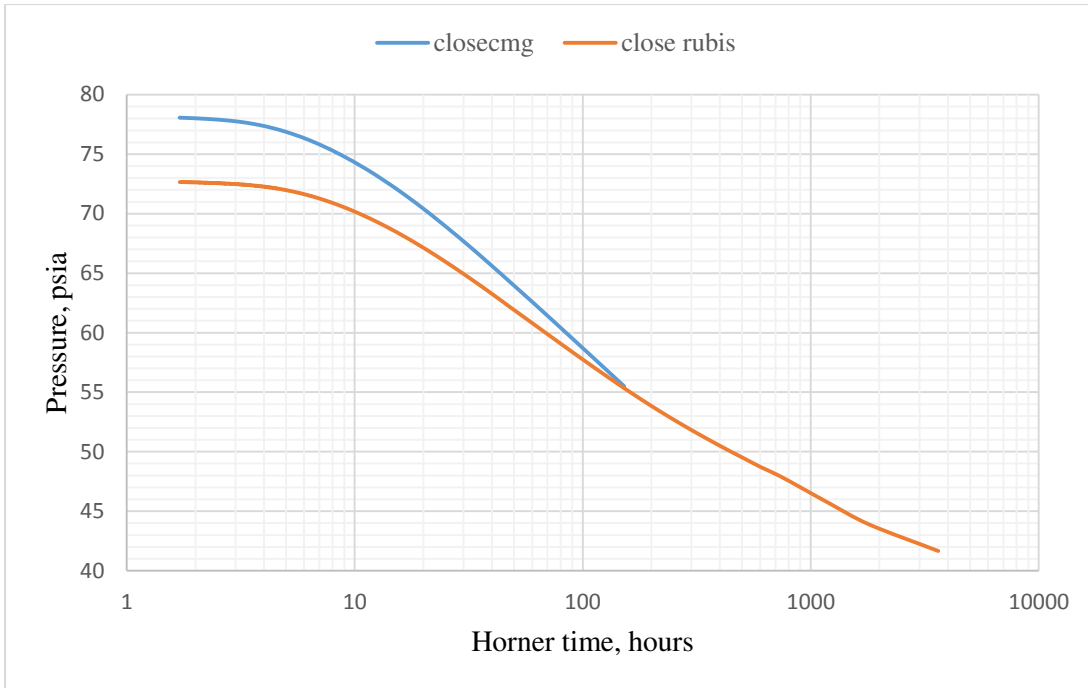


**Figure 8-22.** Horner Plot based on CMG IMEX and ECRIN Rubis pressure values.

The following plot shows how Rubis pressure values are different from each other considering horizontal and inclined fault model:

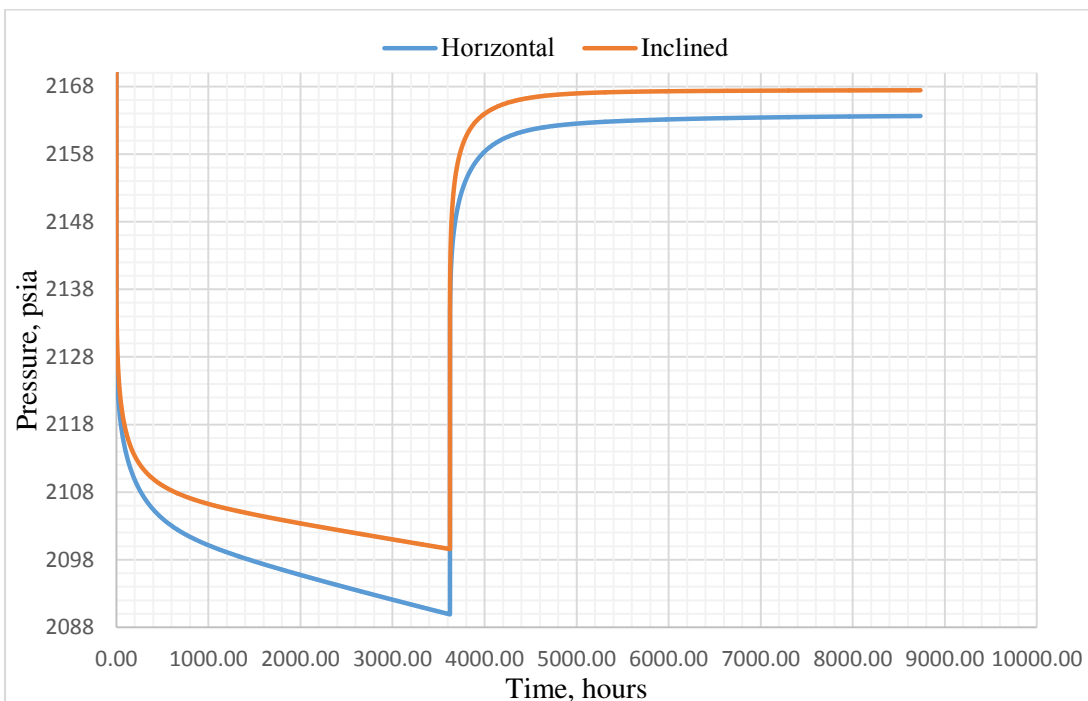


**Figure 8-23.** Ecrin Rubis Pressure Values comparison for horizontal and inclined faults.

In this plot there is good agreement between the curves except that bottom part. Next plot, accordingly, illustrates CMG IMEX pressure values difference for horizontal and inclined fault models:

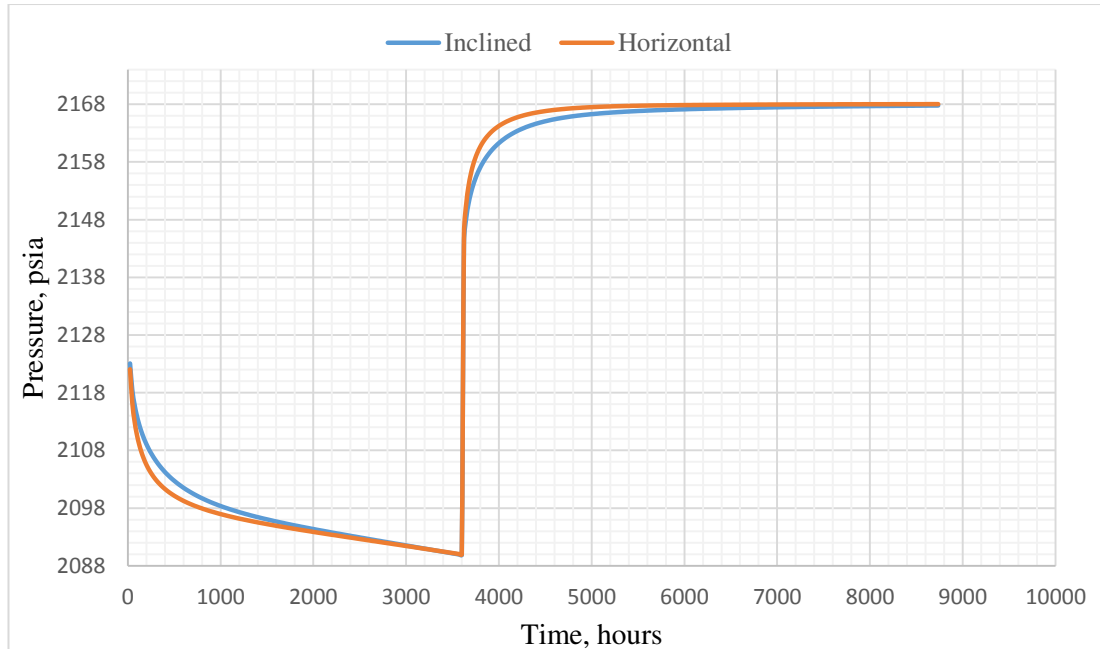


**Figure 8-24.** CMG IMEX Pressure values difference for horizontal and inclined fault models.

The same statement seems to be valid for CMG IMEX also, there is overall a good match except that bottom part of the curves.

### 8.2.2 SATURATED RESERVOIR

In this case gas phase was added to our reservoir model and it was checked how Voronoi gridding is precise on simulating this kind of reservoirs by comparing against the unstructured gridding results.

The aim here is also to check how Voronoi gridding technique applicable for saturated reservoir models when there is horizontal or inclined fault. There are 3 sub-cases and each their conclusions and discussions are provided.

- **Case 1.** Saturated Reservoir Model without fault.

So, simple reservoir model was constructed by using Ecrin Rubis and CMG IMEX without any fault and compared their results. The following excel file illustrates how these pressure values match with each other:

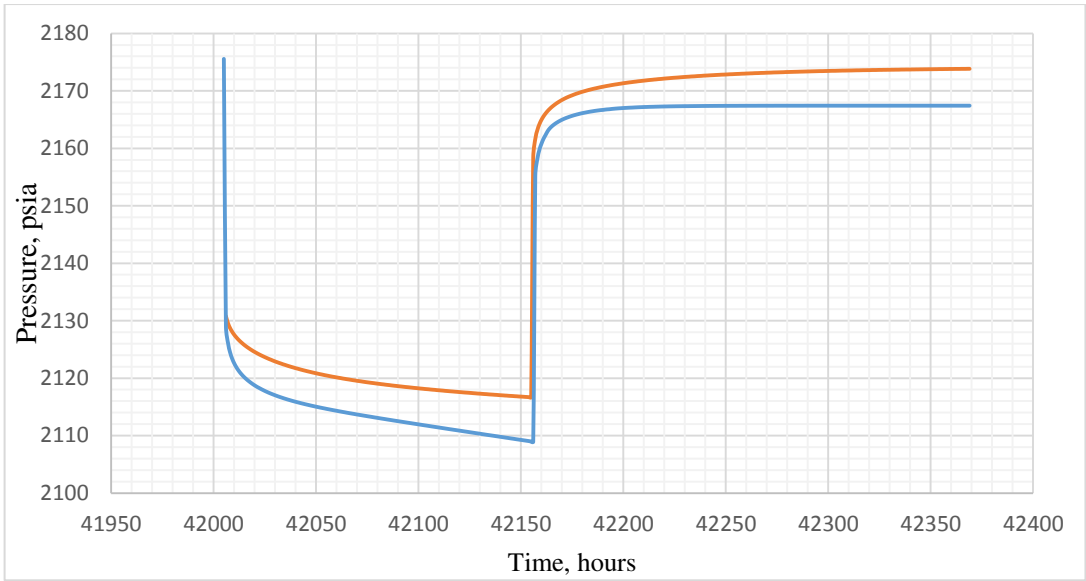


**Figure 8-25.** CMG IMEX Pressure values match with Ecrin Rubis for saturated reservoir model.

Now, if to compare this figure with previous figures it's apparent that with gas phase the difference is higher. Unstructured gridding can lead similar results to structured gridding when there is no gas phase, but with gas phase the difference is more tangible.

Based on the Ecrin Saphir results using both CMG IMEX and Ecrin Rubis it is obvious that there is an actual difference also for the end of transient flow regime. This was expected, because in above figure it was illustrated how their pressures differ from one another.

Now if to compare their Horner Plots, the following results are obtained:

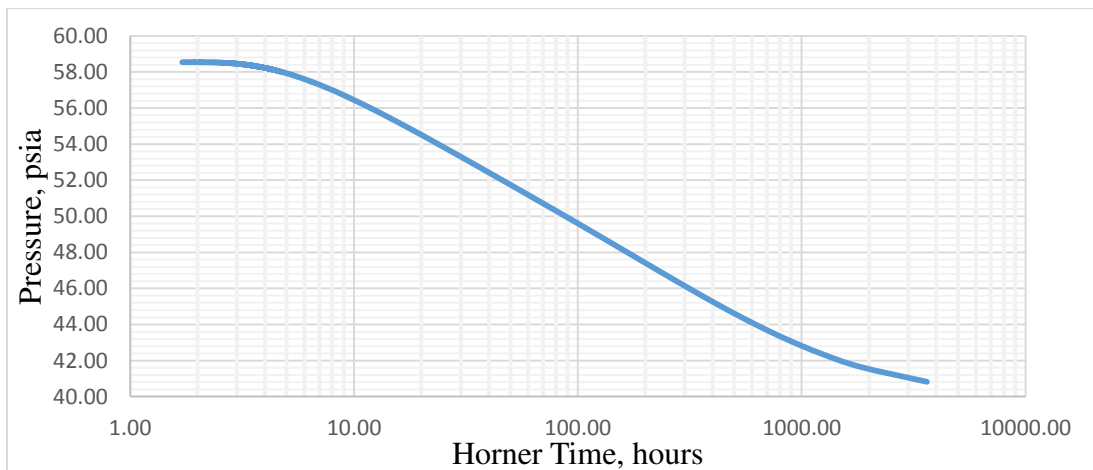


**Figure 8-26.** Horner Plot by using Ecrin Rubis Pressure Values.

If to add straight line to see the transition to pseudo-steady state regimes, then the following plot will be acquired:



**Figure 8-27.** Horner plot based on Ecrin Rubis pressure values with straight line.

Accordingly, the next plot was prepared by using CMG IMEX pressure values:

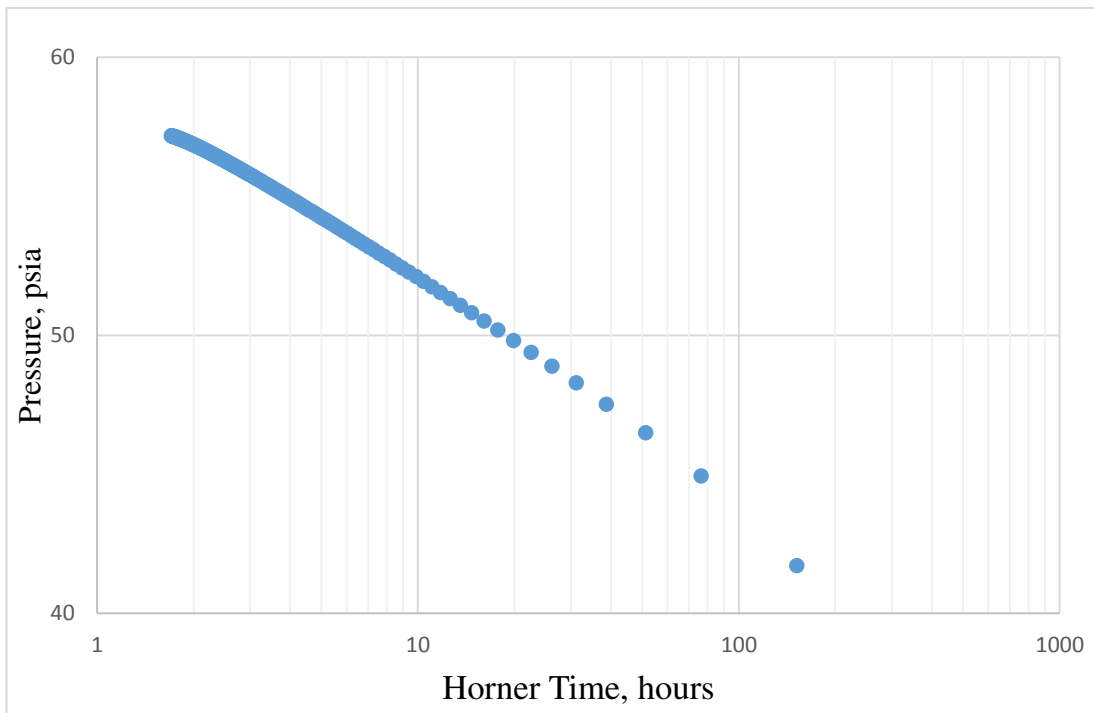


**Figure 8-28.** Horner Plot based on CMG IMEX pressure values.

Alternatively, if to add straight line to see the transition zone to pseudo-steady state, the following plot is obtained:

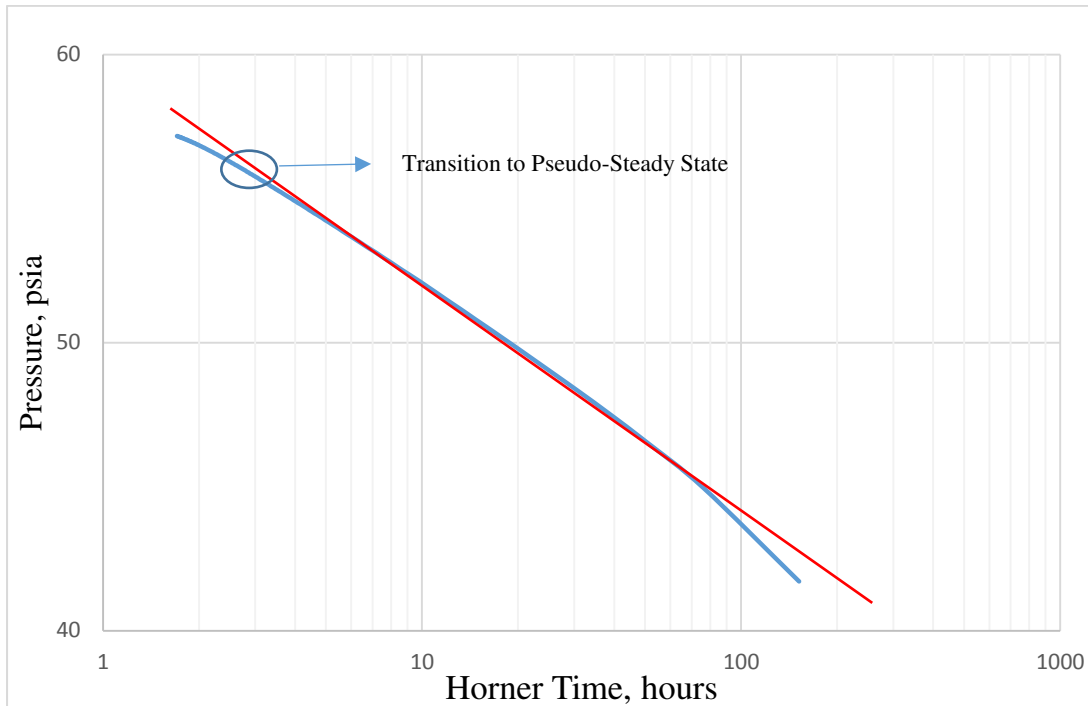


**Figure 8-29.** Horner Plot by using CMG IMEX values with straight line.

- **Case 2.** Saturated model with horizontal fault model

In this model, it was checked Voronoi gridding usage preciseness in terms of representing horizontal fault model by comparing with structured gridded reservoir mode. So, the same reservoir with the same rock and fluid properties was built by using CMG IMEX and Ecrin Rubis. Following excel file illustrates how these two models distinguish:

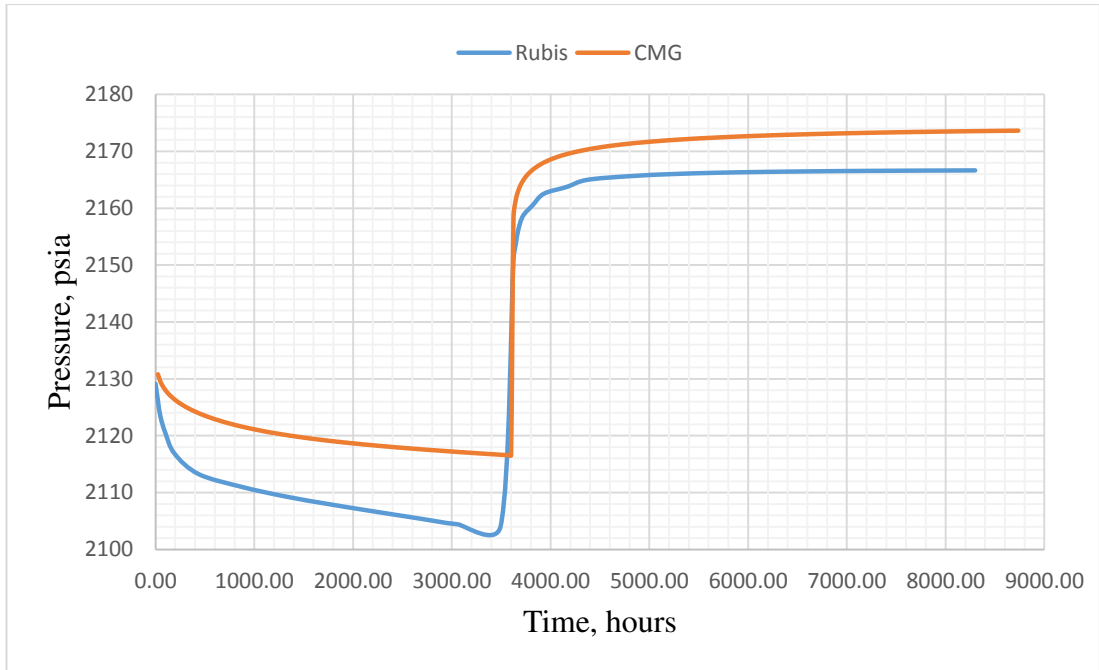


**Figure 8-30.** CMG IMEX-Ecrin Rubis pressure values match for saturated reservoir with horizontal fault.

As in the previous case, it's apparent that these models results are different when there is gas phase or fault. From the last two comparisons it can be concluded that with more complexities, these models results will also be different.

If to concentrate on Ecrin Saphir results that used both simulators pressure output values, one can conclude that Voronoi gridding technique can represent fault more appropriately because in Ecrin Saphir plot that used CMG IMEX pressure data (Figure 7-55) the second straight line is hardly.

But, to be more confidently assured which of them is more precise, the distance from well to fault for this case was also calculated. So, the following plot describes a Horner Plot by using Ecrin Rubis pressure values:

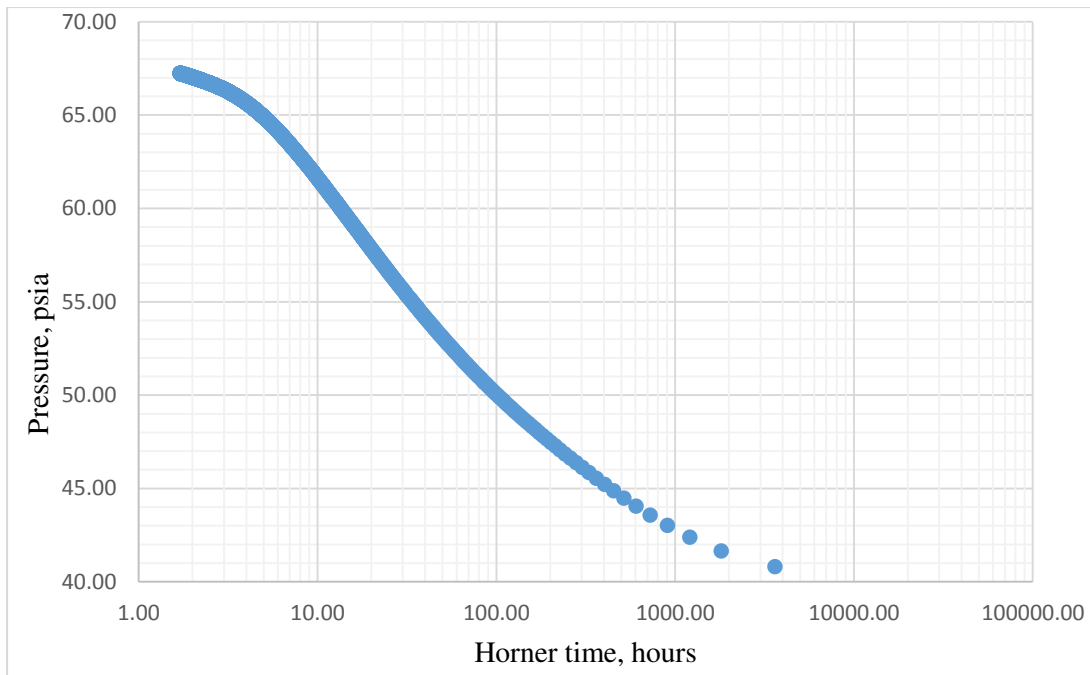


**Figure 8-31.** Horner Plot by using Ecrin Rubis pressure values for saturated reservoir model with a horizontal fault.

If to add two straight lines to see the intersection point between those two lines, one would get the following:

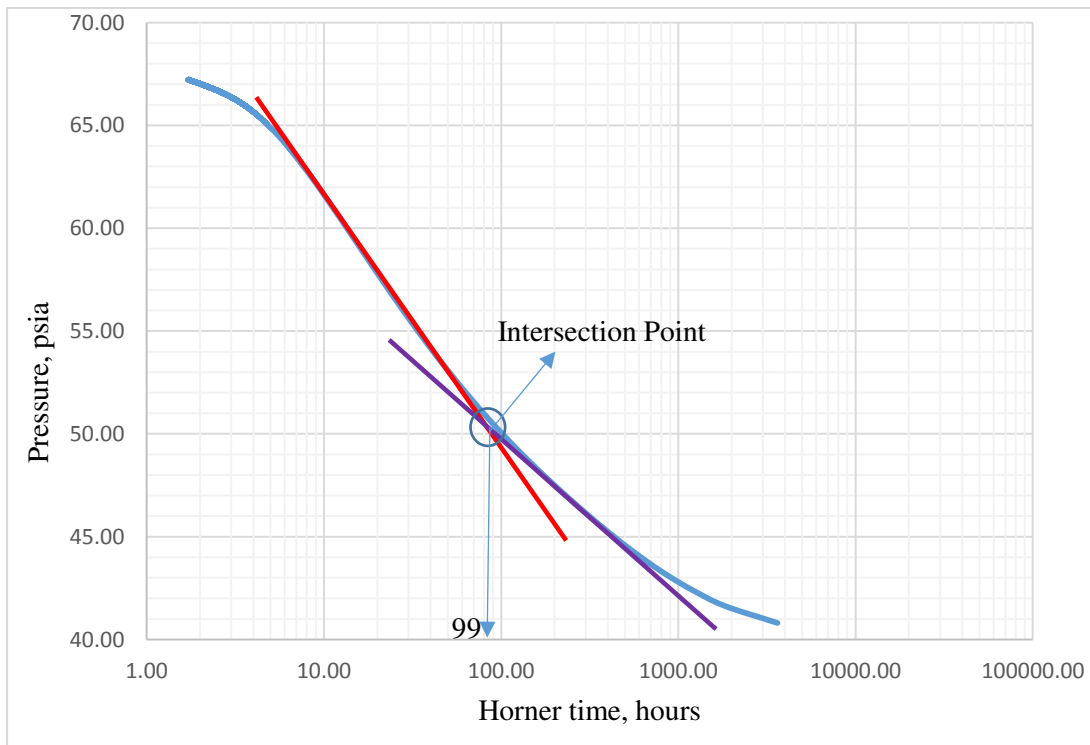


**Figure 8-32.** Horner Plot for Saturated reservoir model with horizontal fault by using Rubis pressure values.

In this plot the intersection point for two lines is 99 hours. So, by using equation (8-1) and (8-2), the distance from well to fault is found to be 519 ft as opposed to 500 ft to our actual data. So there is a good agreement between these values.

Now the same distance can be checked based on Horner plot by using CMG IMEX pressure values. Firstly, the next plot shows how Horner plot looks like for this case:

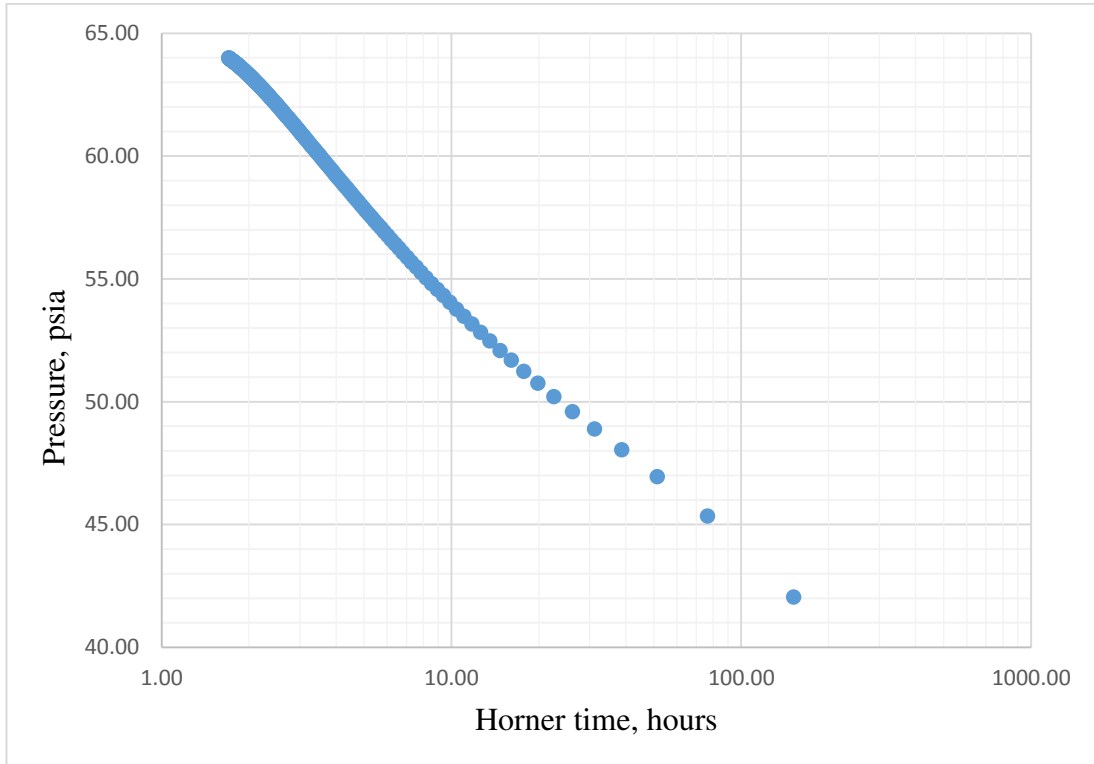


**Figure 8-33.** Horner Plot based on CMG IMEX pressure values for the saturated reservoir model with horizontal fault.

Now, for checking the intersection point between the two straight lines because of fault presence, these lines are added to the plot which in turn the following figure can be acquired:

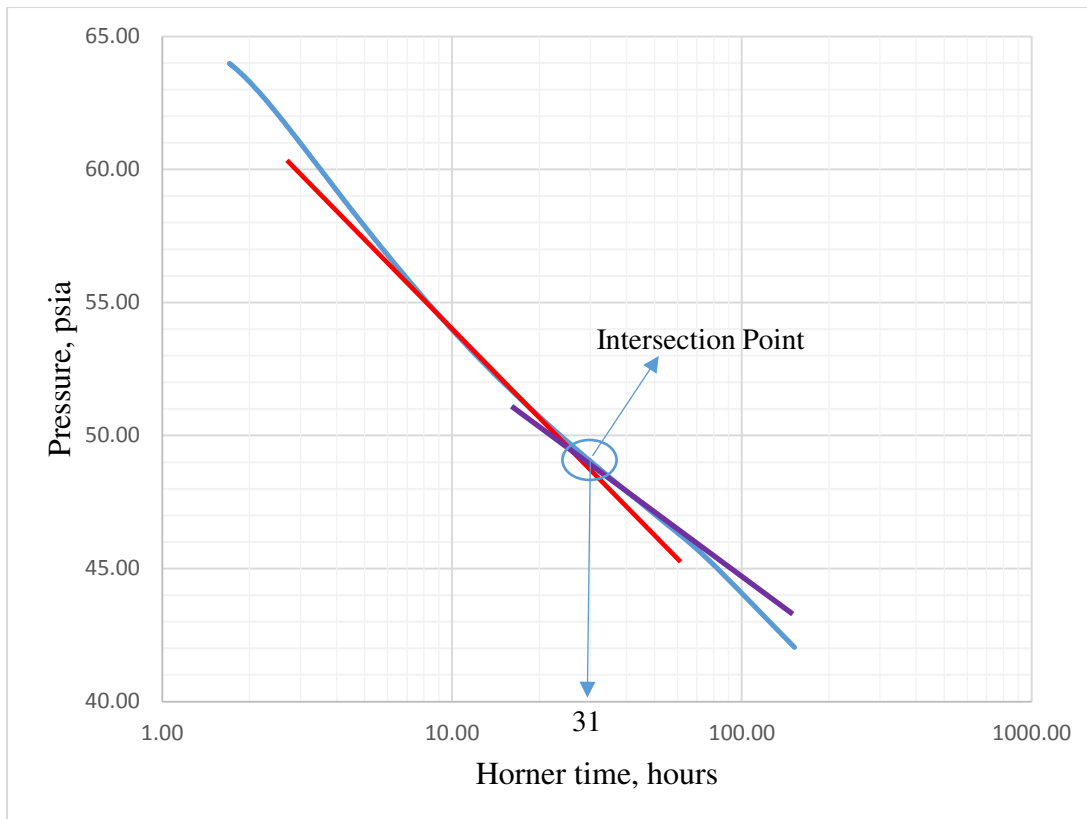


**Figure 8-34.** Horner Plot by using CMG IMEX pressure values.

However, in this plot the intersection time equals to 31 hours. Again by using equation (8-1) and (8-2), the distance is calculated to be 939 ft as opposed to 500 ft of actual data.

So, in this example it was illustrated that unstructured Voronoi gridding offers more precise and representative results than CMG IMEX.

- **Case 3.** Saturated Reservoir Model with inclined Fault channel.

Now in this case inclined fault channel was introduced to the reservoir system and again the same reservoir model was built with the same oil, gas and rock properties on CMG IMEX and Ecrin Rubis. Having obtained the pressure values, these data were compared on excel file and the following figure illustrates this difference:

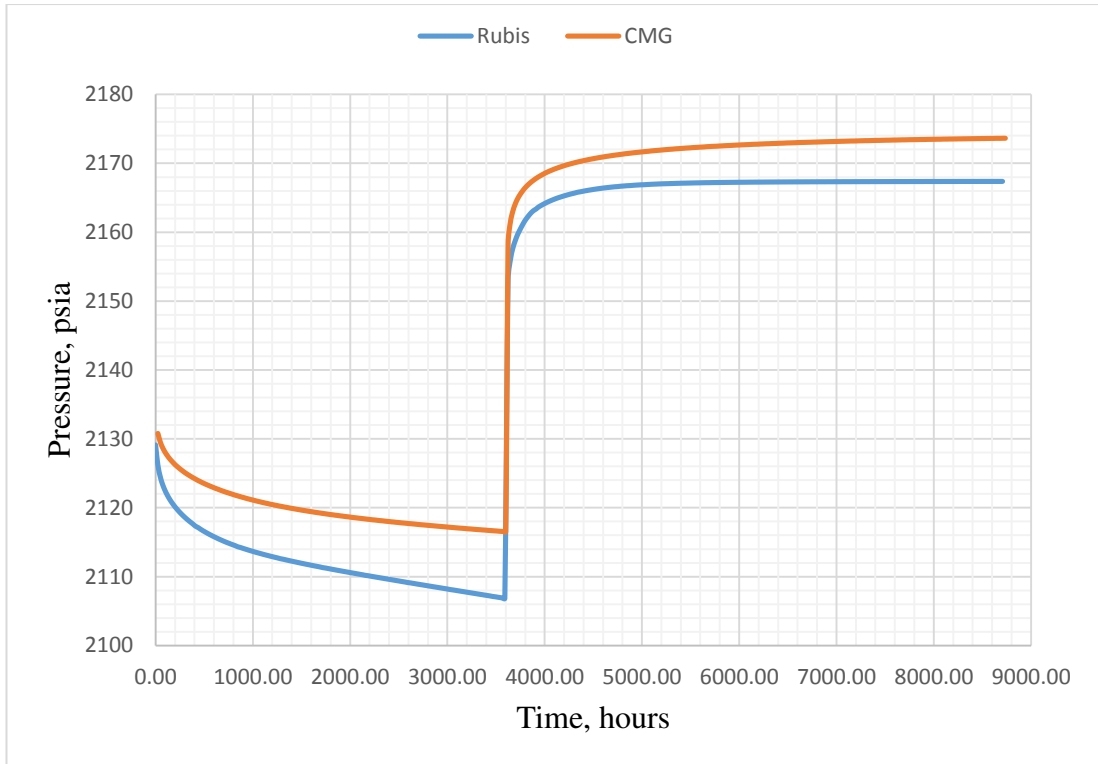


**Figure 8-35.** CMG IMEX pressure values comparison with Ecrin Rubis for the saturated reservoir model with inclined fault.

So, this plot also supports the idea that with more complexities, the discrepancy between the pressure values will be more conspicuous. For instance, their inequality is more evident with fault than without any fault, and additionally with gas phase their agreement also gets deteriorated.

Again for being more confident which of them offers more precise results, the distance between the well and the fault can be estimated by using Horner plots. Note that, actual distance equals to 283 ft. So, the following plots were generated by using Rubis and CMG Ecrin values respectively:

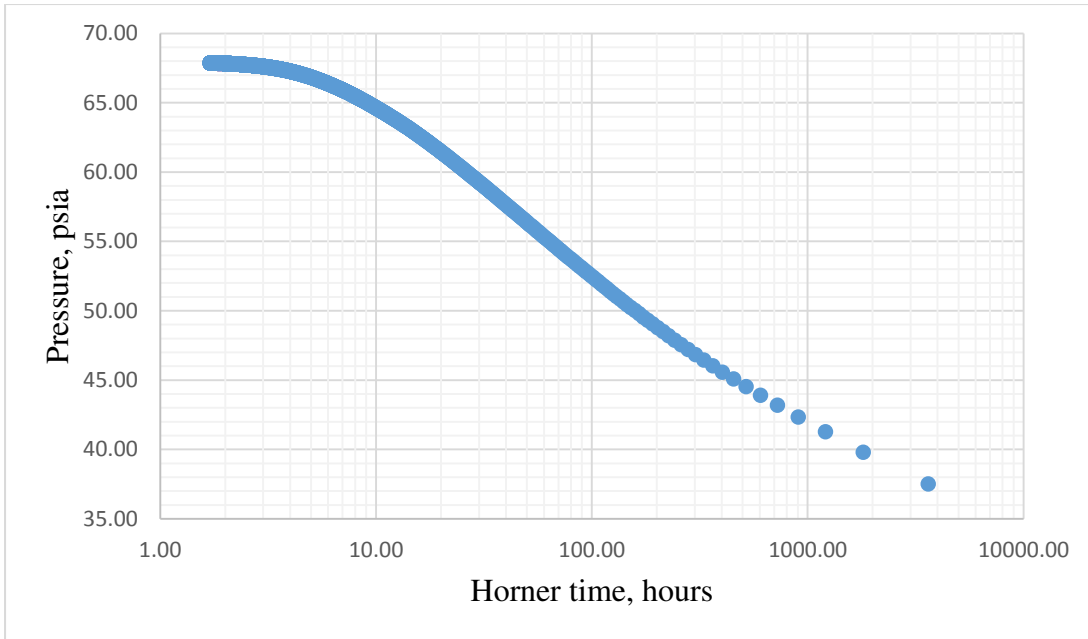


**Figure 8-36.** Horner Plot based on Ecrin Rubis values for saturated reservoir with inclined fault.

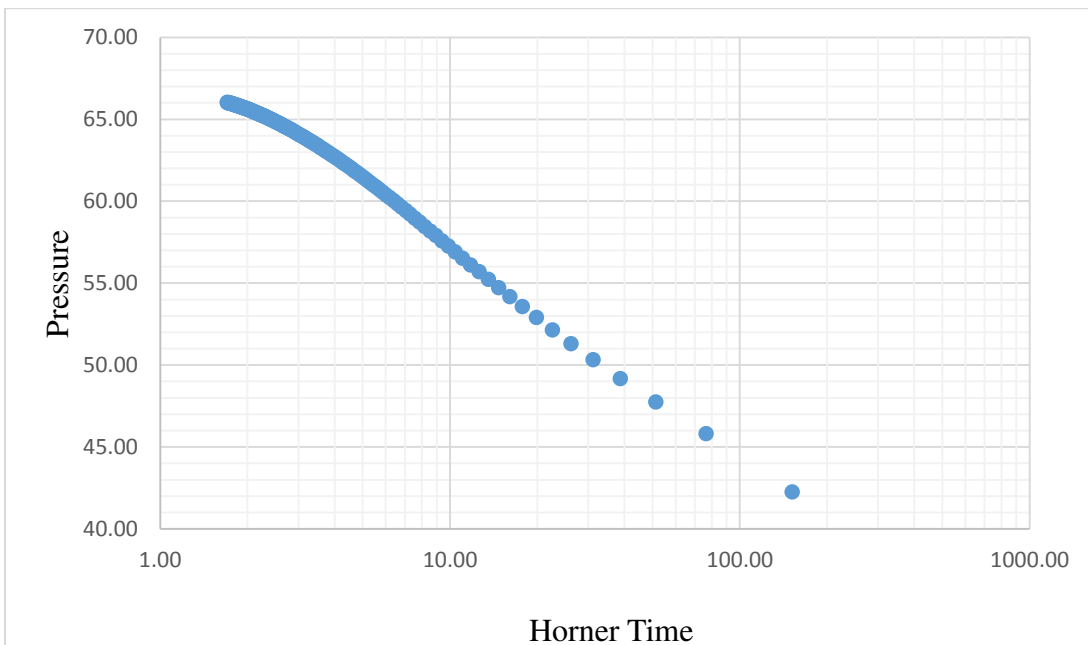


**Figure 8-37.** Horner Plot based on CMG IMEX pressure value for saturated reservoir with inclined fault.

Now, after introducing these plots 2 straight lines can be added to each of these plots to find the intersection point between the lines. So, the next plot was generated based on Ecrin Rubis pressure values:

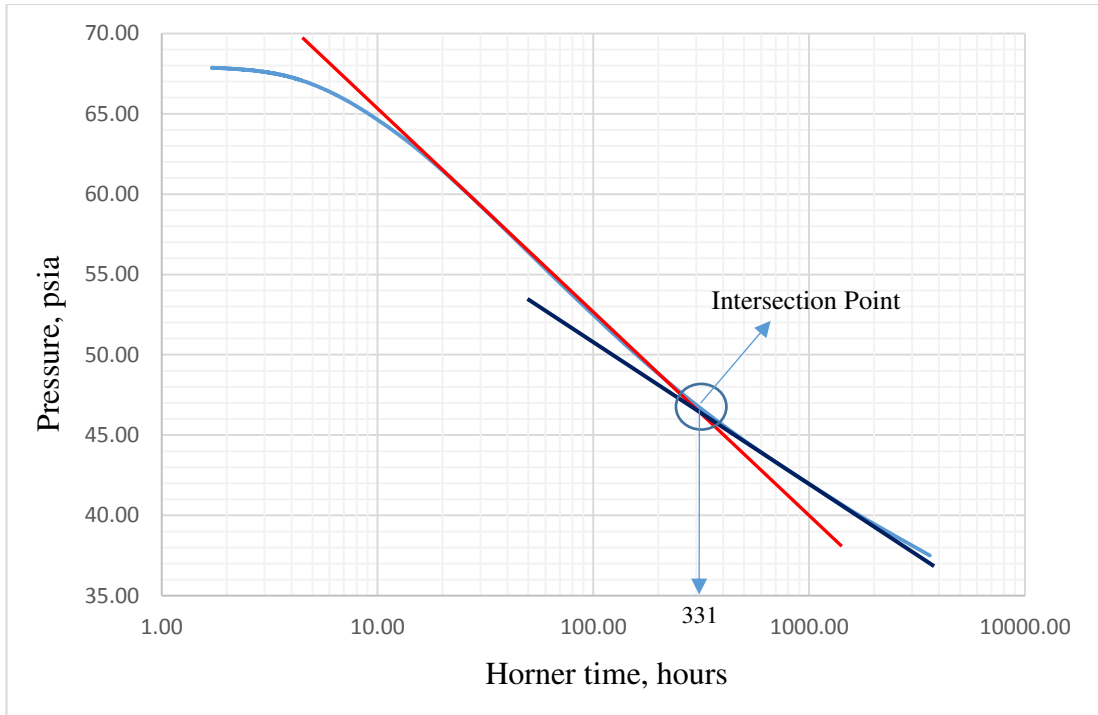


**Figure 8-38.** Horner Plot based on Ecrin Rubis pressure values for the saturated reservoir with inclined fault.

In this plot, it's apparent that the intersection point here is 331 hours. So, based on equations (8-1) and (8-2), the distance was found to be equal to 283 ft. Perfect match with the actual distance is obtained. This proves the fact that Voronoi gridding technique is accurate even with inclined fault channel orientation in a saturated reservoir.

Now, the actual distance can be compared with the value that's obtained from Horner plot by using CMG IMEX pressure values. So, the next plot illustrates the intersection point between the lines:



**Figure 8-39.** Horner Plot based on CMG IMEX pressure values for saturated reservoir model with inclined fault.

In this figure it's seen that the intersection point is 51 hours, which in its turn leads to 727 ft of distance based on equations (8-1) and (8-2) as opposed to 283 ft of actual distance data. So, not as accurate results as it was obtained from Ecrin Rubis pressure data, in fact the true distance has not been preserved. The explanation behind this fact is the manner how structured gridding simulates the inclined fault which is in the form of zig-zag is totally different how unstructured gridding behaves, in the latter the fault distance and length is preserved, whereas in the former case it is not preserved.

From these conclusions it can be stated than Voronoi gridding technique is capable of generating more accurate and representative results for well test design than unstructured gridding technique.

This conclusion can be even supported with the reference of comparison between Ecrin Saphir results which used both numerical simulators. With Figure 7-58 one can more confidently say that there is a fault in our system, whereas Figure 7-59 does not offer such extent of confidence, in fact it's hardly noticed second straight line there.

Table 8-1 illustrates the end of transient flow regime for each case obtained from analytically and numerically.

**Table 8-1.** End of Transient flow regime comparison

<b>End of Transient Regime</b>		
<b>Reservoir Models</b>	<b>Analytical (hours)</b>	<b>Numerical (hours)</b>
OILWATER Model	96.8	98
BLACKOIL Model	96.8	14.7
Reservoir Model with 2 wells	96.8	14.2
Rectangular Reservoir Shape	581	370
Square Reservoir Shape	97	96.8
Reservoir with vertical fault	407	335
Reservoir with inclined fault	407	196

Alternatively, Table 8-2 indicates the comparison between Ecrin Rubis and Analytical Methods results considering six different cases. Analytical calculations results don't change, because no fluid and rock property were changed for each case, only different shut-in times, production rates, and production times were considered.

**Table 8-2.** End of transient regime comparison for 6 different cases

Cases	<i>End of Transient Regime</i>	
	<b>ECRIN RUBIS</b>	<b>Analytical (hours)</b>
Case 1	222	209
Case 2	225	209
Case 3	392	209
Case 4	337	209
Case 5	<i>No transition</i>	<i>No transition</i>
Case 6	248	209

Table 8-3 presents the results of calculated well to fault distance by using CMG IMEX and Ecrin Rubis for each reservoir cases considering both horizontal and inclined faults with saturated and undersaturated reservoirs.

**Table 8-3.** Well to Fault distance estimation for different reservoir models.

<i>Well to Fault Distance (ft)</i>		
Reservoir Models with Fault	<b>Ecrin Rubis</b>	<b>CMG IMEX</b>
Undersaturated Model with Horizontal Fault <i>Real Distance is 500 ft</i>	499.78	590
Undersaturated Model with Inclined Fault <i>Real Distance is 283 ft</i>	284	594
Saturated Model with Horizontal Fault <i>Real Distance is 500 ft</i>	519	939
Saturated Model with Inclined Fault <i>Real Distance is 283 ft</i>	283	727

## CHAPTER 9

### CONCLUSIONS

To sum all the results and discussions up, it can be concluded for the first part that analytical calculations can exhibit similar results with numerical simulators under ideal circumstances, where the reservoir is ideally square, only oil phase is flowing and reservoir is not specified with any flow barriers, i.e. faults or pinch-outs. In these cases sophisticated reservoir simulators may not be economically preferred, in fact analytical equations can be used in these cases. However most of the reservoirs around the world can be irregular in shape where oil, gas, and water can flow simultaneously through the reservoir, even it can be entrenched with a number of faults with different channel orientations. So, in these cases numerical simulators are evidently the best option to design a well test.

For the second part it can be concluded that because of flexibility of Voronoi gridding technique, it represents and simulates faults with better accuracy than structured gridding. In the example of finding the distance from well to fault, it was apparent that Voronoi gridding results are much closer to actual distance than CMG ECRIN generated data. Even with inclined fault example, the actual distance was preserved through the accurate simulation of unstructured Voronoi gridding. Based on this, conclusion is that Voronoi gridding can offer the same preciseness irrespective of whether reservoir is saturated or unsaturated.

The next conclusion for six cases was that for better well test design procedure, production time, shut-in duration, and production rate should be selected optimally, otherwise because of weak pressure disturbance through lower production rate or

because of short shut-in time preventing the pressure to increase and stabilize, well test design can't yield accurate and reliable information to be relied upon.

## CHAPTER 10

### FUTURE WORK

The future work for the first section of this study which is highlighting the differences of numerical model results over analytical equation results, oil reservoir models with fault together with the gas phase can be investigated, because in this study it was assumed that there is only oil phase flowing throughout the reservoir when there's a fault. So, analytically, the end of flow regime can be calculated for this kind of reservoir and pressure drop also can be calculated based on analytical equations. Numerically, build-up log-log plot can yield the time required to reach the pseudo-steady state as well as bottom-hole flowing pressure for each time step is also provided from CMG IMEX simulator. Subtracting these values from initial reservoir pressure will give pressure drop acquired by using numerical simulators. Corresponding differences in time for the end of radial flow regime and pressure drops can yield how analytical equation results match with numerical simulator results under these circumstances.

For the second section of this study which is investigating the applicability of using Voronoi gridding in well test design, multiple faults in a rectangular reservoir shape model with multiple wells can be studied as a future work. In this study, Voronoi gridding was applied to square reservoir model with only one fault along with one well, and all calculations were performed under these assumptions. However, introducing more complexities to reservoir system, i.e. multiple faults which some of them are horizontal, some of them are inclined in an irregular reservoir shape with multiple wells and additionally gas phase flowing with the oil phase can give more insight about the preciseness of Voronoi gridding applicability for well test design purposes.



## REFERENCES

1. Abdus Satter, James L. Buchwalter: "Practical Enhanced Reservoir Engineering assisted with Simulation Software", 2008
2. Ahmed Tarek, "Reservoir Engineering Handbook", 2001
3. Al-Thaward, F.M., Liu, S.J., Banerjee, R. " Linking Well Test Interpretations to full Field Simulations", SPE pape 105271, Kingdom of Bahrain, 11-14 March, 2007
4. Amanat U. Chaudry: "Oil Well Testing Handbook", 2004
5. Azarkish, A., Khaghani, E. "Interpretation of Water Injection/Falloff Test- Comparison between Numerical and Levitan's Analytical Method", SPE Conference and Exhibition, China, 2012
6. Aziz K.; "Analytical Well Models for Reservoir Simulation," SPEJ (Aug. 1985) 573-79
7. Aziz, K. and Settari, A.: "Petroleum Reservoir Simulation", Applied Science Publishers Ltd., London, 1979
8. Aziz, K.: "Notes for Petroleum Reservoir Simulation", Stanford University, Stanford, 1991.
9. Bixel. H.C., Larkin, B.K. and Van Poolen. H.K, "Effect of Linear Discontinuities on Pressure Build-Up and Drawdown Behaviour",1963
10. Blasingame, T.A.. Johnston. J.L. and Lee. W.J. "Type-Curves Analysis Using the Pressure", 1989
11. Boe, A., Skjaeveland, S.M. and Whitson C.H. "Two-Phase Pressure Test Analysis", 1981
12. Bourdarot, G., "Well Testing Interpretation Methods", 1998
13. Bourdet Dominic,:"Well Test Analysis, The Use of Advanced Interpretation Models", 2002.
14. Boutaut J., Dumay C., "Use of DST for Effective Dynamic Appraisal", SPE 97113, Texas, 2005

15. Brand, C.W., Heinemann, Z.E. and Aziz, K.: "The Grid Orientation Effect in Reservoir Simulation," paper SPE 21228, 1991.
16. Burgess K.A. "An integrated Approach to the Design and Interpretation of Reservoir Tests and Well Productivity Analysis", SPE Paper 23715, 1992
17. Clark, N., "A Review of Reservoir Engineering," World Oil, June 1951
18. Dake L.P., "Fundamentals of Reservoir Engineering", 1977
19. Daungkaew, S. "Forecasting the productivity of Laminated Sands with Single Well Predictive Model", SPE 116370, 2008
20. Deng, H., A., Mohammed "Reservoir Characterization and Flow Simulation of a Low Permeability Gas Reservoir: An integrated approach for Modelling Tommy Lakes Gas Field", SPE paper 137507, 2010
21. Dietz, D.N.: "Determination of Average Reservoir Pressure from Build-Up Surveys", 1998.
22. Ding, Y., and Jeannin, L., "New Numerical Schemes for Near-well Modelling Using Flexible Grid", SPE journal 9(1):109-121, 2004
23. Escobar, F.H., Djebbar, T., "PEBI Grid Selection for Numerical Simulation of Transient Tests", Alaska, October, 2002.
24. Forsyth, P.A. and Sammon, P.H.: "Local Mesh Refinement and Modelling of Faults and Pinchouts", 2002
25. Fung, L., Dogru, A.H. "Distributed Unstructured Grid Infrastructure for Complex Reservoir Simulation", Annual Conference and Exhibition, Rome, Italy, 2011.
26. Garcia J.P., and Mehran, P.D., "Well Testing in Tight Gas Reservoirs", SPE 100576, presented in Calgary, Canada, 2006
27. George Stewart: "Well Test Design and Analysis", 2010
28. Goode, P. A. "Pressure Drawdown and Buildup Analysis of Horizontal Wells", 1996
29. Gordon Adamson, Martin Crick, Brian Gane, Omer Gurpinar, "Simulation Throughout the life of a Reservoir", 1998
30. Gray, K.E.: "Approximating Well-to-Fault Distance From Pressure Buildup Tests", 1958
31. Gringarten, A.C., Ramey, H.J., and Raghavan, R.: "Pressure Analysis for Fractured Wells", paper SPE 4051, 1972.

32. He, N., and Chambers, K.T., "Calibrate Flow Simulation Models with Well-Test Data to Improve History Matching", SPE paper 56681, presented in Houston, Texas, 3-6 October, 1999`
33. Heinemann, Z. E. "Interactive Generation of Irregular Simulation Grids and its Practical Applications", SPE paper 27998, Tulsa, Oklahoma, August 1994
34. Hui, D., Xia, B., Zhangxing, C., "Numerical Well Testing Using Unstructured PEBI Grids", SPE Paper 142258, 2011
35. Jargon, J.R. "Effect of Wellbore storage and Wellbore Damage at the Active Well on Interference Test Analysis", 2010.
36. John Lee : "Well Testing", 1997
37. Kamal, M.M., Braden, J.C. and Park, H., "Use of Pressure Transient Testing To Identify Reservoir Damage Problems", 1992
38. Kuchuk, F.J., "Radius of Investigation for Reserve Estimation from Pressure Transient Well Tests", 2009
39. Kuifu, D., "Use of Advanced Pressure Transient Anlysis Techniques to Improve Drainage Area Calculations and Reservoir Characterization", SPE 109053, 2007
40. Kumar, V., James D., and Theodore K., "The use of Wireline Formation Tester for Optimization of Conventional Well Test Design and Interpretation", 2010
41. Larry S.K., Xiang Y.D., "An unstructured Gridding Method for Densely-Spaced Complex Wells in Full-Field Reservoir Simulation", 2013
42. Matthews, C.S. and Russell, D.G.: "A Method for Determination of Average Reservoir Pressure in a Bounded Reservoir", 1995
43. Merland, R., Ganzer, L., Nghiem, L.X. "Building Centroidal Voronoi Tessellations for Flow Simulation in Reservoir Using Flow Information", SPE 141018, The Woodlands 21-23, Feb. 2011
44. Michael, M., "Application of Water Injection/Fall off test for Reservoir Appraisal", SPE 77532, 2006.
45. Miller, C.C., Dyes, A.B., and Hutchinson, C.A. Jr.: "Estimation of Permeability and Reservoir Pressure From Bottom-Hole Pressure", 1998
46. Mlacnik, M. J., and Heinemann Z. E. "Using Well Windows in Full Field Reservoir Simulation", SPE Reservoir Evaluation and Engineering, 2003
47. Muskat, M., 1934. "The Flow of Compressible Fluids Through Porous Media and some Problems in Heat Conduction", 1992

48. Palagi, C.L.: "Generation and Application of Voronoi Grid to Model Flow in Heterogeneous Reservoirs", 1992
49. Palagi, C.L., "Use of Voronoi grid in Simulation, April", SPE 22889, 1994
50. Peaceman, D.W.: "Fundamentals of Numerical Reservoir Simulation", Elsevier Scientific Publishing Company, Amsterdam, Oxford, New York, 1977
51. Perrine. R.L.: "Analysis of Pressure Buildup Curves", 1994
52. Ramey, H.J. Jr.: "Non-Darcy Flow and Wellbore Storage Effects on Pressure Buildup and Drawdown of Gas Wells", 1994
53. Raghavan, R., Dixon T.N., Phan, V.Q., "Integration of Geology, Geophysics, and Numerical Simulation in the Interpretation of the Well Test", SPE Reservoir Evaluation and Engineering Journal, June, 2001
54. Robert C. Earlougher: "Advances in Well Test Analysis", 1997
55. Ronald N. : "Modern Well Testing Analysis", 1990
56. Russel D.G.: "Determination of Formation Characteristics From Two-Rate Flow Tests", 1985
57. Sinha, S.P., and Al-Qattan, R. " Numerical Simulation to Design and Analyse Pressure Transient Tests in a Shaly Interbedded Reservoir, SPE 93941, 2005
58. Schlumberger: "Modern Well Testing", 1994
59. Streltsova, T.D., "Buildup Analysis for Interference Tests in Stratified Formations", 1984.
60. Streltsova, T.D. and McKinley, R.M., "Effect of Flow Time Duration on Build-Up Pattern for Reservoirs with Heterogeneous Properties", 1984